

University of Warwick institutional repository: <http://go.warwick.ac.uk/wrap>

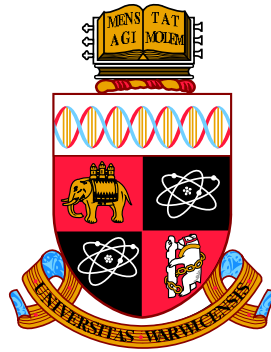
A Thesis Submitted for the Degree of PhD at the University of Warwick

<http://go.warwick.ac.uk/wrap/60376>

This thesis is made available online and is protected by original copyright.

Please scroll down to view the document itself.

Please refer to the repository record for this item for information to help you to cite it. Our policy information is available from the repository home page.



Graphical representation of range of motion in the assessment of total hip arthroplasty

by

Glen Alan Turley

An Innovation Report submitted in partial fulfilment of the
requirements for the degree of
Doctor of Engineering (EngD)

The University of Warwick, WMG: Innovative Solutions

March 2012

THE UNIVERSITY OF
WARWICK

Abstract

Total Hip Arthroplasty (THA) is a successful technique restoring lost mobility to patients suffering from osteoarthritis. A successful THA normalises the biomechanics of the hip joint so that a patient can achieve the required range of motion to fulfil their daily activities. A recent development in THA implant technologies has been the introduction of femoral neck modularity. Assessment of femoral neck modularity has been limited by two factors. Firstly, range of motion requirement is not well understood and secondly previous clinical reports have lacked a comparison against an established successful THA implant. This study has successfully addressed these limiting factors by developing an innovative range of motion benchmark which considers the activities a person is required to undertake during their daily routine. The benchmark was developed using a systematic review of the literature focussing on hip joint biomechanics. This has been the first study to provide a clinically meaningful representation of hip joint range of motion which permits operative outcome to be directly compared against an established benchmark. Integration of the range of motion benchmark within the surgical environment was achieved by using a surgical navigation measurement device. Intra-operative measurement meant that post-operative range of motion could be simulated and compared against the requirement set by the range of motion benchmark. Distinct outcome measures have been able to be developed using this comparison which has allowed the surgical process to be assessed like a manufacturing system. Using these outcome measures, it was found that femoral neck modularity has greater potential to adjust implant orientation in comparison to non-modular femoral neck implants to achieve the ideal range of motion. However, this potential is being limited due to the current modular neck options available and because of difficulty experienced by the surgeon in assessing implant orientation. These findings have been used to develop a medical device which provides guidance to the surgeon about the THA implant orientation and thus allow them to be able to make the correct modular neck choice to maximise range of motion and improve the operative outcome for the patient.

Acknowledgements

This Engineering Doctorate would not have been possible without the aid and support of a number of people. Firstly, I would like to thank my mentor's Prof. Mark Williams and Prof. Damian Griffin. The work presented crosses engineering, clinical, commercial and academic boundaries and required not only their guidance but also their trust in me over the past four years. I would also like to thank Shahbaz Ahmed, Austin Fearnside, Martin Bishop and Dr-Ing. Martin Haimerl who have provided the benefit of their experience on numerous occasions. The work also required collaboration between a number of organisations and I would like to thank the staff at WMG, Warwick Medical School, Coventry and Warwickshire NHS Trust, Nikon Metrology, Brainlab and Wright Medical Technology for making this happen.

My deepest gratitude goes to my family. They have provided more than generous understanding throughout my years of education and have given me the freedom to develop whilst also showing unwavering support. My life over the past four years has transformed beyond all recognition because of one person, my wife Kieu Anh. She has shown remarkable patience and faith in me of the like I have never experienced. I am looking forward with excitement to my life ahead with her beyond the Engineering Doctorate.

Declaration

I declare that all work and innovation contained and described within this Engineering Doctorate Innovation Report was undertaken by myself unless otherwise acknowledged within the text. In particular, the study protocol for the application of the innovation was designed by the Clinical Trials team within Warwick Orthopaedics led by Professor of Trauma and Orthopaedics Damian Griffin. The integration and the design of how the innovation was applied within the study protocol was undertaken by myself with all subsequent analysis and new knowledge generated as a result of this study being my own. This work has not been previously submitted for any other academic degree or qualification.

Glen Alan Turley

March 2012

Contents

Abstract	i
Acknowledgements	iii
Declaration	iv
Contents	v
Glossary of Terms	viii
List of Figures	ix
List of Tables	xi
1 Introduction	1
1.1 Background to the research	1
1.2 Research scope	4
1.3 Outline of EngD portfolio	5
1.4 Outline of innovation report	7
2 Literature Review	9
2.1 Introduction	9
2.2 Principles of human movement	10
2.3 Biomechanics of the hip joint	12
2.3.1 Body segment coordinate frames	12
2.3.2 Joint coordinate frame	15
2.3.3 Summary	21
2.4 Biomechanics of total hip arthroplasty	22
2.4.1 Acetabular cup	24
2.4.2 Femoral stem	26
2.4.3 Summary	28
2.5 Hip joint reference frames	29
2.5.1 Pelvic reference frame	29
2.5.2 Femoral reference frame	31
2.5.3 Summary	33
2.6 Femoral neck modularity	35
2.6.1 Overview of neck modularity	35

2.6.2	Previous studies	37
2.6.3	Femoral neck integrity	40
2.6.4	Summary	41
2.7	Literature review summary	42
3	Research Methodology	44
3.1	Introduction	44
3.2	Selection of research design	45
3.3	Systematic review methodology	47
3.3.1	Literature search	47
3.3.2	Systematic review validity	50
3.3.3	Validation of the range of motion benchmark	51
3.3.4	Summary	53
3.4	Randomised controlled trial design	54
3.4.1	Trial design	54
3.4.2	Participants	61
3.4.3	Methods	61
3.4.4	Outcome measures	62
3.4.5	Sample size	67
3.4.6	Sampling errors	68
3.4.7	Summary	69
3.5	Summary	70
4	Establishing a range of motion benchmark	71
4.1	Introduction	71
4.2	Establishing range of motion values	72
4.2.1	Pure joint motion	72
4.2.2	Activities of daily living	75
4.2.3	Summary	77
4.3	Constructing the graphical representation	78
4.3.1	Initial representation	78
4.3.2	Final representation	81
4.3.3	Defining the position of the range of motion benchmark	85
4.3.4	Summary	87
4.4	Validation of the range of motion benchmark	88
4.4.1	Results	90
4.4.2	Discussion	91
4.4.3	Summary	94
4.5	Summary	95
5	Post-operative assessment using the range of motion benchmark	96
5.1	Introduction	96
5.2	Implementation	97
5.2.1	Measurement protocol	97
5.2.2	Graphical representation of prosthetic range of motion	100
5.2.3	Summary	102
5.3	Measurement system assessment	103

5.3.1	Measurement validity	103
5.3.2	Measurement reliability	107
5.3.3	Summary of results	109
5.4	Summary	110
6	Assessment of femoral neck modularity	111
6.1	Introduction	111
6.2	Influence of femoral neck modularity	112
6.2.1	Definition of independent variables	113
6.2.2	Screening results	114
6.2.3	Full factorial results	117
6.3	Effectiveness of femoral neck modularity	120
6.3.1	Clinical trial results	121
6.4	Effectiveness of range of motion benchmark	124
6.5	Summary	126
7	Discussion	127
7.1	Introduction	127
7.2	Research objectives	128
7.2.1	Establishing a prosthetic range of motion benchmark	128
7.2.2	Graphical representation of the range of motion benchmark	131
7.2.3	Assessment of post-operative outcome using the graphical representation	134
7.2.4	Assessment of femoral neck modularity	135
7.2.5	Effectiveness of graphically representing hip joint range of motion	141
7.3	Research question	144
7.4	Innovation	145
7.5	Research limitations	147
7.6	Further innovation	150
7.7	Further Work	154
7.8	Summary	156
8	Conclusion	157
8.1	Introduction	157
8.2	Key findings	158
8.3	Implications of the research	160
8.4	Final summary	162
	References	163
A	Calculation of hip-joint centre	178
B	Validation experiment	180
C	Inter-observer experiment	182

Glossary

AEP	Ankle Epicondyle Piriformis Plane, 92
APP	Anterior Pelvic Plane, 27
ASIS	Anterior Superior Iliac Spine, 10
BMI	Body Mass Index, 57
CAD	Computer Aided Design, 8
CAS	Computer Aided Surgery, 8
CT	Computer Tomography, 30
CTE	Comparative Treatment Efficacy, 52
DDH	Development Dysplasia of the Hip, 33
ISB	International Society of Biomechanics, 12
NHS	National Health Service, 1
NURBS	Non-Uniform Rational B-Spline, 49
OA	Osteoarthritis, 1
PSIS	Posterior Superior Iliac Spine, 10
PTUB	Pubic Tubercles, 27
PV	Percentage Variance in Scores, 50
RCT	Randomised Controlled Trial, 43
rms	root mean square, 84
THA	Total Hip Arthroplasty, 1
TPP	Transverse Pelvic Plane, 11

List of Figures

1.1	Example of component-on-component impingement (Klues et al., 2007).	2
1.2	Structure of EngD portfolio.	6
1.3	Structure of innovation report.	7
2.1	The anatomical coordinate frame (Brinckmann et al., 2002).	11
2.2	Body segment coordinate frames of the hip joint (Wu et al., 2002).	13
2.3	Motion of the hip joint (Luttgens and Wells, 1982).	14
2.4	Hip joint coordinate system <i>adapted from</i> Grood and Suntay (1983).	16
2.5	Clinical rotations for the left hip joint.	20
2.6	Effect of component orientation on range of motion.	23
2.7	Illustration of acetabular cup orientation conventions <i>adapted from</i> Murray (1993).	24
2.8	Acetabular cup impingement limits (Jaramaz et al., 1997).	25
2.9	Femoral stem orientation <i>adapted from</i> Yoshimine and Ginbayashi (2002).	27
2.10	Clinical interpretation of the pelvic reference frame (a) The anterior pelvic plane (APP) <i>and</i> (b) Alignment of the APP with whole body (DiGioia et al., 1998).	30
2.11	Illustration of femoral anteversion measurement conventions.	32
2.12	Femoral neck modularity (a) Lateral view of modular femoral neck system <i>and</i> (b) Antero-posterior view of modular femoral neck system (Sakai et al., 2000).	36
2.13	Modular femoral neck options: straight, varus-valgus 8° and 15° (not shown), ante-retroverted 8° and 15°, combination of ante-retroverted 4.5° with varus-valgus of 6° - AR-VV1 and AR-VV2 options (Traina et al., 2009a).	36
2.14	Example independent offset adjustment with modular necks (Traina et al., 2009a).	38
3.1	Two-stage research process.	45
3.2	Randomised controlled trial methodology (Piantadosi, 2005; Schulz et al., 2010).	46
3.3	The patient CT segmentation process (a) The original Dicom slice image (b) The thresholded slice image <i>and</i> (c) The cleaned slice image.	52
3.4	Consort flow diagram (Schulz et al., 2010).	56
3.5	Femoral stem.	57
3.6	Specification of prosthetic components.	58

3.7	Intervention group femoral stem specifications (a) Profemur neck interfacing with stem <i>and</i> (b) Profemur neck length (Wright Medical Technology, Inc, 2010).	59
3.8	Procotyl-L liner options (Wright Medical Technology, Inc, 2009).	60
3.9	The Brainlab surgical navigation measurement system (Brainlab AG, 2008).	63
3.10	Outcome measures for randomised controlled trial.	64
3.11	Overview of research design.	70
4.1	Initial three-dimensional range of motion representation (a) view of the initial range of motion in the sagittal plane <i>and</i> (b) view in the coronal plane.	80
4.2	Deviation of daily activity fixed axis of rotation away from the transverse plane.	82
4.3	Modelling axes of rotation (a) representation of rotation axes in the transverse plane <i>and</i> (b) visual of rotation axes on the initial range of motion representation.	83
4.4	Knee centre joint angles in the coronal-transverse plane; impingement shown in red.	84
4.5	Final graphical representation of the range of motion benchmark.	84
4.6	The range of motion benchmark directional axis.	87
4.7	Two dimensional plot of patient average range of motion compared to the benchmark.	93
4.8	Three dimensional plot of patient average range of motion compared to the benchmark.	93
5.1	The surgical navigation setup.	98
5.2	Femoral coordinate frame construction and implant registration.	99
5.3	Total hip prosthetic position.	100
5.4	Implementing the hip joint graphical range of motion benchmark.	101
6.1	Percentage contribution of the control group independent variables.	117
6.2	Percentage contribution of the intervention group independent variables.	118
6.3	Percentage contribution of the intervention group independent variables using only neck ante-retroversion.	119
6.4	Percentage contribution of the intervention group independent variables using only neck varus-valgus.	119
7.1	Examples of areas of impingement in prosthetic motion.	135
7.2	Interaction plots: modular neck version and component positioning.	137
7.3	Interaction plots: modular neck-shaft angle and component positioning.	138
7.4	Example of the effect of modular neck choice.	140
7.5	Plot of the size of the prosthetic motion area compared to its position.	142
7.6	Distribution of control (purple) and intervention (blue) directional axes.	143
7.7	Comparison of the graphical representations of hip joint motion.	145
7.8	Illustration of acetabular cup and femoral stem orientations.	151
7.9	The trial femoral head.	152
7.10	The trialling process for the prototype femoral head.	156

List of Tables

3.1	Strategy for literature search.	48
3.2	Screening results from literature search.	49
3.3	Healthy subject range of motion analysis using CT scans.	53
3.4	BioloX ceramic acetabular liner rotation centre.	58
4.1	Recommended reference and distribution figures for pure joint motion of the hip. .	74
4.2	Activities of daily living.	76
4.3	Summary of patient characteristics.	89
4.4	Comparison of experimental results with previous studies.	90
5.1	Gait analysis method: angle between pelvic and femoral medial-lateral axes. . . .	106
5.2	Inter-observer results for the surgical navigation measurement system.	108
6.1	Acetabular cup and femoral stem orientation.	112
6.2	Prosthetic high-low values.	113
6.3	Control group screening results - prosthetic motion area.	116
6.4	Control group screening results - prosthetic angle deviation.	116
6.5	Intervention group ante-retroverted screening results - prosthetic motion area. . .	116
6.6	Intervention group ante-retroverted screening results - prosthetic angle deviation. .	116
6.7	Intervention group varus-valgus screening results - prosthetic motion area.	116
6.8	Intervention group varus-valgus screening results - prosthetic angle deviation. . . .	116
6.9	Clinical trial result - propensity to impinge.	121
6.10	Clinical trial result - impingement severity.	122
6.11	Non-modular intervention result - propensity to impinge.	123
6.12	Non-modular intervention result - impingement severity.	123
6.13	Intervention treatment group - modular neck choice.	123
6.14	Ideal modular neck choice result - propensity to impinge.	123
6.15	Clinical trial result - combined version.	125
6.16	Clinical trial result - size of prosthetic motion area.	125
6.17	Clinical trial result - position of prosthetic motion area.	125

Chapter 1

Introduction

1.1 Background to the research

Total hip arthroplasty (THA) is a successful technique which restores lost mobility to patients suffering from osteoarthritis (OA) and acute trauma (Enocson et al., 2009; Soong et al., 2004). Today, THA is one of the most frequently performed reconstructive operations with excellent intermediate to long term results (Huo et al., 2008). However, there are still complications which require the initial procedure to be revised. In 2010, 11.4% of hip replacement procedures performed in England & Wales were revision procedures. The most prominent indication for surgery was aseptic loosening secondary to wear representing 45% of revision cases while 15% of cases were due to dislocation (National Joint Registry, 2011). Analysis of Scandinavian joint registeries have shown that over time aseptic loosening becomes more predominant while dislocation becomes less predominant, although still an important factor (Kurtz et al., 2007).

A successful THA normalises the biomechanics of the hip joint enabling a patient to regain mobility without pain or discomfort (Sakai et al., 2000). Normalisation of hip joint biomechanics is dependent upon achieving joint stability and the ideal range of motion to be able to fulfil daily activities (Duwelius et al., 2010). Scifert et al. (2001), found that 90% of dislocations had evidence of impingement. Prosthetic impingement occurs when

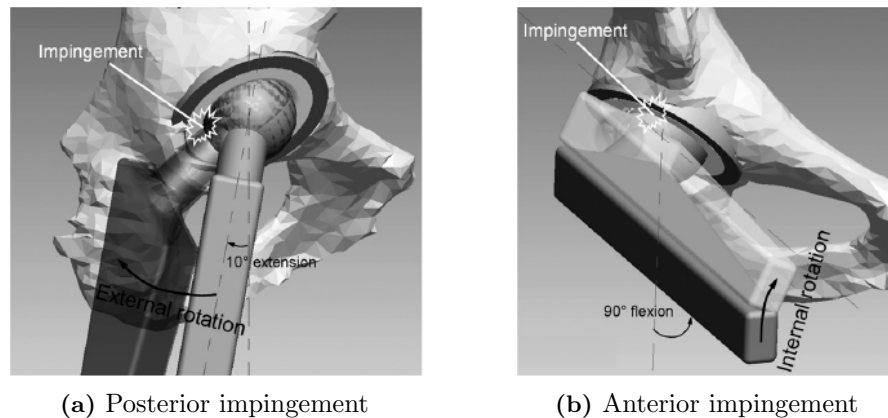


Figure 1.1: Example of component-on-component impingement (Kluess et al., 2007).

the neck of the femoral component contacts with the rim of the acetabular cup, shown in Figure 1.1. Further motion beyond the impingement point leads to subluxation of the femoral head until the joint dislocates (Kluess et al., 2007; Malik et al., 2007; Nadzadi et al., 2003). Therefore, improved range of motion to impingement is directly correlated to improved resistance to dislocation and wear (Nadzadi et al., 2002). The impingement free range of motion of a prosthetic component is set on implantation and is dependent upon both implant positioning and prosthetic design (Kluess et al., 2007). This has driven manufacturers to maximise range of motion and surgeons to orientate components in such a way to exploit this range of motion in areas where it has to be maximised physiologically (Kummer et al., 1999; Widmer and Zurfluh, 2004).

The need to be able to adjust prosthetic component orientation to maximise range of motion has resulted in a trend towards modular design solutions (Anderson et al., 2007). Modular designs have been well reported in being able to help reconstruct the femoral anatomy to aid joint stability and to maximise range of motion (Widmer and Majewski, 2005; Yoshimine, 2006). A recent development has been the introduction of femoral neck modularity. Modular necks provide the surgeon with the ability to independently adjust femoral neck length, femoral neck-shaft angle and the version angle of the femoral neck (Miki et al., 2009; Sakai et al., 2000; Toni et al., 2001). Initial clinical reports of femoral neck modularity have been positive. However, they have been limited by two factors.

Firstly, the impingement free range of motion requirement is not well understood and secondly these reports have lacked a comparison against an established hip replacement implant which does not have a modular femoral neck.

Determining the boundary within which an impingement free range of motion is required would allow surgeons to assess the operative procedure (Thornberry and Hogan, 2009). At present, specifications for range of motion outcome post-THA has been based on limits of pure joint motion in each of the anatomical planes (D'Lima et al., 2000; Seki et al., 1998; Widmer and Zurfluh, 2004; Yoshimine, 2005), or from measuring joint rotations for specific activities of daily living (Hemmerich et al., 2006; Johnston and Smidt, 1970; Ko and Yoon, 2008; Nadzadi et al., 2003). Only one study has attempted to graphically represent a range of motion boundary as a continuum (Thornberry and Hogan, 2009). The purpose of this study is to determine a representation of the required range of motion which surgeons can use to assess operative success and to use this representation to assess the effectiveness of femoral neck modularity with regard to its resistance to dislocation against a non-modular control.

1.2 Research scope

The scope of this research is focussed upon total hip arthroplasty and determining the required operative parameters to achieve a successful outcome for the patient. The research question and objectives for this study have been detailed.

“How can range of motion be graphically represented and modelled physiologically to assess resistance to dislocation in total hip arthroplasty?”

- To establish a prosthetic range of motion benchmark for total hip replacement.
- To graphically represent the range of motion benchmark to assess risk of dislocation.
- To provide an assessment of post-operative outcome using the range of motion benchmark.
- To assess the effectiveness of femoral neck modularity in limiting prosthetic impingement.
- To evaluate the effectiveness of graphically representing hip joint range of motion in the assessment of operative outcome.

It is hypothesised that being able to represent range of motion as a continuum will successfully identify how likely a patient is to impinge and therefore dislocate post-operatively. This is achieved by providing a comparison of the benchmark requirement with a patient’s post-operative prosthetic range of motion. Such a comparison will allow the effectiveness of femoral neck modularity in limiting prosthetic impingement to be evaluated. Before the research question and objectives can be answered, the threshold of current knowledge with regard to hip joint range of motion has to be established. Further, current knowledge from previous studies which have assessed the effectiveness of femoral neck modularity needs to be presented. This theoretical foundation is presented in the form of a review of the literature in chapter 2.

1.3 Outline of EngD portfolio

The research summarised in this innovation report has been compiled from a series of portfolio submissions which demonstrate how the research has developed so that it has been able to answer the research question and objectives presented in section 1.2. The overview of the portfolio submissions and how they fit into the context of the innovation report is shown in Figure 1.2. The research was originally focussed upon orthopaedic procedures in general rather than specifically the hip joint. EngD submission one, details the biomechanical principles of joint articulation which can be generalised to all joints. This work provided the biomechanical foundations which underpins this research. Following completion of this initial portfolio submission, the gaps in knowledge were reviewed and the application of the research was focussed to the hip joint. The second submission dealt specifically with the hip joint and analysed three specific factors - biomechanics of hip joint motion, the biomechanics of total hip arthroplasty and developing a range of motion benchmark requirement. Research relating to the first two factors have been summarised within chapter 2. Research associated with the development of the range of motion benchmark provided the foundation for the work presented in chapter 4.

The development of the range of motion benchmark and its graphical representation was the focus of the third portfolio submission and was the main innovation contained within this study. The fourth portfolio submission presented the application of the innovation where the graphical representation of the range of motion benchmark was used to assess the effectiveness of femoral neck modularity. This was achieved with the incorporation of a surgical navigation measurement device which allowed prosthetic range of motion to be directly compared against the developed range of motion benchmark. This work is presented in chapter 5. The application area for the innovation was chosen in consultation with the Coventry and Warwickshire NHS Trust which is specialised in undertaking randomised controlled trials. Consequently, femoral neck modularity was chosen as the application area, as one of its most significant success factors is range of motion. The results of this randomised controlled trial is presented in chapter 6. The analysis of the results for the

randomised controlled trial allowed for further innovation in the form of a medical device to prevent prosthetic dislocation which was presented in the final portfolio submission and summarised in chapter 7. The development of this medical device represented the completion of this study which went from understanding the biomechanics of human movement, applying it to the hip joint to understand a real clinical problem and finally providing a solution to address this problem.

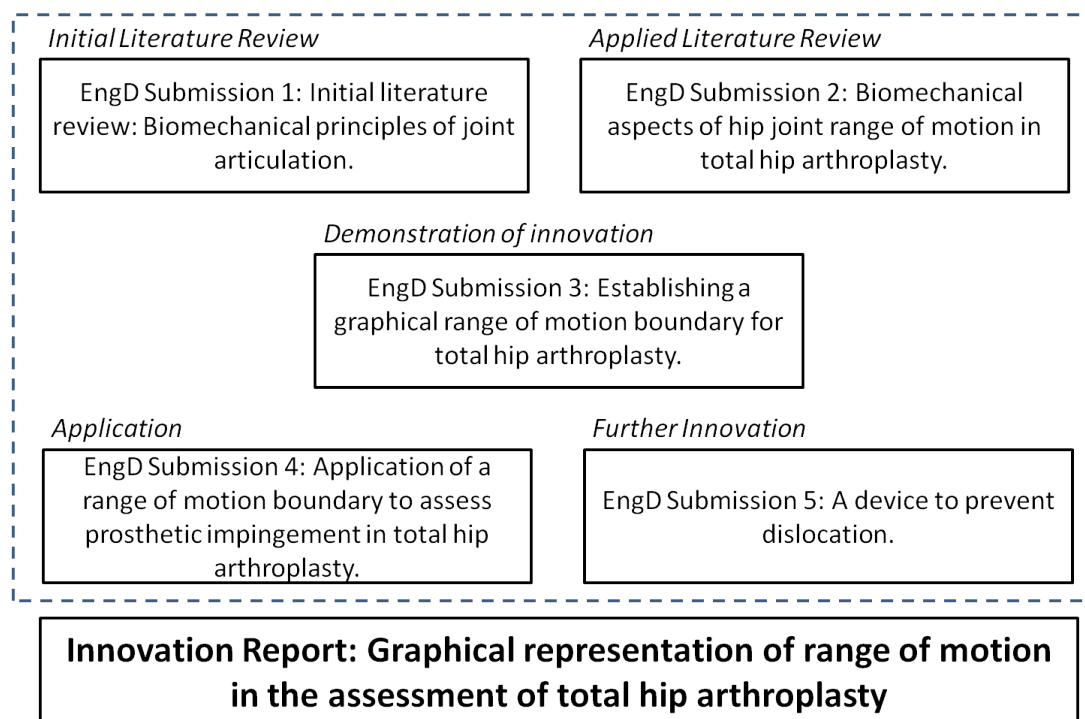


Figure 1.2: Structure of EngD portfolio.

1.4 Outline of innovation report

The structure of this innovation report has been shown in Figure 1.3. Following, a brief description of each of the chapters has been provided to give a general outline to this study.

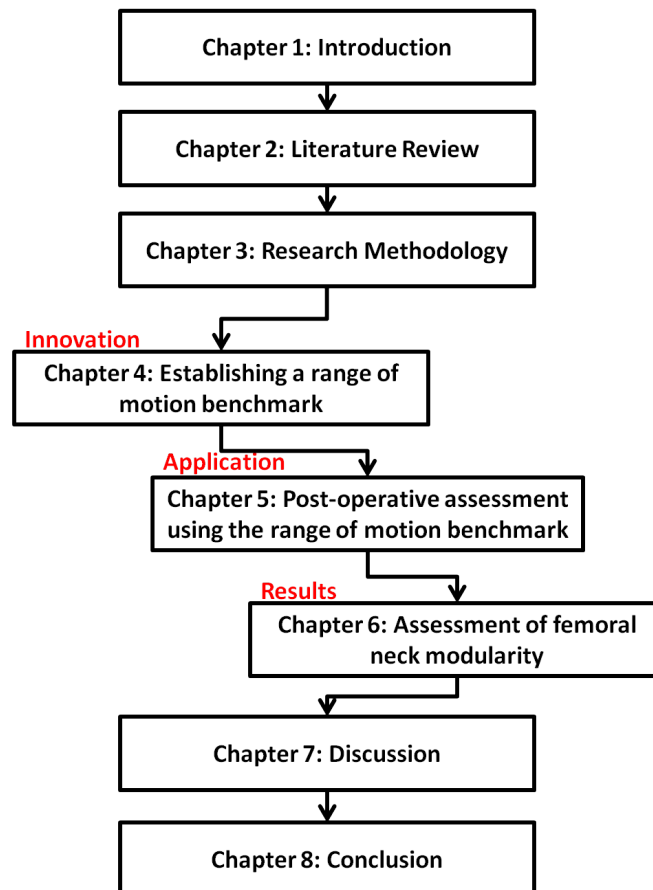


Figure 1.3: Structure of innovation report.

Chapter 1: Introduction - The introduction chapter has presented the background to the research problem and presented a research question and objectives aimed at addressing this research problem.

Chapter 2: Literature review - The literature review details the background information required to be critiqued in order to provide a theoretical foundation from which to base the study. Literature has been separated into the following themes - principles of human movement, hip joint biomechanics, total hip arthroplasty and femoral neck modularity.

Chapter 3: Research methodology - This chapter will use the theoretical foundation to analyse the requirements of each of the research objectives presented in section 1.2. The requirements of these objectives will be used to select an appropriate research design to generate innovation and apply it to meet the aims of the research.

Chapter 4: Establishing a range of motion benchmark - This chapter will present the findings of a systematic review methodology to determine the required range of motion to be achieved by a patient post-THA. This data is used to construct a graphical representation of the hip joint range of motion benchmark.

Chapter 5: Implementing the range of motion benchmark - In this chapter the methodology used to develop the graphical representation of the hip joint range of motion benchmark is used to provide an assessment of patient prosthetic range of motion. The benchmark and prosthetic representations are compared to provide an assessment of operative outcome.

Chapter 6: Assessment of femoral neck modularity - In this chapter the results of a randomised controlled trial to assess the effectiveness of femoral neck modularity will be presented. The results of the clinical trial are also used to evaluate the effectiveness of graphically representing hip joint range of motion in the assessment of operative outcome.

Chapter 7: Discussion - This chapter will bring together all the themes of the research and discuss the extent to which the research objectives have been met and whether the research question has been answered. The level of innovation generated by the research and its application will also be analysed along with evidence of further work.

Chapter 8: Conclusion - This chapter will finalise the research by highlighting its key findings, its implications and in conclusion provide a final summary for this study.

Chapter 2

Literature Review

2.1 Introduction

The aim of this chapter is to review the key subject areas with regard to modelling hip joint range of motion, total hip arthroplasty (THA) and femoral neck modularity. Research into these subject areas will provide the threshold of current knowledge in relation to the research question and objectives that were outlined in chapter 1. The main findings and gaps in knowledge gained from reviewing the literature are presented in section 2.7. These main findings will be used to select an appropriate research design in chapter 3 to address each of the research objectives to allow detailed theory to be developed building upon the theoretical foundation established in this chapter.

2.2 Principles of human movement

Biomechanics is a multidisciplinary speciality. In orthopaedics, it influences the prevention, diagnosis and treatment of most musculoskeletal injuries and diseases (Brinckmann et al., 2002). Biomechanics utilises and applies the principles of mechanics to biological problems to allow description of human movement. Therefore, understanding the biomechanics of the hip joint is critical to be able to answer the research question and objectives.

In biomechanics, it is important that motion and orientation are expressed in clinical terms to ensure meaningful comprehension by the healthcare community. This requires relating findings and expressing them in an anatomical coordinate frame, consisting of three mutually perpendicular cardinal planes (coronal, sagittal and transverse). The subject is considered to be in the neutral posture when they are upright and erect on both legs with arms to the side (Amadi et al., 2008; Brinckmann et al., 2002). Biomechanical assessment of motion uses the principles of rigid-body mechanics, which regards the distances between points on a moving segment to be invariant (Woltring, 1991). A common exception to this rule is skin movement, which is considered non-rigid (Andriacchi et al., 1998; Ehrig et al., 2006). A rigid-body has six degrees of freedom, with three translational and three rotational degrees of freedom which are used to describe the location and orientation of a body segment (Andrews, 1984). Using the illustration in Figure 2.1, translations occur along the coronal, sagittal and transverse planes and rotations occur in the coronal (abduction/adduction), sagittal (flexion/extension) and transverse (internal/external rotation) planes (Brinckmann et al., 2002).

Further definition of the anatomical coordinate frame can be described in terms of the reference axes (x, y, z). For the purposes of integration with the Computer Aided Surgery (CAS) and Computer Aided Design (CAD) packages used in this study. The anatomical axis definition detailed on page 11 will be used. The anatomical planes, axis definitions and clinical rotations that have been described in this section will be applied consistently.

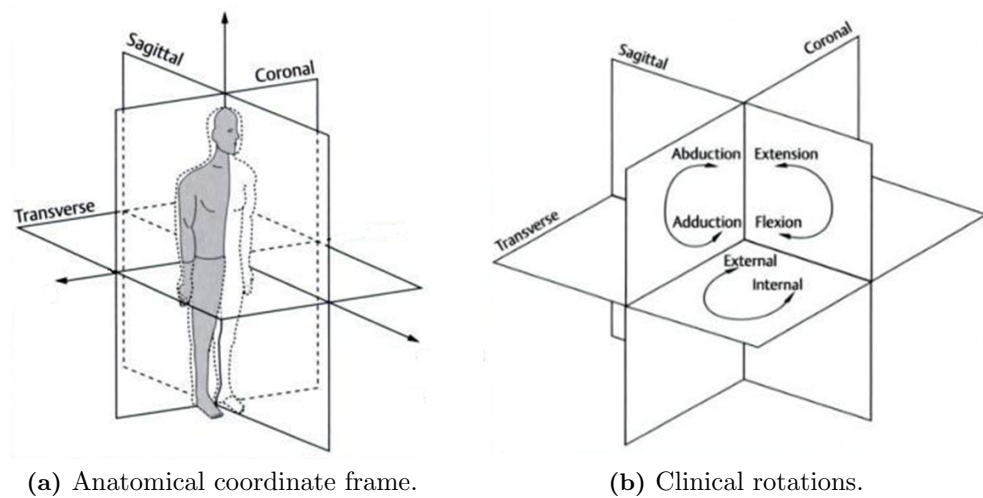


Figure 2.1: The anatomical coordinate frame (Brinckmann et al., 2002).

In orthopaedics, the relative position of one body segment to another is of critical importance to ascertain joint characteristics (Wu and Cavanagh, 1995). In the musculoskeletal system there are seven joints which are commonly modelled and analysed - Elbow, Foot & Ankle, Hip, Knee, Shoulder, Spine and Wrist & Hand (Nordin and Frankel, 2001; Wu et al., 2002, 2005). To be able to describe joint characteristics, a number of coordinate frames have to be used. Broadly, these coordinate systems can be designated into two distinct classes. Body segment coordinate frames which refer to the local coordinate system of a particular bone and the joint coordinate system which is used to define the relationship between two body segments of a joint, for example the pelvis and femur which are the mating bones within the hip joint (Wu et al., 2002). The relative position between the pelvis and femur are expressed within a hip joint coordinate frame. The biomechanics of the hip joint are explained in the following section.

- X-Axis: Medial/Lateral (Inboard to Outboard).
- Y-Axis: Anterior/Posterior (Front to Rear).
- Z-Axis: Superior/Inferior (Head to Toe).

2.3 Biomechanics of the hip joint

This section will outline how the motion of the hip joint is expressed. Firstly, the pelvic and femoral body segment coordinate frames will be introduced. This will be followed by how these body segments are aligned in a hip joint coordinate frame to express joint articulation.

2.3.1 Body segment coordinate frames

To describe the motion of a bone, a Cartesian coordinate frame is established using palpable bony landmarks. Its position and orientation can then be expressed relative to a global coordinate frame (Ehrig et al., 2006; Holt et al., 2005; Morrison, 1970). A minimum of three non-collinear points or landmarks are necessary to define a body segment coordinate frame (Sommer 3rd et al., 1982; Stökdijk et al., 2000). A total of seven landmarks are used to define the body segment coordinate frames of the pelvis and femur. These landmarks are shown in Figure 2.2, and for the pelvis are as follows - hip joint centre, left and right anterior superior iliac spines (ASIS) and the left and right posterior superior iliac spines (PSIS). For the femur the landmarks of the hip joint centre and the medial and lateral epicondyles are used (Wu et al., 2002).

In gait analysis, there are only a limited number of palpable landmarks which can be used to establish a body segment coordinate frame. The femur only has two points that can be measured in a standardised way, the lateral and medial epicondyles. A third point, the hip joint centre is required to be estimated (Kirkwood et al., 1999; Stökdijk et al., 2000). This landmark is modelled as a single kinematic rotation point, whose position is equivalent to the geometric centre of the femoral head (Camomilla et al., 2006; Veeger, 2000). This means that the rotation centre is fixed over the entire range of motion of the hip joint. Consequently, as the origin of the hip joint coordinate frame is located at the centre of the hip, there are no translational effects within the joint and only the rotational motions of flexion/extension, abduction/adduction and internal/external rotation are modelled, as

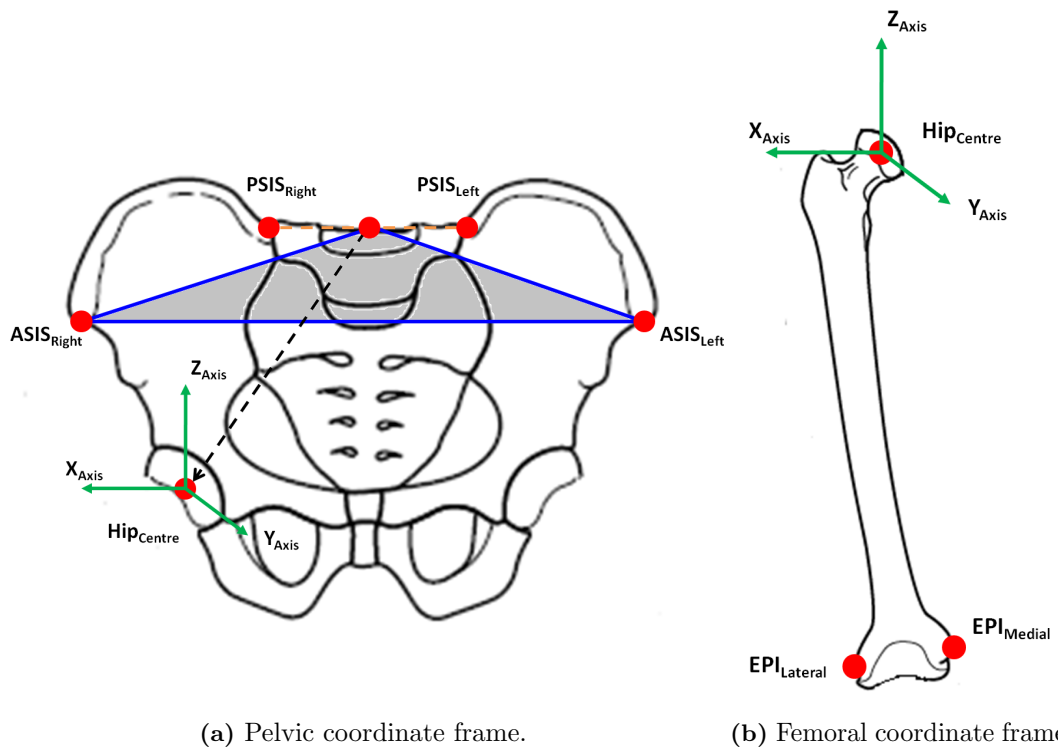


Figure 2.2: Body segment coordinate frames of the hip joint (Wu et al., 2002).

shown in Figure 2.3. This modelling assumption has been tested with a similar ‘ball and socket’ joint, the shoulder, which has the largest range of motion. It was found that between 1-5mm of translation can occur within the joint over the entire range of motion. This is considered negligible and perfect ‘ball and socket’ behaviour can be assumed (Monnet et al., 2007; Stökdijk et al., 2000; Veeger, 2000). Hip joint prostheses are manufactured to be spherical and therefore exhibit this perfect ‘ball and socket’ behaviour, providing there is enough tension in the soft tissue structures and the femoral neck does not impinge against the rim of the pelvic acetabular cup (Klues et al., 2007; Kummer et al., 1999; Nadzadi et al., 2003).

To establish the pelvic coordinate frame, the landmarks shown in Figure 2.2a are required to be palpated or measured to determine their position within three dimensional space. The medial-lateral axis of the pelvic coordinate frame is defined as a line running parallel with the two ASIS running in the positive direction from left to right, originated at the

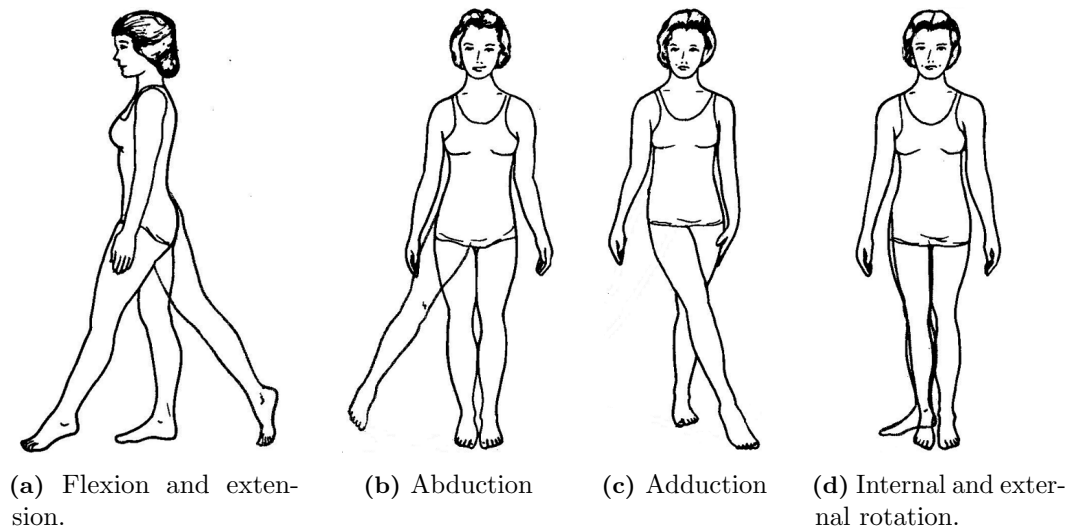


Figure 2.3: Motion of the hip joint (Luttgens and Wells, 1982).

hip joint centre. The Transverse Pelvic Plane (TPP) - shown in grey in Figure 2.2a - is defined as the plane containing the two ASIS and the mid-point of the two PSIS. A line perpendicular to the TPP originated at the hip joint centre defines the superior-inferior direction. Finally, the anterior-posterior axis is constructed orthogonal to the other two axes (Wu et al., 2002).

The landmarks required to establish the femoral coordinate frame are shown in Figure 2.2b. The superior-inferior or mechanical axis is defined as a line running in the positive direction from the knee centre to the hip joint centre. The knee centre is defined by the mid-point of the two femoral epicondyles. Next the coronal plane is defined, which contains the hip joint centre and the medial and lateral femoral epicondyles. The anterior-posterior axis is constructed perpendicular to the coronal plane located at the hip joint centre. The medial-lateral axis is constructed orthogonal to the other two axes (Wu et al., 2002).

Once the pelvic and femoral body segment coordinate frames have been established, their relative motion can be described. However, the body segment coordinate frames of the pelvis and femur may not be aligned. Therefore, axes have to be selected in order to describe the motion of the hip joint. This is presented in the following section.

2.3.2 Joint coordinate frame

It has been established that the three-dimensional location of a body segment can be modelled by knowing the local and global coordinates of three or more landmarks (Carman and Milburn, 2006). This now has to be applied to describe the motion of the hip joint, which means that the clinical rotations shown in Figure 2.3 have to be expressed according to the anatomical planes shown in Figure 2.1. There have been a number of joint coordinate systems that aim to model this behaviour, with significant ones being proposed by Cheng et al. (2000), Grood and Suntay (1983) and Woltring (1994). The International Society of Biomechanics (ISB) recommends the approach of Grood and Suntay (1983) and has applied this methodology beyond its original application to the seven joints of the human body (Wu et al., 2002, 2005). This approach has been used in many studies, as revealed by the systematic search of the literature presented in chapter 4. Therefore, the Grood and Suntay (1983) joint coordinate method will be described in this section. Further, all joint motions of flexion/extension, abduction/adduction and internal/external rotation reported will be aligned to this method of reporting joint rotations.

Referring to Figure 2.1a, when the body is posed in the neutral standing posture although they share a common origin the coordinate frames of the pelvis and femur may not be aligned. Therefore, from these six axes a meaningful joint coordinate frame has to be derived. Taking first the femur, based on the interpretation of Wu et al. (2002), internal/external rotation of the femur is of clinical importance. Therefore, the superior-inferior z-axis of the femur is termed the 'body fixed' axis of the femur. Next considering the pelvis, the flexion/extension of the femur about the hip joint centre is of clinical importance. Consequently, the medial-lateral x-axis is selected to be the 'body fixed' axis of the pelvis. Now that two axes have been defined a third axes can be derived from the vector cross-product of these axes, which forms an axis perpendicular to the two 'body fixed' axes (Grood and Suntay, 1983). This is termed the 'floating axis' and rotation about this axis is allied with the clinical rotation of abduction/adduction.

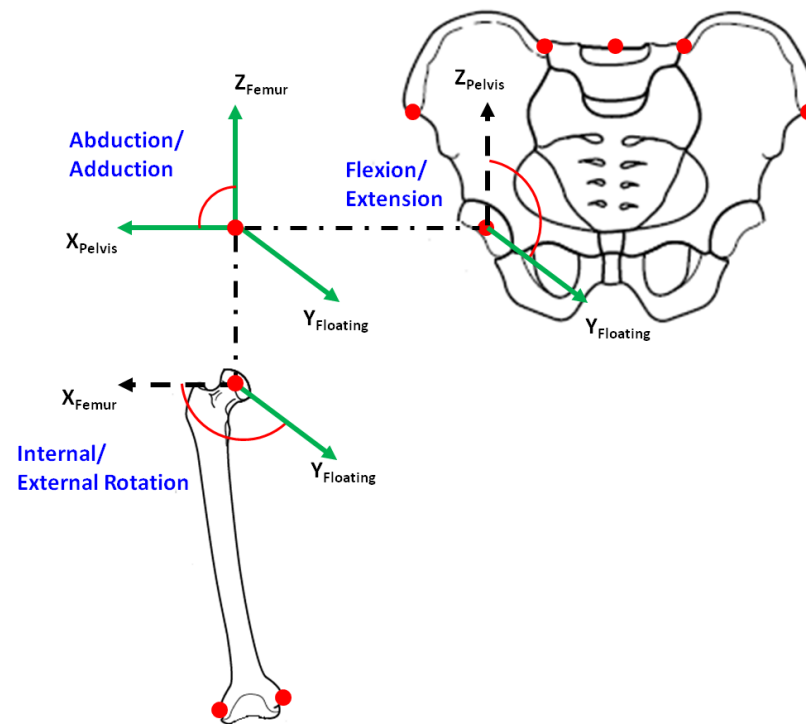


Figure 2.4: Hip joint coordinate system *adapted from* Grood and Suntay (1983).

The clinical rotations of flexion/extension, abduction/adduction and internal/external rotation occur about each of the three axes of the joint coordinate system described and presented in Figure 2.4. As the hip joint flexes or extends the orientation of the ‘floating axis’ changes as the relationship between the two ‘body fixed’ axes alters. Therefore, the amount of flexion/extension (f) can be determined as the angle between the ‘floating axis’ and the pelvic z -axis. Similarly, internal/external rotation (r) can be visualised as the angle between ‘floating axis’ and the femoral x -axis. This means that abduction/adduction (a) can be found through the relationship between the two ‘body fixed’ axes.

To be able to describe joint motion mathematically, the position of the inferior body segment has to be expressed in the coordinate frame of the superior body segment, to achieve a common coordinate expression (Grood and Suntay, 1983). As well as determining the axes of the joint coordinate system, the sequence in which the clinical rotations are applied is of critical importance. This is because while any desired orientation can be achieved by performing rotations about three axes in sequence (Brinckmann et al., 2002). The word

sequence is vital to note because matrix multiplication is non-commutative which means that $R_{x-axis} \cdot R_{y-axis} \neq R_{y-axis} \cdot R_{x-axis}$. Therefore, any orientation is dependent upon the order in which the rotations are applied (Heard, 2005; Woltring, 1991). Consequently, Grood and Suntay (1983) proposed a strict temporal order in which rotations occur. There has been concern regarding this sequence (Baker, 2001, 2003). However, many studies use this approach when reporting motion data. Therefore, determining the amount of hip joint motion using this convention will be explained.

- First rotation: flexion/extension (f) about the pelvic x-axis.
- Second rotation: abduction/adduction (a) about the ‘floating axis’
- Third rotation: internal/external rotation (r) about the femoral z-axis.

A rotation θ about a reference axis can be represented in the form of a component rotation matrix. These component rotations matrices have been shown in equation 2.1 for the motions of flexion/extension, abduction/adduction and internal/external rotation. Euler’s theorem states that *“two component rotations about different axes passing through a point are equivalent to a single rotation about an axis passing through a point”* (Hibbeler, 2009). This means that these component rotation matrices can be merged to create a composite rotation matrix. This composite matrix is formed by multiplying the component rotations in sequence, equation 2.2 (Brinckmann et al., 2002). The resulting rotation matrix is shown in equation 2.3 (Spring, 1986). If the composite rotation matrix takes the form presented in equation 2.4. Then the constituent joint angles can be calculated, as shown in equation 2.5.

$$R_x = \begin{bmatrix} 1 & 0 & 0 \\ 0 & \cos f & -\sin f \\ 0 & \sin f & \cos f \end{bmatrix}, R_y = \begin{bmatrix} \cos a & 0 & \sin a \\ 0 & 1 & 0 \\ -\sin a & 0 & \cos a \end{bmatrix}, R_z = \begin{bmatrix} \cos r & -\sin r & 0 \\ \sin r & \cos r & 0 \\ 0 & 0 & 1 \end{bmatrix} \quad (2.1)$$

$$\text{Composite rotation sequence} = \{[(R_x \cdot I)R_y]R_z\} \quad (2.2)$$

$$\begin{bmatrix} \cos r \cdot \cos a & -\sin r \cdot \cos a & \sin a \\ \sin r \cdot \cos f + \cos r \cdot \sin a \cdot \sin f & \cos r \cdot \cos f - \sin r \cdot \sin a \cdot \sin f & -\cos a \cdot \sin f \\ \sin r \cdot \sin f - \cos r \cdot \sin a \cdot \cos f & \cos r \cdot \sin f + \sin r \cdot \sin a \cdot \cos f & \cos a \cdot \cos f \end{bmatrix} \quad (2.3)$$

$$\begin{bmatrix} a_{11} & a_{12} & a_{13} \\ a_{21} & a_{22} & a_{23} \\ a_{31} & a_{32} & a_{33} \end{bmatrix} \quad (2.4)$$

$$\sin a = a_{13}, \quad \cos a = \begin{matrix} + \\ - \end{matrix} \sqrt{1 - (\sin a)^2}, \quad \cos a = \begin{cases} -\cos a, & \text{if } |\arccos(\cos a)| > \frac{\pi}{2}, \\ +\cos a, & \text{otherwise} \end{cases}$$

$$\cos r = \frac{a_{11}}{\cos a}, \quad \sin r = \frac{-a_{12}}{\cos a}, \quad \cos f = \frac{a_{33}}{\cos a}, \quad \sin f = \frac{-a_{23}}{\cos a}$$

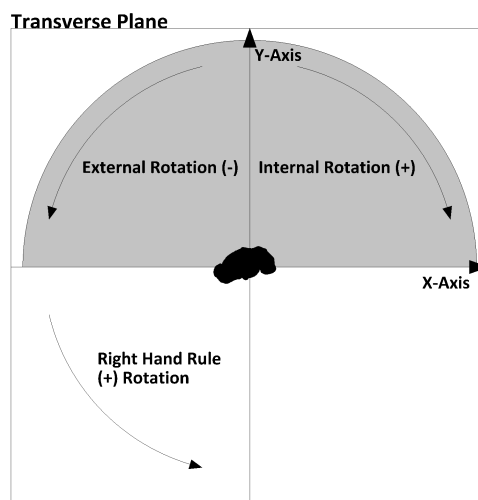
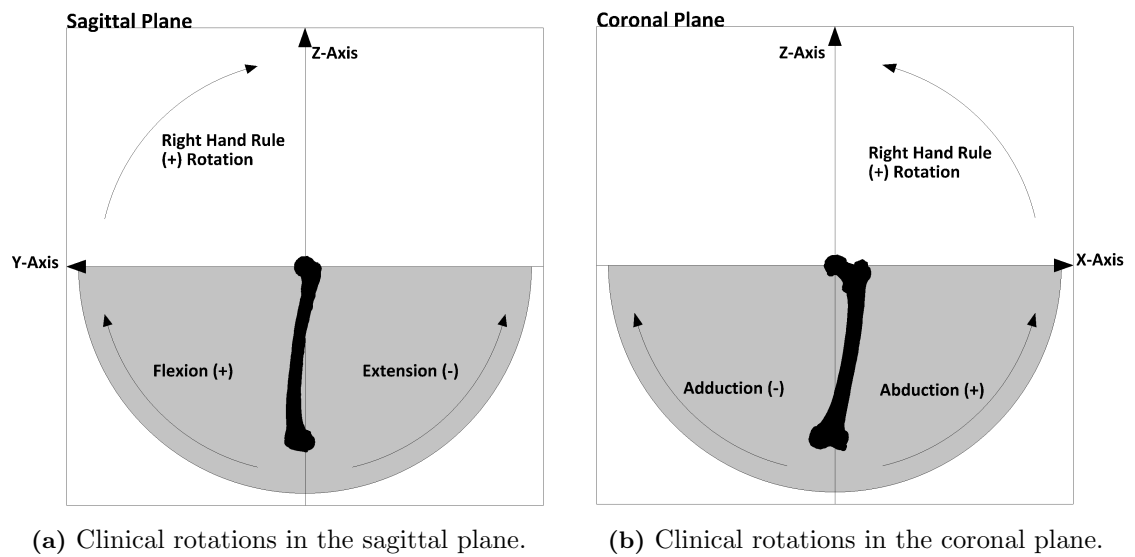
$$\text{flexion/extension} = \text{atan2}(\cos f, \sin f) \quad (2.5)$$

$$\text{abduction/adduction} = \text{atan2}(\cos a, \sin a)$$

$$\text{internal/external rotation} = \text{atan2}(\cos r, \sin r) - 1$$

There are a number of points that need to be noted when considering equations 2.1-2.5. Firstly, the component rotation matrices shown in equation 2.1 and thus the subsequent composite matrix in equation 2.3 are point rotation matrices (Kuipers, 1999). There are two types of rotation matrix - point and frame. A point rotation matrix considers the coordinate frame fixed while points rotate about it. In a frame rotation the relationship is reversed. Therefore, a coordinate frame rotation through angle θ about an axis is exactly the same as a point rotation about the same axis by $-\theta$ (Kuipers, 1999). Consequently, the two rotation perspectives have the same vector frame relationship. Point rotation has been considered in this section because the construction of the graphical representation of hip joint range of motion presented in chapters 4 and 5 requires this type of matrix in its construction.

The second item to note is the restriction with regard to $\cos a$. This is placed, due to Euler angles exhibiting a singularity when the hip joint approaches 90° abduction/adduction (Cappozzo et al., 2005). However, in the case of the hip joint, this position is not anatomically possible. Finally, equation 2.5 considers the joint angle calculations for a left hip joint. Figure 2.5, shows the clinical interpretation of rotations in each of the anatomical planes for the left hip joint (Brinckmann et al., 2002). Referring to Figure 2.5c, it is evident that the clinical interpretation of internal/external rotation defies the right-hand rule. Consequently, all reported internal/external rotation joint angles should be multiplied by a factor of -1 for a left hip joint. For a right hip joint all reported abduction/adduction joint angles should be multiplied by a factor of -1.



(c) Clinical rotations in the transverse plane.

Figure 2.5: Clinical rotations for the left hip joint.

2.3.3 Summary

In this section, the joint coordinate frame methodology developed by Grood and Suntay (1983) has been presented to explain hip joint motion. There are issues with regard to how mathematically representative this joint coordinate system is. This is because it does not satisfy the requirements of an ideal Cartesian coordinate frame, as it is not necessarily orthogonal. This makes it difficult to represent hip motion graphically. However, as Cappozzo et al. (2005) identifies, if the pelvic and femoral coordinate frames are aligned when the body is posed in the neutral standing posture, shown in Figure 2.1a. Then the ‘floating axis’ is congruent to the y-axis of the femur, resulting in an orthogonal joint coordinate frame. Further, if the neutral standing posture description provided by Luttgens and Wells (1982) is considered, when in the neutral position the knee centre should be directly below the hip joint centre. If the pelvis is considered fixed, then in this situation, the z-axis of the pelvis and femur will be aligned. This means that the vector cross product of the pelvic x-axis and femoral z-axis would produce a ‘floating axis’ in an orthogonal coordinate frame, although this axis may not be coincident with the femoral y-axis. Further consideration of these reference frames will be discussed in section 2.5. First the biomechanics of total hip arthroplasty are discussed.

2.4 Biomechanics of total hip arthroplasty

A successful THA normalises the biomechanics of the hip joint enabling a patient to regain mobility without pain or discomfort (Sakai et al., 2000). Normalisation of hip joint biomechanics is dependent upon achieving joint stability and the ideal range of motion to be able to fulfil daily activities (Duwelius et al., 2010). To achieve joint stability, the surgeon is required to make appropriate adjustments to the femoral neck-shaft angle, femoral offset, femoral version, pelvic hip centre position and femoral head coverage (Duwelius et al., 2010; Malik et al., 2007; Sakai et al., 2002; Traina et al., 2009b). Post-operative range of motion is dependent upon the positioning of the prosthetic components, in particular, the inclination of the acetabular cup and the combined version of the pelvic acetabular cup with the neck of the femoral component (Sakai et al., 2002; Yoshimine, 2006). Consequently, there is a trade off between stability and impingement with regard to prosthetic component orientation (Widmer, 2007).

Mal-orientation of prosthetic components has been reported to be a cause for post-operative instability and dislocation (Barsoum et al., 2007). Malchau et al. (2011) analysed the acetabular cup inclination and anteversion measurements of 1,954 THA procedures. It was found that only 47% of patients had a cup orientation within both the ideal defined cup inclination and anteversion limits. As well as positioning, design factors such as head-neck ratio, cup-opening plane and neck-shaft angle also influence the post-operative range of motion (Widmer and Zurfluh, 2004). These design factors determine the amount of movement a THA can achieve which can be calculated using equation 2.6 where A is the opening angle of the acetabular cup, n is the thickness of the femoral neck and r is the radius of the femoral head (Yoshimine and Ginbayashi, 2002). This total movement has been termed as the oscillation angle (θ). However, it should be noted that the oscillation angle as described by equation 2.6 only calculates the amount of movement an implant can achieve if the geometry of the femoral neck is cylindrical, which is uncommon. Consequently, more involved calculations are required to determine the oscillation angle of implants with a non-axis symmetric femoral neck (Nikou et al., 1998). The oscillation angle is one of five factors

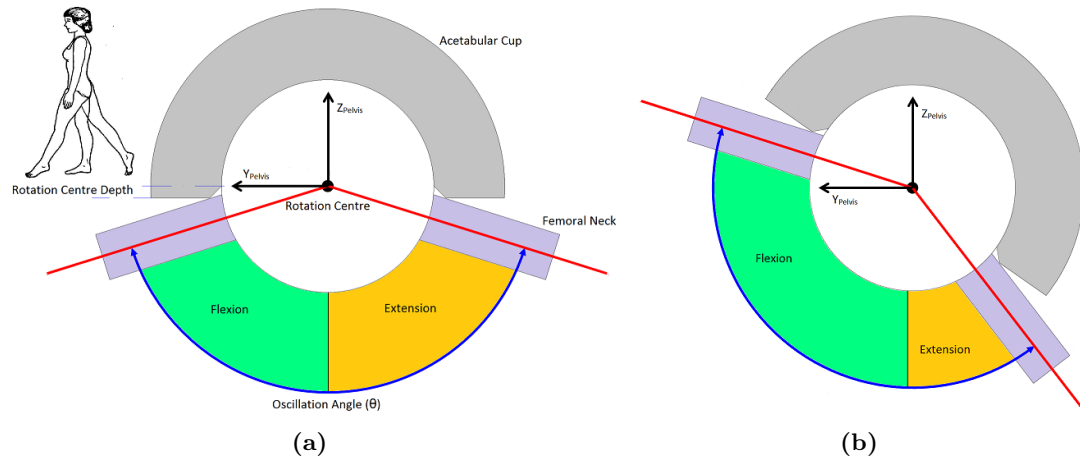


Figure 2.6: Effect of component orientation on range of motion.

which can influence range of motion (Yoshimine and Ginbayashi, 2002). The other four factors combine to influence the relative amounts of flexion/extension, abduction/adduction and internal/external rotation that can be achieved within the impingement limits set by the oscillation angle (θ) (DiGioia et al., 1998; Jaramaz et al., 1997; Ko and Yoon, 2008; Yoshimine and Ginbayashi, 2002). The change in the relative amount of joint motion is illustrated in Figure 2.6 for the motion of flexion/extension in the sagittal plane. The other four factors are **(1)** the inclination of the acetabular cup (α) **(2)** the anteversion of the acetabular cup (β) **(3)** the angle between the femoral neck and the transverse plane (a) and **(4)** the version angle of the femoral neck (b). Surgeons have to ensure that the relative orientations of the acetabular and femoral components are positioned in such a way that the required physiological range of motion is impingement free (Barsoum et al., 2007; Widmer, 2007). This is achieved by attaining a prosthetic range of motion larger than the necessary physiological range of motion (Ko and Yoon, 2008; Miki et al., 2007; Nadzadi et al., 2003). This section provides an overview of the geometrical aspects which influence post-operative range of motion. Section 2.4.1 will cover the acetabular cup and section 2.4.2 the femoral stem.

$$\theta = A - \sin^{-1} \left(\frac{n/2}{r} \right) \quad (2.6)$$

2.4.1 Acetabular cup

The orientation of the acetabular cup determines the boundary within which the femoral neck can move freely. Acetabular cup orientation is defined by the angle of its opening plane with respect to the pelvic coordinate frame, expressed by its angle of inclination (α) and anteversion (β) (Murray, 1993). However, there are three different conventions with regard to acetabular cup inclination and anteversion in standard use - anatomical, operative and radiographic - these have been illustrated in Figure 2.7 (Murray, 1993; Jaramaz et al., 1998; Wolf et al., 2005).

The difference between acetabular cup orientation convention is based upon the axis from which the angle of anteversion is measured (Murray, 1993). It is important to note that this difference, if the same inclination and anteversion angles were quoted for each of the conventions, would result in different spatial orientations. This requires nonograms to be used to convert between these conventions (Murray, 1993; Yoon et al., 2008). The conventions are applied in different areas of the treatment process. The radiographic method is used in the measurement of cup orientation using two-dimensional planer x-rays. The operative approach is associated with the mechanical guides that are used to align the acetabular cup during surgery and the anatomical definition is used when measuring cup orientation using three-dimensional medical images (DiGioia et al., 2002).

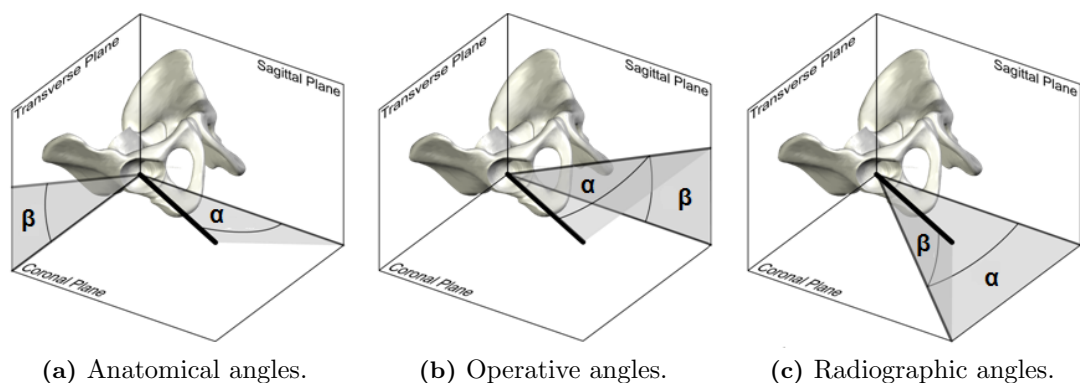


Figure 2.7: Illustration of acetabular cup orientation conventions *adapted from Murray (1993)*.

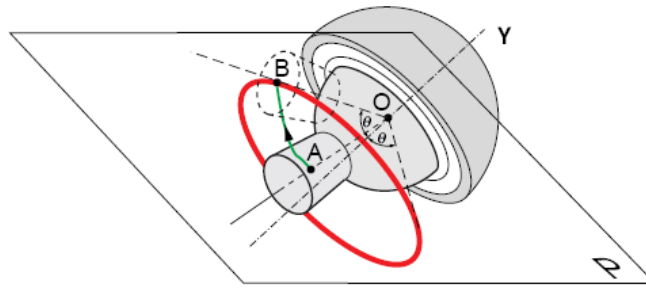


Figure 2.8: Acetabular cup impingement limits (Jaramaz et al., 1997).

Once the acetabular component has been fitted into position, the limits of impingement are fixed. These limits are set by the rim of the acetabular cup. The femoral neck is able to move freely within these limits, as shown in Figure 2.8. Acetabular cup orientation is one of the major factors affecting dislocation (Yoon et al., 2008). Many authors have presented figures for cup inclination and anteversion in which dislocation is minimised (Lewinnek et al., 1978; McCollum and Gray, 1990; Seki et al., 1998; Widmer and Zurfluh, 2004; Yoshimine, 2005). Yoon et al. (2008) compared these figures, by converting them all to the radiographic convention, and found on average these recommendations aim to place the acetabular component between 32-50° inclination and between 8-25° anteversion.

Due to a number of clinical reasons it may not be possible to place the acetabular cup in its desired orientation (Widmer, 2007). This is where the neutral position of the femoral neck becomes important. It determines the amount of flexion/extension, abduction/adduction and internal/external rotation that can take place within the impingement limits set by the acetabular cup. Therefore, to obtain a good THA outcome, the surgeon should consider not only the orientation of the acetabular cup but also the position of the femoral component (Barsoum et al., 2007; Tannast et al., 2005). Orientation of the femoral component is discussed in section 2.4.2.

2.4.2 Femoral stem

The relative amount of joint motion that can be achieved within the impingement limits of the acetabular cup is determined by the orientation of the femoral neck. Of importance is the location of the femoral neck in the neutral standing posture which determines the amount of flexion/extension, abduction/adduction and internal/external rotation before impingement. Two factors determine the neutral position of the femoral component - femoral neck angle from the transverse plane (*a*) and femoral neck anteversion (*b*) (Yoshimine and Ginbayashi, 2002). Femoral component orientation is shown in Figure 2.9 and it is described by the anatomical convention (Ko and Yoon, 2008; Yoshimine and Ginbayashi, 2002).

The femoral neck angle from the transverse plane (*a*) is governed by two factors, the implant neck-shaft angle and the stem varus-valgus orientation in the femoral canal. These factors alter the orientation of the neck relative to the impingement limits set by the acetabular cup, hence range of motion (Widmer and Majewski, 2005; Yoshimine, 2005). Femoral anteversion (*b*) is measured as an angle between two planes - the coronal plane and the plane of anteversion. The plane of anteversion is formed by the long axis of the femoral stem and the femoral neck axis (D'Lima et al., 2000; Murphy et al., 1987). Ideally, the reference planes of the pelvis and femur should be aligned so that measured acetabular cup and femoral stem orientation relate to allow subsequent inference with regard to range of motion.

There has been less written about the optimum positioning of the femoral component with regard to femoral version (*b*) and especially femoral neck axis away from the transverse plane (*a*) (Soong et al., 2004). This is because, pathologically, the position of the femoral stem is influenced by the geometry of the femoral canal and hence difficult for the surgeon to control (Malik et al., 2007). Recommended values for femoral version range between 0°-25° (Charnley, 1979; Harris, 1985; McCollum and Gray, 1990; Ritter, 1980; Sakai et al., 2000). Combined version values have been posed by adding recommended values of acetabular cup anteversion with those recommended for femoral version (Sakai et al., 2002; Soong et al., 2004). However, these can only be added if both acetabular cup and femoral stem

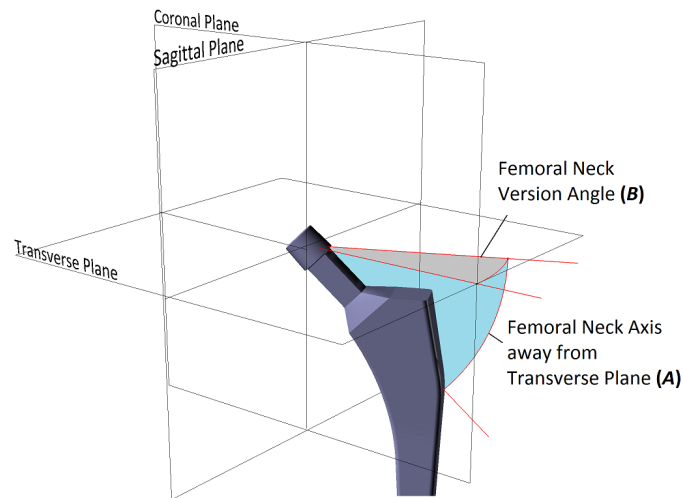


Figure 2.9: Femoral stem orientation *adapted from* Yoshimine and Ginbayashi (2002).

orientation are measured according to the same convention and their reference frames are aligned (Widmer, 2007; Yoon et al., 2008). Clinical recommendations for the amount of combined version range between 25° - 60° (Dorr et al., 2009; Jolles et al., 2002; Ranawat and Maynard, 1991; Sakai et al., 2002). This range reflects differences in subject anatomy which can vary considerably (Maruyama et al., 2001; Yoshioka and Cooke, 1987). However, these recommendations do not acknowledge inter-dependence with regard to acetabular inclination, oscillation angle, femoral stem varus-valgus and its neck-shaft angle. All of which, alter the combined version required to be attained to achieve the required anatomical range of motion (Widmer, 2007; Yoshimine, 2006).

2.4.3 Summary

It has been shown that there is a wide variation in the recommended values for component positioning in THA to avoid impingement and achieve a stable joint. However, discrete recommendations for individual acetabular cup and femoral anteversion values should only act as a guideline for component placement. Due to the inter-dependence of femoral and acetabular positioning, adjustments of one component position should be based on knowledge regarding the position of the other component (Dorr et al., 2009; Malik et al., 2007; Widmer, 2007). There are other influencing factors, such as femoral head-neck ratio, acetabular cup and femoral neck design and individual patient and group morphological conditions. Further, there has been difficulty relating surgical measurements of component orientation to post-operative range of motion. This has been due to an incongruity between the reference frames used in the surgical field and those which were presented in section 2.3, when discussing hip joint articulation measured by gait analysis. This will be discussed further in the following section.

2.5 Hip joint reference frames

In section 2.3, the reference frames used to describe hip joint motion were discussed. In section 2.4, the measurement of component orientation was presented. These measurements need to be based from anatomical references to be meaningful for the clinician and allow subsequent inference with regard to range of motion post-THA. This section will present the reference frames used in THA and comment on their alignment with regard to the reference frames presented earlier in this chapter in section 2.3.

2.5.1 Pelvic reference frame

The orientation and measurement of the acetabular cup is dependent upon the reference frame from which the surgeon bases their cup alignment or measurement (Nikou et al., 2000; Tannast et al., 2005). Therefore, as well as defining the convention used to measure the angle of inclination and anteversion of the acetabular cup. The reference frame that cup orientation is measured from needs to be considered. In clinical situations, the acetabular cup is usually measured from a pelvic coordinate frame based on the landmarks used to define the Anterior Pelvic Plane (APP), shown in Figure 2.10a (Dandachli et al., 2006). These landmarks are the left and right anterior superior iliac spines (ASIS) and the left and right pubic tubercles (PTUB). Consequently, it differs from the TPP pelvic coordinate frame used in the joint coordinate system presented in Figure 2.2a in section 2.3. The relationship between the APP and the TPP is not necessarily orthogonal (Dandachli et al., 2006; Miki et al., 2007). However, Dandachli et al. (2006), states that the relationship is almost perpendicular with an average difference of 104° between the two planes. Any deviation away from a 90° relationship creates ambiguity comparing prosthetic range of motion with the required physiological range of motion based on gait analysis studies.

The pelvic coordinate frame based on the landmarks of the APP is shown in Figure 2.10a. The origin of the pelvic reference frame is the hip joint centre and the medial-lateral x-axis is located at this origin running in the positive direction parallel to a line connecting the

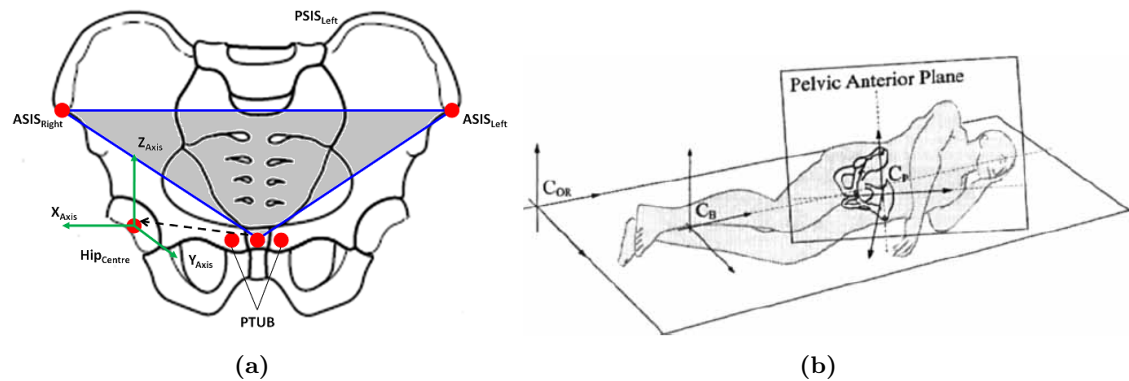


Figure 2.10: Clinical interpretation of the pelvic reference frame **(a)** The anterior pelvic plane (APP) and **(b)** Alignment of the APP with whole body (DiGioia et al., 1998).

left ASIS to the right ASIS. The APP is defined as the plane containing the two ASIS and the mid-point of the two PTUB. A line perpendicular to the APP originated at the hip joint centre defines the anterior-posterior y-axis. Finally, the superior-inferior z-axis is constructed orthogonal to the other two axes (Dandachli et al., 2006).

In conventional hip arthroplasty procedures, the mechanical guides that are used to position the prosthetic component assume that the patient's trunk and pelvis are aligned during surgery, Figure 2.10b (Najarian et al., 2009). McCollum and Gray (1990), claim that accurately aligning the pelvis with respect to the patient is an almost impossible task, leading to improper cup alignment. Interpretation of acetabular cup orientation with respect to the whole-body is only possible if additional information on the tilt, rotation and obliqueness of the patient's pelvis is known (Chen et al., 2006; Tannast et al., 2005; Wolf et al., 2005; Yoon et al., 2008). These angles can then be used to correct the misalignment, which is usually most significant with regard to pelvic tilt (Lembeck et al., 2005; Nishihara et al., 2003). However, when stood in the neutral standing posture, the pelvis according to the APP - may not be parallel or coincident with the whole body coordinate frame (Chen et al., 2006; Malik et al., 2007). Therefore, it is unclear whether this correction is required in order to determine the correct prosthetic range of motion post-THA.

2.5.2 Femoral reference frame

Femoral version, in a joint coordinate frame is regarded to be the angle between the femoral neck axis and the coronal plane (Ko and Yoon, 2008; Seki et al., 1998; Yoshimine, 2006). Clinically, femoral version has been defined by both Murphy et al. (1987) and Yoshioka and Cooke (1987), with the later labelling their definition as functional anteversion. Similarly, both define femoral anteversion as the angle between the femoral neck axis and an axis defined by the inferior aspect of the femur translated to the centre of the knee. The difference relates to the landmarks from which this axis is constructed. Murphy et al. (1987), base their axis, termed the condylar axis, from the posterior aspect of the femoral condyles with Yoshioka and Cooke (1987) constructing their axis from the medial and lateral epicondyles, similar to the femoral coordinate frame in section 2.3.1. Figure 2.11, provides illustrations of both definitions. The definition provided by Murphy et al. (1987) is considered to define the neutral rotation of the femur, where the condylar plane is congruent to the coronal plane of the anatomical coordinate frame presented in Figure 2.1a. The condylar plane is defined by the posterior aspects of the femoral condyles and the long axis of the femur. Femoral anteversion (b) is then measured as the angle in the transverse plane between the condylar plane and the plane of anteversion. The plane of anteversion is defined by the femoral neck axis and the long axis of the femur (Murphy et al., 1987). Significantly, as the condylar plane is considered to define the neutral rotation of the femur. The Murphy et al. (1987) definition is aligned to the anatomical definition of anteversion shown Figure 2.9. This is because the neck axis of the femoral component is measured from the coronal plane, which the condylar plane defines (Ko and Yoon, 2008; Seki et al., 1998; Yoshimine, 2006).

The Yoshioka and Cooke (1987) definition of femoral anteversion would equate to the angle measured between the femoral neck axis and the coronal plane, if in the neutral position the transepicondylar axis lies in the coronal plane. However, as Yoshioka and Cooke (1987) noted the femur is naturally externally rotated. This is supported by Maruyama et al. (2001), who stated that in order to achieve the correct offset measurement from an

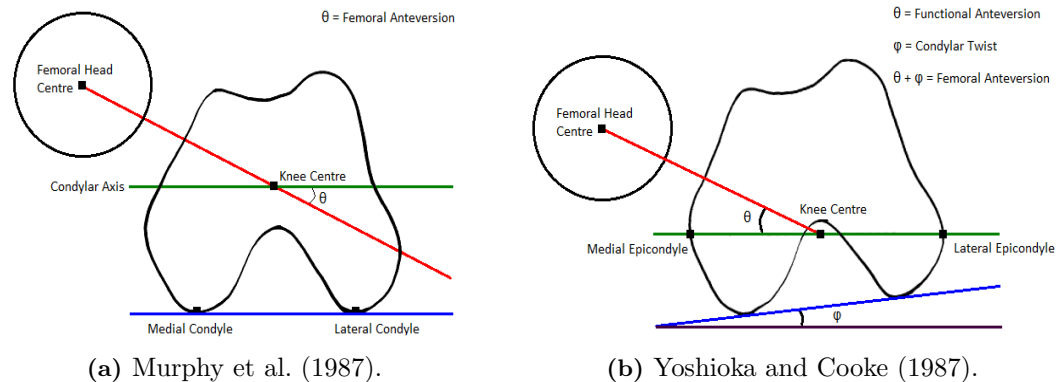


Figure 2.11: Illustration of femoral anteversion measurement conventions.

antero-posterior radiograph the femur is required to be internally rotated by the patient to bring the femoral neck axis in line with the coronal plane. Measurements by Yoshioka and Cooke (1987) have shown that on average the transepicondylar axis is externally rotated in comparison to the coronal plane by 5.6° ($\sigma = 2.2^\circ$), shown by the condylar twist angle in Figure 2.11b. Consequently, the body segment coordinate frame of the femur, presented in section 2.3.1, would not align with the pelvic reference frame in the anatomical neutral standing posture. Therefore, inferring post-operative range of motion based on the measurements of acetabular cup inclination (α), anteversion (β) and femoral neck axis away from the transverse plane (a) and version (b) would result in incorrect deductions due to the pelvic and femoral reference frames not being aligned.

Based on these findings, clinicians use the condylar axis to define the neutral rotation of the femur. Therefore, the posterior aspect of the femoral condyles are used instead of the femoral epicondyles as the basis from which to construct the femoral body segment coordinate frame. Where the superior-inferior z-axis is a line running in the positive direction from the knee centre to the hip joint centre. The knee centre is defined by the mid-point of the two femoral epicondyles. The coronal plane is defined as a plane containing the hip joint centre and a line parallel to the posterior aspect of the femoral condyles located at the knee centre. The anterior-posterior y-axis is constructed perpendicular to the coronal plane located at the hip joint centre. The medial-lateral axis is constructed orthogonal to the other two axes (Nikou et al., 2000). It is this reference frame that is

used to provide measurement with regard to femoral anteversion and neck axis away from the transverse plane. Further, motion analysis studies using Computer Tomography (CT) scans of the patient anatomy have used the pelvic and femoral coordinate frames described in this section as the basis of their analysis (Kubiak-Langer et al., 2007; Kurtz et al., 2010; Tannast et al., 2007, 2008). Therefore, there is a conflict between clinical measurement of prosthetic positioning and subsequent range of motion analysis with the standards proposed and used in gait analyses.

2.5.3 Summary

This section has discussed the reference frames that are used in THA to base measurement of acetabular cup and femoral stem orientation. It has been found that these reference frames differ from those which are used in gait analyses. The APP is used instead of the TPP in the pelvic coordinate frame and the posterior aspect of the femoral condyles rather than the femoral epicondyles in the femoral coordinate frame. It has been found that the posterior aspect of the femoral condyles define the neutral rotation of the femur. However, they are not directly palpable and can only be assessed via medical imaging. Consequently, a surrogate known as the figure-of-four axis is used in surgery to determine the neutral rotation of the femur (Mayr et al., 2007).

In the case of the posterior aspect of the femoral condyles being used to define the neutral rotation of the femur. The medial-lateral axes of both the femur and pelvis would be aligned. The medial-lateral axis of the pelvis is defined as running from the left ASIS to the right ASIS in both the APP and TPP conventions. This means that the remaining issue regarding pelvic and femoral reference frame congruence is alignment of the anterior-posterior and superior-inferior axes, which can be measured in the sagittal plane, known as pelvic tilt. The degree of tilt could depend on whether the APP or TPP pelvic reference frames are used. Lembeck et al. (2005) found an 8° forward tilt in the pelvic APP plane in comparison with the whole-body. While Dandachli et al. (2006) found that the relationship between the APP and TPP planes is not necessarily orthogonal.

The gait analysis methodology outlined in section 2.3 allows for a non-orthogonal reference frame, meaning the pelvic and femoral reference frames do not necessarily have to be aligned. This creates a problem with regard to inferring range of motion clinically based on the measurements of THA prosthetic positioning which require reference frames to be aligned. Consequently, any range of motion benchmark derived from gait analysis data needs to be validated for congruence with the clinical reference frames described in this section.

2.6 Femoral neck modularity

There has been a trend towards modular design solutions in the hip replacement market, giving the surgeon the versatility to adjust particular prosthetic options (Anderson et al., 2007). Traditionally, modularity has been associated with femoral prosthetic head offset and diameter and different neck offset and neck-shaft angle options (Toni et al., 2001; Traina et al., 2004). These have been well reported in being able to help reconstruct the femoral anatomy to aid joint stability and maximising the oscillation angle (Widmer and Majewski, 2005; Yoshimine, 2006). This section discusses a further evolution with regard to THA prosthetic modularity, a modular femoral neck.

2.6.1 Overview of neck modularity

Hip replacement procedures are classified into two distinct types cemented and uncemented procedures (National Joint Registry, 2011). In cemented procedures, the surgeon has the flexibility to adjust the orientation of the femoral stem. However, the options for the surgeon to control the degree of anteversion are more limited with uncemented procedures and are influenced by the geometry of the femoral canal (Malik et al., 2007). It has been proposed that greater control with regard to the orientation of the femoral component can be achieved with neck modularity (Sakai et al., 2000). Most non-modular femoral neck stems have only 10 options, in contrast to the 60 options that having a modular femoral neck provide (Duwelius et al., 2010). A schematic of the femoral neck options is shown in Figure 2.13.

It has been reported that modular femoral necks offer more options with regard to improving the head centre position and allows both pre-operative planning and independent intra-operative adjustment for offset and leg length to improve joint stability (Duwelius et al., 2010; Traina et al., 2009b). This is because in traditional non-modular neck stems, offset and neck length are directly proportional to the size of the femoral stem, as shown in Figure 2.14. Independent intra-operative adjustment has also been considered a solution

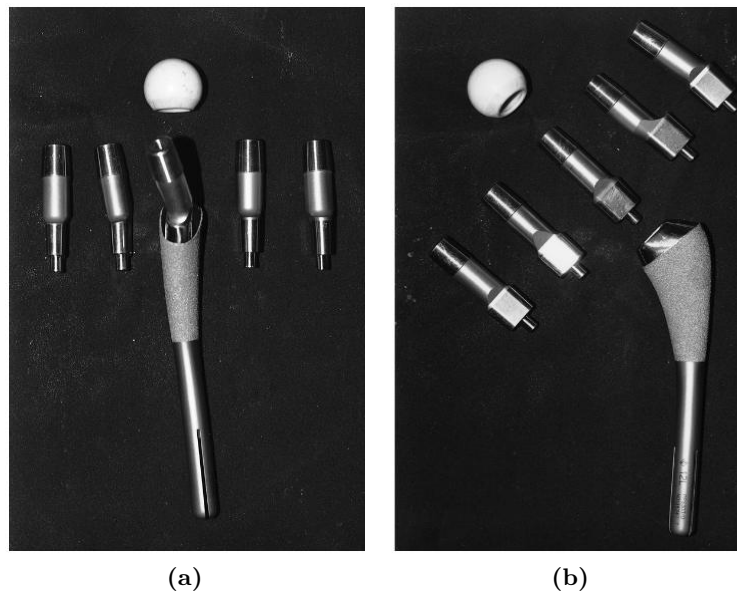


Figure 2.12: Femoral neck modularity (a) Lateral view of modular femoral neck system and (b) Antero-posterior view of modular femoral neck system (Sakai et al., 2000).

to prosthetic impingement by allowing adjustment of the femoral neck-shaft angle, but more significantly femoral neck version adjustment (Miki et al., 2009; Sakai et al., 2000; Toni et al., 2001; Widmer and Majewski, 2005). A modular neck allows adjustment of the femoral neck within the impingement limits set by the orientation of the acetabular cup, providing flexibility to move the range of motion that the THA can accept to a position where it enables a patient to fulfil their daily activities (Jaramaz et al., 1997; Ko and Yoon, 2008; Yoshimine, 2005). This is proposed to be beneficial in cases with normal and abnormal anatomy, such as development dysplasia of the hip (DDH), a major cause of secondary osteoarthritis (Miki et al., 2009; Toni et al., 2001). There have been a number of clinical and engineering assessments of modular femoral necks and these will be analysed in the following section.

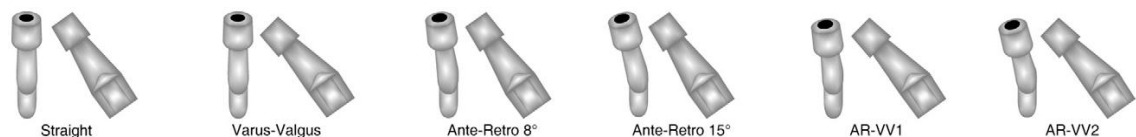


Figure 2.13: Modular femoral neck options: straight, varus-valgus 8° and 15° (not shown), ante-retroverted 8° and 15°, combination of ante-retroverted 4.5° with varus-valgus of 6° - AR-VV1 and AR-VV2 options (Traina et al., 2009a).

2.6.2 Previous studies

There have been a number of clinical (Duwelius et al., 2010; Sakai et al., 2002; Toni et al., 2001; Traina et al., 2004, 2009a, b, 2011) and engineering (Miki et al., 2009; Sakai et al., 2000) evaluations of modular femoral necks. Toni et al. (2001) evaluated 347 cementless arthroplasties mainly treating primary osteoarthritis or DDH. The study found 100% cup and stem stability and patients reported a considerable improvement in pain, walking and range of motion one year post-operation. In terms of neck options selected, a straight neck was used 71.7% of the time. The study of Traina et al. (2004) and Duwelius et al. (2010) diagnosed their clinical cohorts into groupings based on assessment of their anatomy. Traina et al. (2004), found that modularity became more effective with increasing case difficulty, where 56.5% of patients classified as having a normal hip morphology received a straight neck, compared to only 21.6% of patients classified as having a severe hip deformity. In the Duwelius et al. (2010) study, over half the patients were classified as outlier patients meaning a non-standard modular neck was fitted to correct hip joint anatomy. Following treatment, both the Traina et al. (2004) and Duwelius et al. (2010) studies had a post-operative dislocation rate of 0.3%, better than the rate reported in the literature. Both studies noted how modularity corrected abnormal anatomy. Traina et al. (2004) also noted that the risk of impingement was reduced by the surgeon intra-operatively adjusting the femoral neck until optimum range of motion was achieved.

Sakai et al. (2002) employed CT in the assessment of 116 modular femoral neck cementless prostheses, in comparison to 23 non-modular cemented hips. It was found that the use of the retroverted neck in DDH patients resulted in post-operative version being significantly smaller in the modular femoral neck group. Also, the anteverted neck was able to increase post-operative anteversion in those patients who had a pre-operative version of less than 15°. It concluded that the modular neck system could be used to correct femora with various pre-operative conditions. However, there was a practical limit to the extent that the modular neck system could aid post-operative outcome to bring post-operative reconstruction within ideal limits.

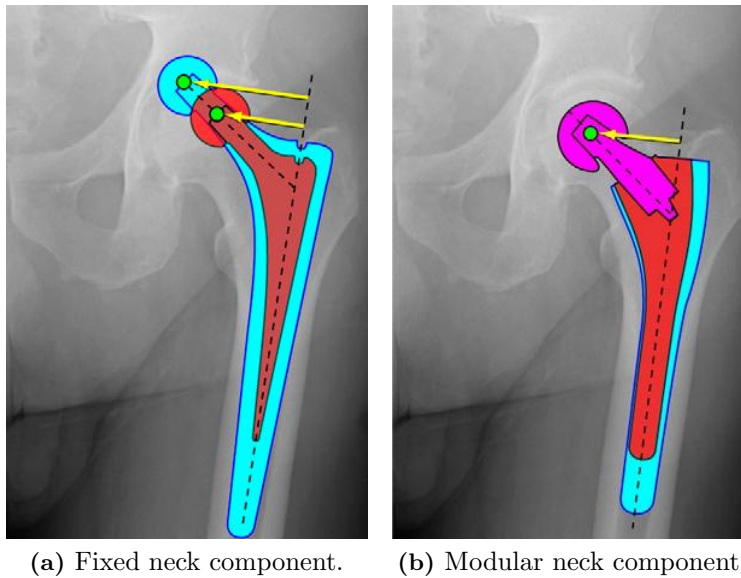


Figure 2.14: Example independent offset adjustment with modular necks (Traina et al., 2009a).

The studies by Traina et al. (2009a; 2009b; 2011) looked at the effectiveness of femoral neck modularity at providing benefit in a number of clinical scenarios. Traina et al. (2009a), analysed the effectiveness of modularity in restoring hip anatomy in both men and women. The study found a different distribution of neck choice between men and women, with women having shorter and more anteverted or retroverted necks fitted. It was stated that these differences correspond to those which are seen anatomically between men and women. The follow-up results showed that the dislocation ratio of women compared to men was 2:1, lower than the 4:1 ratio reported in literature. This was cited to be due to the flexibility of modularity in being able to restore hip anatomy in women as well as men. Traina et al. (2009b) assessed the effectiveness of implanted modular stems with a high centre of rotation, to enable an easier surgical technique in DDH patients. It comprised of 44 hips constructed with a normal anatomical centre of rotation and 44 hips with a high anatomical centre of rotation. The study found that there were no statistically significant differences in the radiographic and clinical results of both groups. This differed in comparison with other studies that had to construct a high hip centre through means other than femoral neck modularity. These cases usually suffered from poor clinical results with significant risk of aseptic loosening and prosthetic failure. Therefore, the modular femoral neck was found to be useful and effective in THA procedures where the acetabular cup cannot be placed in its

anatomical position because of poor bone stock. Finally, the study by Traina et al. (2011) analysed the 10 year follow-up results of 61 THAs diagnosed with secondary osteoarthritis due to DDH and fitted with a modular femoral neck. The clinical results of this series were good with hip function being restored almost every time with only one failure due to ceramic acetabular liner fracture.

The engineering investigations of Miki et al. (2009) and Sakai et al. (2000) used computer simulation and CT analysis of a medical model, respectively. Sakai et al. (2000) found that femoral modularity was useful in achieving the correct version and offset to prevent prosthetic, bony and soft-tissue impingement. However, similar to the author's later clinical study they noted that there was a practical limit when trying to correct offset and version to within the normal 15° - 30° range for severe cases of pre-operative anteversion. Therefore, the significance of this practical limit could be magnified if the acetabular cup is incorrectly positioned. Miki et al. (2009) found that modularity made range of motion until impingement less sensitive to acetabular cup position in comparison to a straight neck prosthesis. Therefore, as well being able to cope with a range of femoral morphologies, the surgeon can also adjust femoral version to suit a range of acetabular positions.

This section has presented a summary of the case series and engineering investigations that have assessed the effectiveness of femoral neck modularity. At present, the studies of femoral neck modularity have predominantly been cohort studies. This type of study inherently has a number of biases which can potentially affect the validity of the result (Chung and Burns, 2008; McCulloch et al., 2002). No studies have been found which have attempted to assess the potential benefits of femoral neck modularity with a suitable control - an equivalent hip implant without a modular femoral neck. This type of study, as assessed using a randomised controlled trial represents the highest level of evidence in clinical studies. As well as the case series and engineering investigations detailed in this section, there have been further engineering investigations and case reports relating to the integrity of the modular femoral neck and these are presented in section 2.6.3.

2.6.3 Femoral neck integrity

As well as clinical and engineering evaluations of modular neck femoral stems, there have been concerns with regard to integrity of the modular femoral neck (Toni et al., 2001). These concerns relate to the taper fitting of the femoral neck to the femoral stem, Figure 2.12, which potentially cause excessive fretting and crevice corrosion to the modular neck. Laboratory tests have been performed to assess the risk of catastrophic corrosion occurring in-vivo (Viceconti et al.1996; 1997). It was found that while the samples exhibited mechanical wear, none had evidence of corrosion.

While laboratory experiments do not indicate risk with regard to modular femoral neck integrity, there have been case reports of modular femoral necks fracturing (Wilson et al., 2010; Wright et al., 2010). One patient, fitted with a long 8° retroverted neck, experienced catastrophic failure of the femoral neck two years after a previous revision for an unrelated issue. The second case of modular femoral neck fracture occurred two months after the patient had slipped on ice. Examination of the fractured neck retrievals using microscopy, revealed extensive fretting and corrosion damage with the fracture surface showing evidence of fatigue (Wilson et al., 2010; Wright et al., 2010).

A retrieval study by Kop and Swarts (2009), examined sixteen implant retrievals of modular femoral necks which were explanted for issues unrelated to femoral neck integrity. Analysis showed significant fretting and crevice corrosion at the modular stem-neck junction in six of the retrievals. The amount of corrosion was significantly more than at other taper sites (Kop and Swarts, 2009). The modular neck failure rate is reported to be 0.027% (Traina et al., 2009a). There are a number of hypotheses related to why neck fracture occurs, which relate to the increased moment arm that is created with the use of long necks and is further increased when anteverted or retroverted necks are used. Coupling this with a heavier patient, then the increased functional demand places high neck stress upon the implant. The increased stress combined with increased amount of corrosion and fretting could lead to degradation and failure at the stem-neck junction (Kop and Swarts, 2009; Wilson et al., 2010; Wright et al., 2010).

2.6.4 Summary

This section has presented the current research with regard to hip joint reconstruction with femoral neck modularity. A review of the clinical series and engineering investigations have shown potential benefits for its use in THA as well as noted areas of risk. However, none of the previous studies have assessed the potential benefits of femoral neck modularity with a suitable control. Therefore, the benefit of this feature needs to be assessed in comparison to other variables such as component positioning and other modular features such as femoral head size and offset adjustments. This would allow a true evaluation of the effectiveness of femoral neck modularity in improving range of motion until impingement and therefore dislocation. The findings of the review of the literature will now be summarised in section 2.7.

2.7 Literature review summary

Literature relevant to this study has been reviewed within this chapter to be able to understand the requirements of post-operative hip joint range of motion. It has been found that as well as the positioning of the pelvic acetabular cup, the orientation of the femoral component is of critical importance. This has been difficult to achieve in the past, which has led to femoral neck modularity being introduced to aid the surgeon in the intra-operative joint reconstruction to improve joint stability and range of motion. The key findings of the review of the literature have been summarised.

- A successful THA normalises the biomechanics of the hip joint which is dependent upon two factors, joint stability and range of motion.
- The joint coordinate frame used in gait analysis studies of human motion are not mathematically representative and does not satisfy the requirements of an ideal Cartesian coordinate frame. This makes it difficult to represent hip motion graphically.
- It has been shown that there is a wide variation in the recommended values for component positioning in THA. This is because of the inter-dependence of femoral and acetabular component orientation. Therefore, adjustment of one component position should be based on knowledge regarding the position of the other component.
- There has been difficulty relating surgical measurements of component orientation to post-operative range of motion. This has been due to an incongruity between the reference frames used in the surgical field and those which are used in gait analysis measurement of human motion. Therefore, the exact requirement is not understood.
- In the THA market modularity has been introduced to increase head-neck ratio, control offset and limb length requirement. It seeks to balance joint stability requirement while maximising range of motion. Femoral neck modularity is the most recent addition allowing for adjustment of femoral version and neck-shaft angle to aid both joint stability and range of motion.

- Previous case series and engineering simulations have shown the potential of femoral neck modularity at being able to restore the biomechanics of the hip joint improving stability and range of motion until impingement. However, retrieval studies and case reports have highlighted the risk with regard to femoral neck integrity.
- The benefit of femoral neck modularity needs to be assessed in comparison to other THA features to allow a true evaluation of its effectiveness in improving range of motion until impingement and therefore resistance to dislocation.

The literature researched has determined the theoretical foundation with regard to being able to understand which factors influence hip joint range of motion post-THA. It has also presented the limitations with regard to graphically representing hip joint range of motion to evaluate impingement and dislocation in THA. Finally, it has also assessed the current clinical knowledge with regard to the effectiveness of femoral neck modularity. The key points highlighted above that have arisen from the research have determined the current threshold of knowledge and identified gaps in knowledge which need to be addressed to be able to answer the research question and objectives defined in chapter 1. A research methodology will now be developed to be able to address the gaps in knowledge so that the current theoretical foundation can be built upon to be able to answer the research question posed in this study.

Chapter 3

Research Methodology

3.1 Introduction

In chapter 1 the research question and objectives for this study were outlined. These objectives were designed to generate innovation and be applied within the surgical field to assess the effectiveness of femoral neck modularity in improving resistance to dislocation. To be able to address each of these research objectives, the current limitations with regard to modelling hip joint motion had to be considered. These were presented in chapter 2 and form the theoretical foundation from which a range of motion benchmark for the hip joint was able to be developed and applied. To do this, the theoretical foundation had to be combined with a suitable research methodology. The selection and design of the research methodology for this study is presented in this chapter.

3.2 Selection of research design

The research undertaken in this study involved developing an innovative engineering solution and applying it into a clinical setting to assess the effectiveness of a medical technology. The work presented to this point in the study has followed the traditional research approach. This has involved defining the research problem and understanding it in the context of what is already known (Kumar, 2011; Welman et al., 2005). A research design needs to be developed that can be used to achieve the studies research question and objectives. Analysing the research objectives further revealed the requirement for a two-stage research design shown in Figure 3.1.

The first stage of the overall research design required a data collection method to be designed from which to establish a range of motion benchmark. This required obtaining data from the biomechanics and clinical fields to develop an evidence based benchmark. The systematic review methodology has established itself as the key element in evidence based education to guide healthcare policy (Torgerson, 2003). This methodology differs from the traditional narrative literature review in that it is replicable so that it can be repeated by other researchers, reliable as it minimises researcher bias and valid as the purpose for the literature review is clearly stated. Further, information from independent studies can be combined to allow for meta-analysis of the range of motion data yielded from the systematic search of the literature. This provides the opportunity for more precise estimates on the required range of motion (Higgins and Green, 2008). Based on this opportunity, the systematic review methodology was chosen to be the data collection instrument to fulfil the first part of the study, rather than a single gait analysis study.

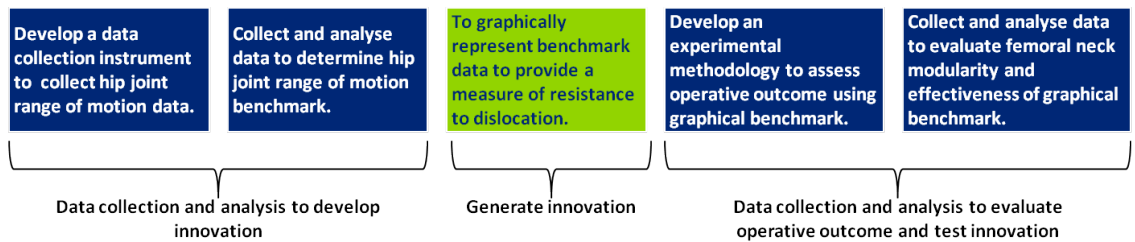


Figure 3.1: Two-stage research process.

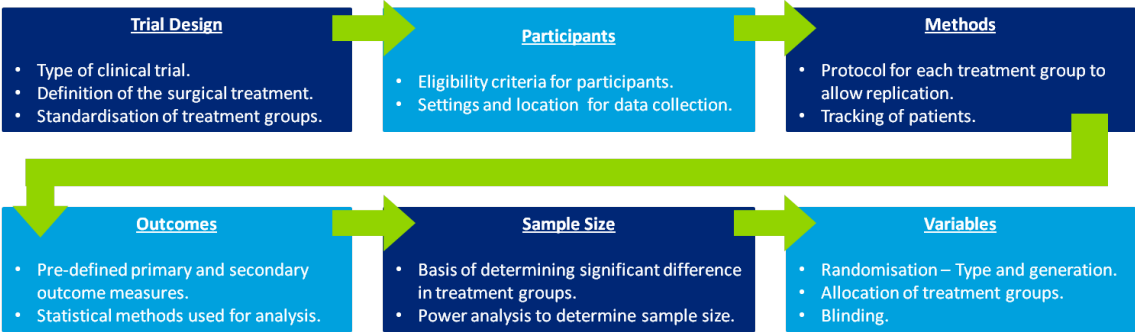


Figure 3.2: Randomised controlled trial methodology (Piantadosi, 2005; Schulz et al., 2010).

The second stage of the research process required an experimental methodology to collect data which could be compared with the benchmark established in the first stage of the research process. The purpose of this comparison was to evaluate the clinical efficacy of femoral neck modularity and to assess the effectiveness of the developed range of motion benchmark in evaluating operative outcome. Evaluation of THA outcome requires the clinical observation of cases in orthopaedic surgery (Chung and Burns, 2008; McCulloch et al., 2002). In orthopaedics literature, most studies are retrospective cohort series, which have a number of biases potentially affecting the validity of the result (Chung and Burns, 2008; McCulloch et al., 2002). This is especially true with regard to comparing two different implant groups where differences are small and consequently any bias can affect the outcome of the study (Boutron et al., 2007). At present, studies of femoral neck modularity have predominantly been cohort studies. In addition, none of the studies have attempted to assess the potential benefits of femoral neck modularity with a suitable control - an equivalent hip implant without a modular femoral neck. Therefore, a Randomised Controlled Trial (RCT) with a non-modular control was selected as the best research design to assess the effectiveness of femoral neck modularity. Figure 3.2, outlines the steps in designing a RCT methodology.

3.3 Systematic review methodology

The objective for the systematic review of the literature was to obtain kinematic data for hip joint range of motion from experimental studies. This included information on both pure joint motion and activities of daily living. Pure joint motion refers to the maximum extents of flexion/extension, abduction/adduction and internal/external rotation in each of the clinical planes presented in Figure 2.1 on page 11. Activities of daily living are those activities such as tying ones shoe laces or sitting on a low chair which contain out of anatomical plane motion. The process of setting up the systematic review and executing the search of the literature followed the guidelines presented by Higgins and Green (2008) and Torgerson (2003). Section 3.3.1, will outline the process implemented for the systematic review of the literature. Section 3.3.2, will present how research validity was ensured during the study.

3.3.1 Literature search

A systematic review of the literature was conducted to obtain experimental data with regard to pure joint motion and activities of daily living. The MEDLINE database was used for the systematic search of the literature, with articles from 1950 until October 2009 being reviewed. After a number of iterations, the field search shown in Table 3.1 was felt to yield the strongest most concise search results.

Table 3.1 shows that 345 articles were obtained from the systematic search of the literature. The article titles were reviewed for relevance to range of motion of the hip joint. Criteria for selection included experimental data for healthy subjects with regard to hip range of motion, benchmark range of motion targets for THA and details relating to activities of daily living. Table 3.2, details the reasons why papers were eliminated through the title review process. If article titles had more than one reason to be eliminated, an order of importance for exclusion was established following the order set out in Table 3.2.

Following the title review process, the remaining 77 articles were assessed for relevance to the subject area. A total of 47 articles were eliminated during this process, 16 of the articles could not be accessed, on 3 occasions the incorrect article was accessed, 13 papers contained post-operative or test results with no control group or benchmark range of motion target, 8 articles had no range of motion or activity of daily living information, 3 articles presented results of mechanical testing and 3 articles presented range of motion data not as joint angles in the anatomical planes. This left a total of 30 relevant articles (Ahlberg et al., 1988; Amstutz et al., 1975; Barrack et al., 2001; Boone and Azen, 1979; Burroughs et al., 2001, 2005; Chandler et al., 1982; D’Lima et al., 2000; Davis et al., 2007; Hagio et al., 2004; Hemmerich et al., 2006; Jaramaz et al., 1998; Kessler et al., 2008; Kluess et al., 2007; Ko and Yoon, 2008; Krushell et al., 1991; Miki et al., 2007; Mulholland and Wyss, 2001; Nadzadi et al., 2003; Pedersen et al., 2005; Piazza et al., 2004; Roaas and Andersson, 1982; Roach and Miles, 1991; Stuchin, 2008; Sun et al., 2007; Thornberry and Hogan, 2009; Widmer and Zurfluh, 2004; Widmer and Majewski, 2005; Yoshimine, 2005, 2006).

The 30 articles applicable to the topic area were reviewed further, after an evaluation of the articles references, a further 22 articles were identified as potentially being relevant to the subject area. On reviewing these articles, 2 could not be obtained, 1 was not published in English and 2 were deemed not relevant because it provided no or very little range of motion or activity of daily living information. This left a further 17 articles (American

1.	Hip	[Title/Abstract]	(64,633)
2.	Range of	[Title]	(4,209)
3.	Motion OR Movement	[Title]	(39,475)
4.	1 AND 2 AND 3		(135)
5.	Range of	[Title/Abstract]	(257,376)
6.	Motion OR Movement	[Title/Abstract]	(184,529)
7.	5 AND 6		(19,455)
8.	Kinematic*	[Title/Abstract]	(11,349)
9.	7 OR 8		(29,709)
10.	Dislocation OR Impingement	[Title/Abstract]	(24,714)
11.	1 AND 9 AND 10		(238)
12.	4 OR 11		(345)

Table 3.1: Strategy for literature search.

Reason for elimination	Number of Articles
Articles not published in English	38
Articles are comments on particular papers	4
Articles relate to alternative hip surgical procedures (arthroscopy, resurfacing, etc)	89
Articles relate to niche population for ROM measurements (sports, congenital disease, etc)	72
Articles relate to different joint (knee, shoulder, etc)	10
Articles relate to the specifics of a measurement technique (inter/intra-observer, marker sets, etc)	26
Articles relate to mechanical testing (stress distribution, wear, etc)	14
Articles relate to acetabular cup placement	15
Total number of articles eliminated	268

Table 3.2: Screening results from literature search.

Academy of Orthopaedic Surgeons, 1965; Cailliet, 1978; Cole, 1971; Costigan et al., 2002; Daniels and Worthingham, 1972; Gajdosik and Bohannon, 1987; Green and Heckman, 1994; Hoppenfeld and Hutton, 1976; James and Parker, 1989; Japanese Orthopaedic Association, 1995; Johnston and Smidt, 1970; Kendall et al., 1971; Kummer et al., 1999; Mohr, 1989; Rowe et al., 2000; Seki et al., 1998; Weiss et al., 2002). A review of the references to these articles produced one relevant result (Johnston and Smidt, 1969). Finally, 2 key articles were identified within the 47 papers as being well referenced in relation to pure joint motion (Boone and Azen, 1979) or activities of daily living (Johnston and Smidt, 1970). A citation search of these papers produced 4 articles (Kadaba et al., 1990; Noble et al., 2003; Nonaka et al., 2002; Svenningsen et al., 1989). A total of 51 articles were taken forward to be evaluated with regard to establishing a range of motion benchmark in chapter 4. The validity of the systematic review of the literature is considered in section 3.3.2

3.3.2 Systematic review validity

The concept of validity is vital in achieving meaningful results from a systematic review of the literature, which requires the issues of validity and reliability to be assessed (Torgerson, 2003). A valid research methodology means that what is being measured is correct for the research topic. Reliable research indicates that the research can be repeated, yield the same results and be free from bias.

The issue of content validity was addressed during the field search, where two people reviewed the constructed search strategy presented in Figure 3.1. One subject librarian skilled in preparing Cochrane reviews and one clinical research fellow skilled in the research area. This ensured that the search strategy was focussed upon obtaining data for hip joint range of motion (Higgins and Green, 2008). The potential for bias was limited by ensuring that only an electronic search of literature was undertaken to prevent personal knowledge being used to influence the articles that were included in the study (Torgerson, 2003). Further, the electronic search of the MEDLINE database was repeated for the dates specified, from 1950 until October 2009 and the same number of articles were found. This meant that the systematic search of the literature could be carried out by other researchers and produce the same articles.

The screening process had strict exclusion criteria, which could be repeated by a third party. This process was double screened to ensure only a minimal amount of relevant articles were missed. There was however a potential for bias where the 30 articles from the screening process had their references and citations reviewed. This is because the articles yielded were based on the author's opinion, although the same inclusion and exclusion criteria were applied rigorously to minimise this bias. Also, the articles yielded from this part of the systematic search of the literature can be directly correlated to the articles produced from the field search. It was felt adding this additional step with the rigorous inclusion and exclusion criteria ensured the most comprehensive amount of relevant articles were taken forward to establish a range of motion benchmark.

3.3.3 Validation of the range of motion benchmark

As well as considering the validity of the systematic review methodology. The data extracted from the articles to produce the graphical representation of the range of motion benchmark presented in chapter 4 was required to be validated. Further, the construction of the graphical representation used a number of experimental assumptions with regard to hip joint motion which were presented in chapter 2. Consequently, the validity of the data used to establish the range of motion benchmark and the theoretical foundation which underpinned the construction of its graphical representation were required to be assessed. The objectives for this validation study have been detailed.

- To assess the validity of modelling the hip joint as a perfect ‘ball and socket’.
- To assess agreement of pelvic coordinate frames used in range of motion analyses.
- To assess the validity of the graphical representation of the range of motion benchmark.

To evaluate the validity of the graphical representation of the range of motion benchmark, ten CT scans were taken of subjects exhibiting no evidence of osteoarthritis or abnormal morphology. The purpose of the experiment was to simulate the range of motion of these patients for comparison with the constructed range of motion representation. To do this, each of the CT scans was segmented to produce three-dimensional models of the pelvis and the femur, shown in Figure 3.3. These three-dimensional models were then imported into the Rhino 4.0 NURBS modelling package for measurement.

Range of motion of the hip joint is limited by bone-on-bone impingement and soft tissue tension. This experiment only considered the range of motion limit due to bone-on-bone impingement. There have been a number of studies which have used CT scans of patients to evaluate range of motion (Miki et al., 2007; Kubiak-Langer et al., 2007; Kurtz et al., 2010; Sun et al., 2007; Tannast et al., 2007; Thornberry and Hogan, 2009). All of these studies have analysed the effect of prosthetic or bony impingement and have made a number of observations that were applicable to this study. Tannast et al. (2007), identified that motions in flexion are very much associated with bone-on-bone impingement rather than

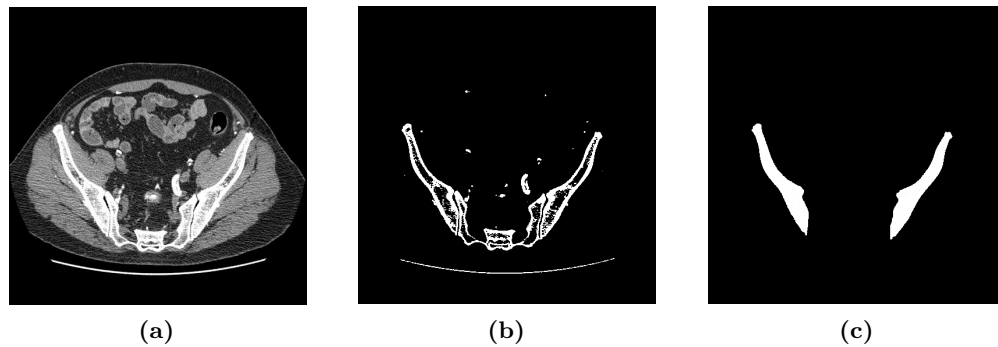


Figure 3.3: The patient CT segmentation process (a) The original Dicom slice image (b) The thresholded slice image and (c) The cleaned slice image.

soft tissue effects. Kurtz et al. (2010), commented on the clinical relevance of bone-on-bone impingement in extension, which was measured to be on average 78° and had little relevance to the activities a person is likely to perform on a daily basis. Finally, Tannast et al. (2007) and Thornberry and Hogan (2009), argued that bone-on-bone impingement will slightly overestimate the required range of motion by approximately 5° because of the absence of soft tissue. Therefore, the experimental hypothesis was that the average patient CT range of motion would be slightly larger in flexion, abduction and adduction than the constructed graphical representation and significantly larger in extension.

To test the validity of the range of motion results, the discrete motions of flexion, extension, abduction and adduction were compared with the findings of Kubiak-Langer et al. (2007) and Tannast et al. (2007) who also analysed range of motion of healthy individuals from CT scans, Table 3.3. The effect size between the current experiment and the experiments by Kubiak-Langer et al. (2007) and Tannast et al. (2007) was used to assess the validity of the experimental range of motion results. The effect size was determined using the percentage variance in scores (PV) (Murphy et al., 2004). PV calculates the variation between the means of the dependent variable measured in the two experiments as a proportion of the total variation. The calculated PV was used to classify the effect size of the difference in means between the experimental methods.

3.3.4 Summary

This section has detailed how articles used to develop the range of motion benchmark were obtained using a reliable method and ensured to be valid. The development of the range of motion benchmark is detailed in chapter 4. This chapter will also present how this benchmark data was used to develop a graphical representation of the range of motion benchmark which was used to assess operative outcome. Further, the validity of the graphical range of motion benchmark and the theoretical foundation which underpins its construction were evaluated using the methodology described in section 3.3.3. Section 3.4, will present how the graphical representation of hip joint range of motion was applied in the assessment of operative outcome.

	Kubiak-Langer et al. (2007)	Tannast et al. (2007)
<i>n</i> =	33	36
Flexion	122° ($\sigma=16.3^\circ$)	121° ($\sigma=11.8^\circ$)
Extension	57° ($\sigma=20.1^\circ$)	58° ($\sigma=20.4^\circ$)
Abduction	63° ($\sigma=10.9^\circ$)	63° ($\sigma=11.1^\circ$)
Adduction	33° ($\sigma=12.3^\circ$)	33° ($\sigma=11.9^\circ$)

Table 3.3: Healthy subject range of motion analysis using CT scans.

3.4 Randomised controlled trial design

In chapter 1, the research question and objectives for this study were presented. A two-stage research process was selected in section 3.2 to fulfil the requirements of the research objectives. The systematic research methodology, presented in section 3.3 was used to address the first two research objectives. The methodology used to construct the graphical representation was used with the method detailed in section 3.4.3 to meet the third research objective. While the final two research objectives were addressed using the results obtained by the randomised controlled trial. Figure 3.2, presented the stages in a randomised controlled trial design. This section will discuss how each stage was developed.

3.4.1 Trial design

The randomised controlled trial required a modular femoral neck total hip replacement design to be assessed against a non-modular control. This is characteristic of a phase III clinical trial, where a new treatment is compared with a historic alternative (Piantadosi, 2005). Comparative treatment efficacy (CTE) trials are employed in the evaluation of outcome in this type of experimental comparison (Chow and Liu, 2004; Piantadosi, 2005). This employed a two-group parallel design in which patients were randomised into non-modular neck control and modular neck intervention treatment groups. Figure 3.4 details the progress through each of the phases of a parallel two-group randomised controlled trial (Schulz et al., 2010). An omission for this study was the follow-up phase as all necessary data was collected intra-operatively. The study protocol was designed by the Clinical Trials team within Warwick Orthopaedics led by Professor of Trauma and Orthopaedics Damian Griffin and administered by Clinical Research Fellow Shahbaz Ahmed. The primary outcome measures and their integration within the study were designed by myself which were the propensity to impinge and impingement severity, these are explained in further detail in section 3.4.4. It was hypothesised that THA performed with an uncemented, stemmed, modular neck component will reduce the risk of prosthetic impingement compared to an identical stem with a non-modular neck.

In clinical trials, clinicians are not able to control for as many sources of variability through the study design as laboratory experiments. Consequently, there are independent variables, other than femoral neck modularity, within the surgeon's control that can influence the operative outcome and bias the study. Four of these independent variables have been discussed in chapter 2 and relate to the parameters defined by Yoshimine and Ginbayashi (2002) - inclination of the acetabular cup (α), anteversion of the acetabular cup (β), the angle between the femoral neck and the transverse plane (a) and the version angle of the femoral neck (b). Further independent variables were identified other than femoral neck modularity which relate to differences in the femoral stem and acetabular liner design. These will be explained later in this section when the non-modular neck and modular neck implant options are discussed. These differences in implant variables was accepted for two principal reasons. Firstly, it was wished to assess the femoral neck modular device against a popular cementless component which was different in design. Differences in range of motion result due to implant geometry could have been avoided if it was wished to assess purely the influence of femoral neck modularity rather than its effectiveness against a historic alternative. If this was the case then the experimental design could have benefited by only using the modular neck implant type. An assessment would have been possible if, in the non-modular control group, only straight necks were permitted to be fitted. However, the second principal reason for accepting a number of independent variables was that the prosthetic options selected in the study could be interchanged in the surgical navigation system described in section 3.4.3 allowing the influence of each of these different parameters to be analysed.

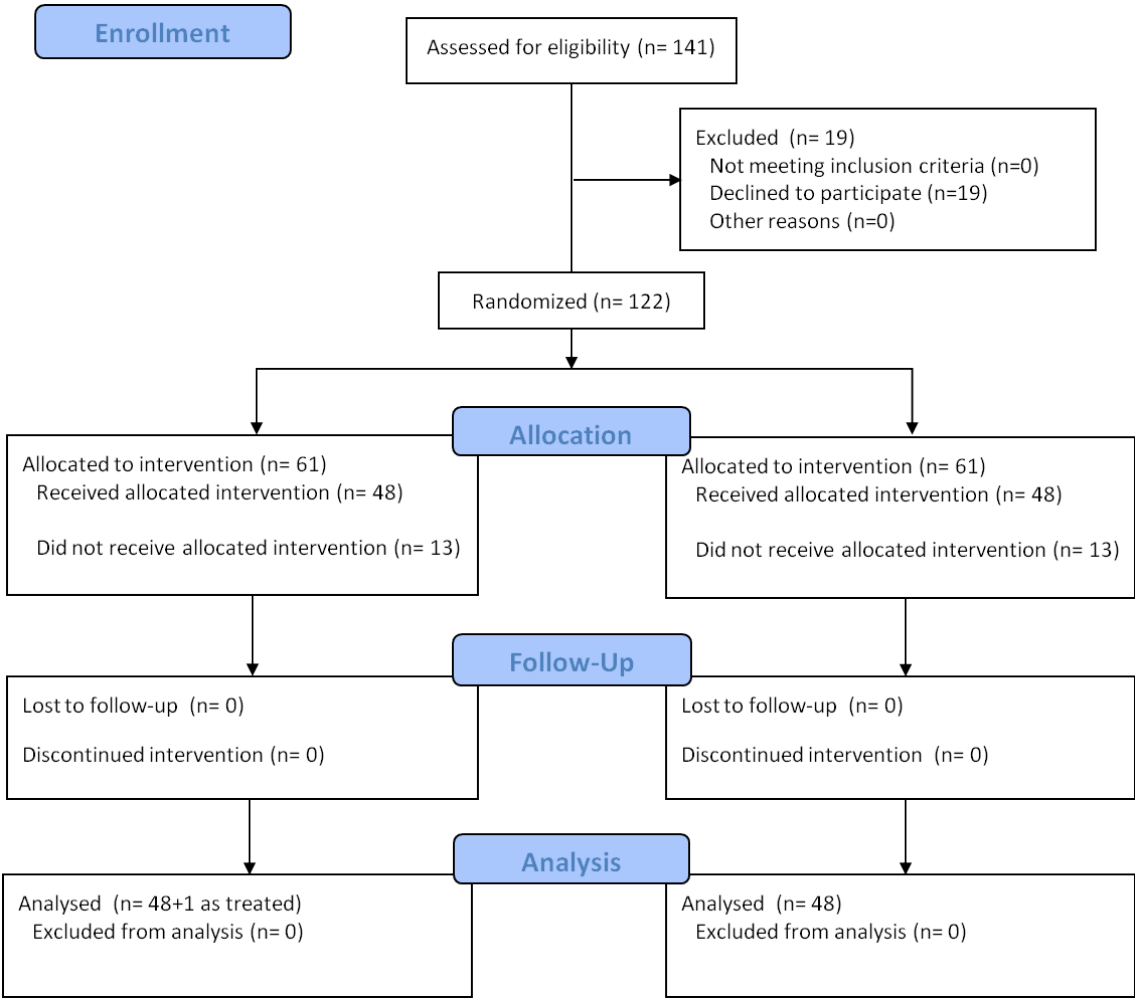


Figure 3.4: Consort flow diagram (Schulz et al., 2010).

The non-modular femoral neck control group

The Depuy Corail straight tapered stem is a popular cementless femoral component used in THA with good follow-up results (Vidalain, 2010). It has three implant options - standard offset, high offset and coxa vara. The standard offset device has a 135° neck-shaft angle, where offset is dependent upon stem size. This ranges from a minimum of 38mm for a small 95mm stem length to an offset of 45.5mm for a 170mm stem length. The high offset stem again has the same 135° neck-shaft angle, however, offset ranges from a minimum of 45.5mm for a 110mm stem to an offset of 52.5mm for a 170mm length stem. The coxa vara has the same offset options as the high offset stem but with a 125° neck-shaft angle. Figure 3.5, presents the stem options (Depuy Orthopaedics Inc, 2010).

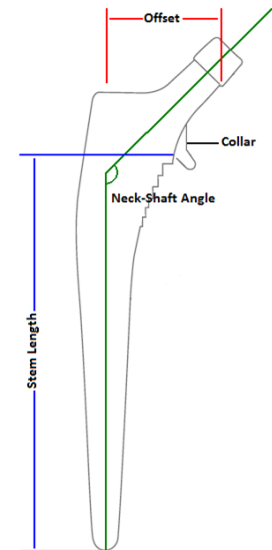


Figure 3.5: Femoral stem.

Implanted along with the Corail tapered stem is the Depuy Pinnacle acetabular cup, which consists of two parts. The acetabular shell and the acetabular liner. The acetabular shell forms the outer part of the acetabular component which is porous coated for cementless fixation to the pelvis. It has an outer diameter ranging from 48mm to 66mm increasing in 2mm increments. The other section of the acetabular component is the acetabular liner which interfaces with the acetabular shell. It is the bearing surface against which the femoral head rotates. The acetabular liner is available in three material choices - polyethylene (Pinnacle Marathon or GVF), metal (Pinnacle Ultamet) and ceramic (BioloX Delta). Each of these acetabular liners has different geometrical characteristics. Using Figure 3.6a as reference, the polyethylene liner has a rotation centre distance of 2mm away from the opening plane of the liner. The metal liner has rotation centre level with the opening plane and therefore is a perfect hemisphere. The position of the rotation centre of the ceramic option is dependent upon the inner and outer diameters of the liner, detailed in Table 3.4.

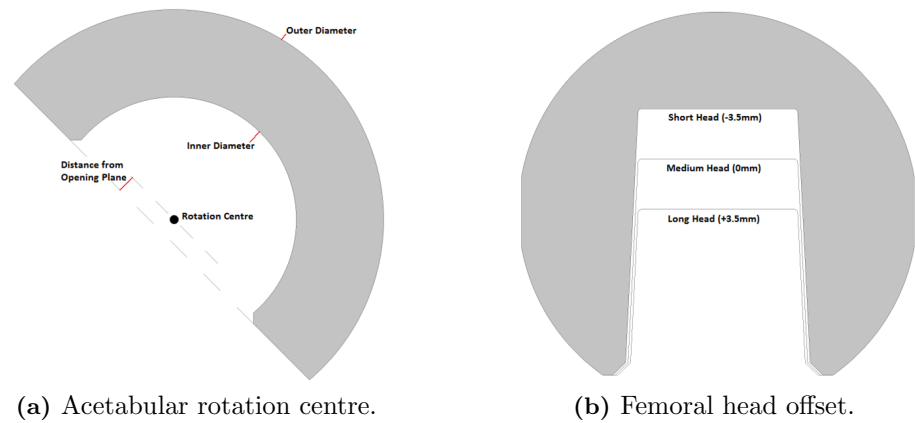


Figure 3.6: Specification of prosthetic components.

The femoral head taper fits to the Corail tapered neck and is available in two materials - metal (Depuy Articuleze) and ceramic (Bilox Delta). Each of these femoral heads is available in three diameters - 28mm, 32mm and 36mm. An increase in the femoral head size increases the femoral head-neck ratio. Consequently, the oscillation angle (θ) increases, resulting in increased range of motion until impingement (Yoshimine and Ginbayashi, 2002). As well as different diameters, the femoral head has three different offsets, -3.5mm, 0mm and +3.5mm, as shown in Figure 3.6b. This has the effect of shortening or lengthening the neck offset shown in Figure 3.5. The femoral head offset, stem size and neck offset all have the effect of changing the location on the femoral neck which impinges against the rim of the acetabular liner, altering the head-neck ratio and ultimately range of motion. Therefore, femoral head diameter, femoral head offset, acetabular liner rotation centre, neck offset, neck-shaft angle and stem length are the independent variables which can affect the range of motion until impingement.

Liner Inner Diameter	Liner Outer Diameter	Rotation Centre
28mm	42-44mm	1mm
32mm	46-48mm	0mm
32mm	50mm	1mm
36mm	+52mm	0mm

Table 3.4: Biolox ceramic acetabular liner rotation centre.

Modular femoral neck intervention group

The Wright Profemur modular femoral neck cementless stem is available in 12 different stem lengths ranging from 109mm to 145.5mm. The proximal modular neck, shown in Figure 3.7b, is available in two lengths for independent offset adjustment, short 28mm and long 38.5mm (Wright Medical Technology, Inc, 2010). The different modular necks have been detailed in Figure 2.13 on page 36 and are available in the following options - straight, varus or valgus 8° and 15° , anteverted or retroverted 8° and 15° , combination of ante-retroverted 4.5° with varus-valgus of 6° - AR-VV1 and AR-VV2 options (Traina et al., 2009a). The straight neck option provides a neck-shaft angle of 135° . The varus option reduces the neck-shaft angle and the valgus option increases the neck shaft angle by 8° or 15° in the pure varus-valgus option, or by 6° in the AR-VV1 and AR-VV2 options. The anteverted neck option increases the distance of the femoral neck axis away from the coronal plane, while the retroverted neck reduces the distance by 8° or 15° in the pure ante-retroverted option, or by 4.5° in the AR-VV1 and AR-VV2 options.

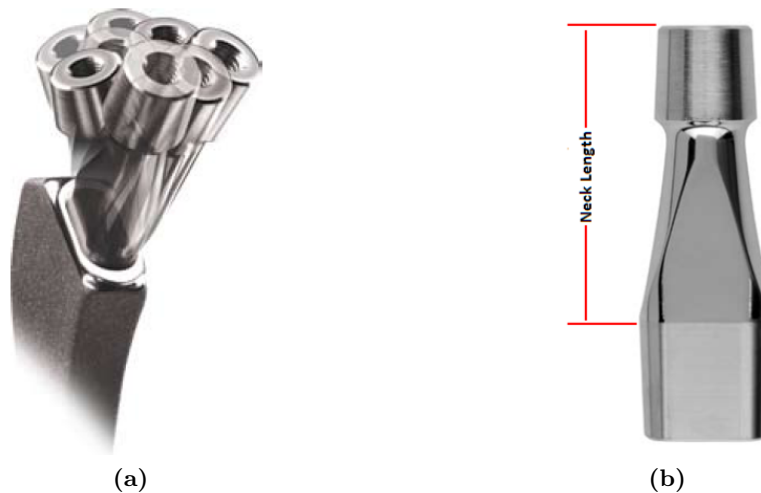


Figure 3.7: Intervention group femoral stem specifications (a) Profemur neck interfacing with stem and (b) Profemur neck length (Wright Medical Technology, Inc, 2010).

Implanted along with the Profemur modular femoral neck stem is the Wright Procotyl-L acetabular cup. Similar to the Depuy Pinnacle, the Procotyl-L consists of a porous coated outer shell to allow cementless fixation. It has an outer diameter ranging from 42mm to 68mm increasing in 2mm increments (Wright Medical Technology, Inc, 2009). The acetabular liner which constitutes the acetabular system bearing surface is available in three material choices, polyethylene, metal and ceramic (Bilox Delta), shown in Figure 3.8. Again, each of these acetabular liners has different geometrical characteristics. Using Figure 3.6a as reference, the polyethylene and metal liners have a rotation centre distance of 1mm away from the opening plane of the liner. While the rotation centre of the ceramic option is dependent upon the inner and outer diameter of the liner, detailed in Table 3.4. The Wright Medical Technology, Inc femoral heads are available in metal or ceramic (Bilox Delta) options. They are each available in three diameters 28mm, 32mm and 36mm with -3.5mm, 0mm and +3.5mm head offsets. The femoral head diameter, femoral head offset, acetabular liner rotation centre, neck length and femoral neck modularity are the independent variables associated with the intervention treatment group.



Figure 3.8: Procotyl-L liner options (Wright Medical Technology, Inc, 2009).

3.4.2 Participants

To minimise inter-patient variability a strict eligibility requirement was established for the clinical trial in accordance with Schulz et al. (2010). Recruitment took place on all patients suffering from primary osteoarthritis suitable for cementless THA within the Coventry and Warwickshire NHS Trust. Exclusion criteria included any patient with a pelvic deformity such as DDH or a lumbar spine deformity. Further exclusion criteria included previous extensive hip surgery (such as osteotomy), if the patient could not understand the study and a Body Mass Index (BMI) of greater than 40. BMI was detailed as an exclusion criteria due to difficulty using the measurement equipment detailed in section 3.4.3 with patients of such size. Finally, if pre- or intra-operatively a lipped acetabular liner was required for a patient within either the control or intervention group, then that patient was excluded from the study. The clinical trial took place at two hospitals within the Coventry and Warwickshire NHS Trust - University Hospital Coventry and the Hospital of St Cross Rugby - between January 2009 and August 2010. Ethical approval was given by the Coventry local research ethics committee on 7th June 2007 for the clinical trial.

3.4.3 Methods

The method with regard to the data collection of prosthetic range of motion is detailed within this section. To acquire the necessary intra-operative measurements to calculate prosthetic range of motion of the implanted components the Kolibri workstation with the Hip Essential 5.1.2 prototype software by Brainlab was used, shown in Figure 3.9. This provided a surgical navigation measurement system consisting of a localisation system with an infrared emitter and stereo infrared cameras used to detect passive marker spheres which reflect the infrared radiation (DiGioia et al., 1998). The combination of this hardware creates a triangulation distance sensor where the infrared radiation emitted from the source is reflected back by the marker spheres (Galloway Jr, 2001). The stereo infrared cameras are located at a fixed angle and distance from each other, known as the triangulation angle. The cameras detect the reflected infrared to determine the markers' coordinate location

relative to the navigation global frame of the workstation camera (Schwenke et al., 2002). If three passive markers are mounted onto a rigid array then, as discussed in chapter 2, a local Cartesian coordinate frame can be established and the six degree of freedom location and orientation of that array can be tracked (Sommer 3rd et al., 1982; Stökdijk et al., 2000).

The surgical navigation system provided a measurement device which could be used intra-operatively to measure the orientation of the pelvic acetabular cup and femoral stem relative to their respective body segment coordinate frames, described in chapter 2, section 2.5. The measurement of prosthetic component orientation and the geometrical specification of the prosthetic components were used to calculate the prosthetic range of motion area. Detailed description of how this was implemented is provided in chapter 5.

3.4.4 Outcome measures

The assessment of operative outcome used the graphical representation of the hip joint range of motion benchmark and a representation of the prosthetic motion area of the patient. The development of the graphical range of motion benchmark is discussed in chapter 4 with the construction of the prosthetic range of motion area presented in chapter 5. Both graphical representations are shown for reference in Figure 3.10. The gold area shows the range of motion benchmark and the prosthetic range of motion in purple. Where the prosthetic range of motion boundary does not encompass the required range of motion. This area is shown in red and is the degree of impingement for a particular patient and used to assess operative outcome. Both the area of impingement, shown in red, and the prosthetic motion area, shown in purple, were expressed as a percentage of the surface area of the range of motion benchmark and used as outcome measures in the experimental analysis. Also used, as an outcome measure, was the 3-dimensional angle between the graphical range of motion benchmark directional axis and the prosthetic motion directional axis, shown in Figure 3.10b. This provided a measure of how well the prosthetic motion area was positioned relative to the benchmark requirement.

**Localisation System -
Emitter & Detector**

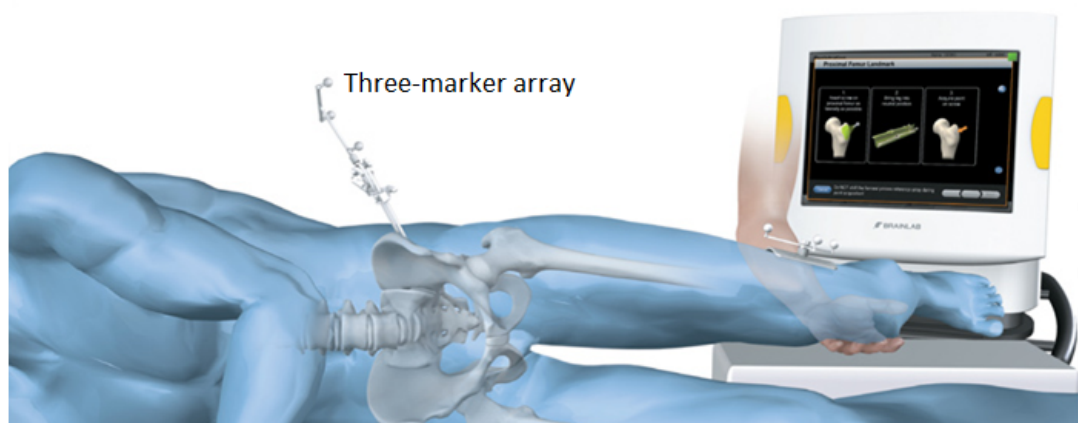
Workstation



(a) Brainlab Kolibri Surgical Navigation Workstation.



(b) Brainlab three-marker pointer.



(c) Brainlab three-marker array.

Figure 3.9: The Brainlab surgical navigation measurement system (Brainlab AG, 2008).

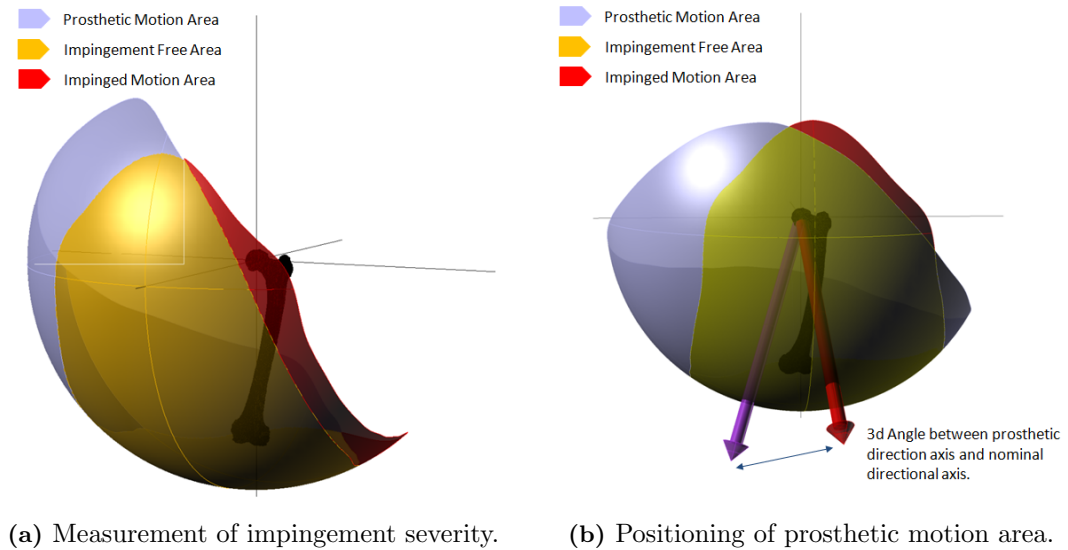


Figure 3.10: Outcome measures for randomised controlled trial.

The fourth research objective presented in chapter 1 required the effectiveness of femoral neck modularity to be evaluated. To do this, the research question was broken down into two further sub-objectives. The first sub-objective provided an assessment of the potential for femoral neck modularity to improve operative outcome. The second sub-objective assessed whether this potential, if any, was being maximised in the operative procedure.

- To evaluate the influence of femoral neck modularity on hip joint range of motion.
- To assess if femoral neck modularity is being effectively used to relieve impingement.

In section 3.4.1, a number of different independent variables were identified which affect the outcome measures that have been described in this section. To be able to fulfil the requirements of the first sub-objective, neck modularity had to be assessed in the context of the other independent variables. For this to be possible, post-operatively, each of the treatment group prosthetic components was able to be changed in the Kolibri workstation to other components within the same treatment group. This allowed independent variables to be assessed with regard to their impact upon the prosthetic motion area. To assess the influence of femoral neck modularity on hip joint range of motion the size of the prosthetic motion area and its position relative to the range of motion benchmark were the primary

outcome measures used. An initial screening, using the systematic fractional replicate design developed by Cotter (1979) was used to screen out those independent variables which were not main factors in influencing the size and position of the prosthetic motion area and therefore range of motion to impingement (Antony, 2003).

Following screening, a full factorial design of experiments was used to assess the contribution and interaction of the independent variables with regard to the size of the prosthetic motion area and its position relative to the range of motion benchmark. This was achieved by setting the main identified factors at their high (+) and low (-) values (Antony, 2003; Montgomery, 2008). During this evaluation, those independent variables not deemed to be main factors were set at their economic values during the full factorial analysis. This economic value was set to be the middle value within the available options for an independent variable. For example femoral head diameter has three possible values 28mm, 32mm and 36mm. The economical value for this independent variable was therefore 32mm. This experimental design allowed for the contribution and interaction of femoral neck modularity, if identified as a main factor, to be evaluated against the other implant variables.

The second sub-objective presented in this section, required an assessment of how effectively femoral neck modularity was being used to relieve impingement. This required direct comparison of the control and intervention treatment groups to assess whether the addition of a modular femoral neck results in a significant reduction in the level of impingement. The primary outcome measures used in this assessment were the propensity to impinge and impingement severity. The propensity to impinge is a measure of whether or not the prosthetic motion area results in impinged motion or not, it is a simple binary 0 or 1 result. The treatment group cohorts were compared using Fisher's Exact Test for Independence to test for any significant differences between the two cohorts in their propensity to impinge (Rees, 2001). If a p-value (one-tail) of less than or equal to 0.05 was calculated then it would be deemed that a significant difference between the treatment groups in their propensity to impinge was found to exist.

The second primary outcome measure was impingement severity. The degree of severity was defined as the size of the impingement area, if any, as a percentage of the range of motion benchmark. Significant impingement was defined as an impingement area greater than 1% of the range of motion benchmark. To evaluate impingement severity a student-t and F-test was used to test for a significant difference in the mean and variance of the two cohorts (Rees, 2001). A significant difference between the control and intervention group was deemed to exist if the p-value for either of the test statistics was less than 0.05. To fully assess the effective use of femoral neck modularity, the neck choice made in the clinical trial was also evaluated, post-operatively. To do this, those implants in the intervention group with impingement were fitted with alternative necks using the Kolibri workstation and reassessed. The propensity to impinge between the original control cohort and the modified neck cohort were then compared using Fisher's Exact Test for Independence to evaluate whether the neck choice made was optimal.

The final research objective presented in chapter 1 required an evaluation of the effectiveness of graphically representing hip joint range of motion in assessing operative outcome. To do this, the sensitivity of modelling prosthetic range of motion to changes in the operative parameters was assessed. An initial assessment of the sensitivity of the prosthetic motion area was made during the factorial experiments. If changes in the high and low values of the independent variables resulted in a change in the size and position of the prosthetic motion area then this would be an initial confirmation of the appropriateness of using the graphical range of motion benchmark to assess operative outcome. Secondly, the measurement of combined component anteversion was correlated to the measurement of the three-dimensional angle between the range of motion benchmark directional axis and the prosthetic motion directional axis, as well as the size of the prosthetic motion area between the control and intervention treatment groups. If correlation was found, then it would show that modelling prosthetic motion area measured against a range of motion benchmark was sensitive at picking up changes in the main independent variable being assessed in the clinical trial, femoral neck modularity (Saltelli et al., 2000).

3.4.5 Sample size

The sample size was calculated based on determining a significant difference between the primary outcome measures of propensity to impinge and impingement severity. This was done using a power analysis, which is used to prevent Type II errors occurring in hypothesis testing (Murphy et al., 2004). A Type II error occurs when the calculation for the study fails to detect statistical significance among groups in the sample population, when in fact there is a significant difference. Type II errors are associated with not having a large enough sample size in the study to detect a significant difference between treatments when one exists. The study of Toni et al. (2001), discussed in section 2.6 of chapter 2, was used as the basis of the power calculation. In their study, almost 20% of primary osteoarthritis patients were required to be fitted with a non-straight modular neck in order to restore hip joint biomechanics. Therefore, using the standard 80% power to detect a 0.2 difference with a significance level of $\alpha = 0.05$ between the modular and non modular treatment groups. Using the statistical tables shown in Murphy et al. (2004), an estimated sample size of 49 in each treatment group was determined. To account for possible losses a total of 141 patients were recruited for the study as shown in Figure 3.4.

3.4.6 Sampling errors

In the previous section, the concept of a Type II error was introduced, when a study infers that a treatment has no effect when in fact it actually does. It is also possible to have a Type I error, where a study infers that a treatment has an effect when in fact it does not (Murphy et al., 2004). This type of error is associated with errors in the sampling strategy and bias. Bias is reduced through the identification and control of confounding variables, which are those variables that cannot be separated (Chow and Liu, 2004). In the planning of the clinical trial various independent variables which effect range of motion were identified. Post-operatively, other than femoral neck modularity, if a difference was found to exist in the distribution of these independent variables. Then the results were able to be reprocessed in the Kolibri workstation removing these effects, so that any difference between the treatment effects were not confounded. Further, in clinical trials randomisation between familiar and unfamiliar procedures can introduce bias against the new treatment (Ahn et al., 2009; Piantadosi, 2005). All surgeons taking part in the clinical trial were experienced with THA procedures using the implants used in both treatment groups. However, none of the surgeons were experienced with using the surgical navigation measurement equipment. To minimise the risk of measurement error, all surgeons took part in training sessions using the navigation equipment. The significance of measurement error in the study design will be discussed further in chapter 5. A further source of variability which was controlled in the study was the surgical approach, the same posterior approach was used in all cases. This ensured that an observed variability between the treatment groups was associated with the implants rather than the surgical technique.

The steps taken detail how possible sources of known variability were controlled for in the clinical trial. However, there were sources of variability that may not have been identified which could affect the validity of the clinical trial result. Randomisation was used to ensure that known and unknown confounding factors were evenly distributed into both groups. Selection bias was avoided by using a computer generated sequence developed by the trial coordinator to allocate patients into either the control or intervention treatment groups

(Chung and Burns, 2008). The coordinator was also blinded to which treatment group they were allocating the patients. This meant that any confounding variables were evenly spread between the two treatment groups. Finally, individuals whom it was thought could subjectively or judgementally bias the study were blinded from any information which could affect their assessment or response to treatment (Chow and Liu, 2004). All surgeons and research staff involved in the administration of the clinical trial were blinded from the individual patient range of motion results until the end of the study. Also, patients were blinded from their allocation of treatment group until the day of the surgery.

3.4.7 Summary

This section has detailed the data collection methods applied in the randomised controlled trial to be able to fulfil the requirements of the final two research objectives for the study. It has also explained how systematic biases and confounding variables were controlled for during the administration of the clinical trial. However, this control only assumed that variables were measured without error (Piantadosi, 2005). There are two concepts which need to be assessed in order to address measurement error, measurement validity and measurement reliability. These will be considered in the chapter 5

3.5 Summary

In this chapter, based on the the scope of the research presented in chapter 1 and findings of the review of the literature presented in chapter 2. The requirements for the research objectives were discussed and a two-stage research design was selected. A systematic review methodology was designed in order to capture hip joint motion data from which to establish a graphical representation of the range of motion benchmark using the knowledge determined through establishing the theoretical foundation. This graphical range of motion benchmark was designed to be implemented into an appropriate experimental methodology to assess the outcome of THA procedures, specifically the effectiveness of femoral neck modularity. The randomised controlled trial was selected as the ideal experimental method, with detailed intervention and outcome measures to both assess the effectiveness of the femoral neck modularity but also the suitability of the developed graphical range of motion benchmark. Each of the research instruments have been considered for reliability and validity in their construction.

Now that the full research design has been developed and discussed, a full research process for the study can be produced which provides an overall schematic for the research linking all the instruments discussed. This research model is shown in Figure 3.11, which provides a detailed overview of the design, theory building, data collection and analysis phases which form the research methodology for this study. The findings from the research design to address the research objectives are discussed in chapters 4-6.

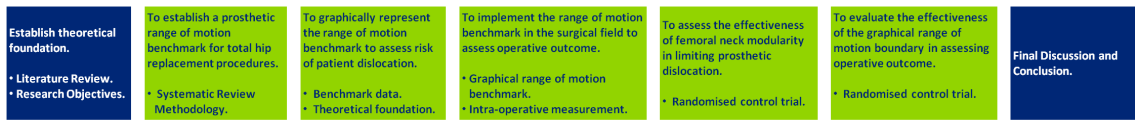


Figure 3.11: Overview of research design.

Chapter 4

Establishing a range of motion benchmark

4.1 Introduction

In chapter 1 it was shown that determining the boundary within which an impingement free range of motion is required would aid surgeons to plan the operative procedure. At present, specifications for range of motion outcome post-THA have either been based on the limits of pure joint motion or from measuring joint rotations for specific activities of daily living. The review of the literature established the current limitations with regard to modelling hip joint motion. Therefore, the need to have range of motion benchmark has been determined and the theoretical foundation regarding its construction established. This chapter aims to answer two of the research objectives detailed in chapter 1.

- To establish a prosthetic range of motion benchmark for total hip replacement.
- To graphically represent the range of motion benchmark to assess risk of dislocation.

Chapter 3 presented a systematic review methodology to extract hip joint range of motion data. This chapter will present the findings of this systematic review and use it to develop a graphical range of motion benchmark which has been published by Turley et al. (2011).

4.2 Establishing range of motion values

The systematic review methodology presented in chapter 3 aimed to obtain information defining typical activities of daily living and experimental data with regard to pure joint motion and activities of daily living. Pure joint motion refers strictly to the motions of flexion/extension, abduction/adduction and internal/external rotation, shown in Figure 2.3 on page 14. These motions occur in only one of the clinical planes - sagittal, coronal and transverse, respectively. Activities of daily living have out of anatomical plane motion. Consequently, they have combined amounts of flexion/extension, abduction/adduction and internal/external rotation. Section 4.2.1, presents the results of the literature search relating to pure joint motion, while section 4.2.2 presents the results relating to activities of daily living.

4.2.1 Pure joint motion

Articles relating to measurement or benchmark values for pure joint motion were identified from the systematic search of the literature. The purpose was to determine reference pure joint motion boundary conditions to ensure impingement free motion. The values for pure joint motion presented in these articles were categorised into three classes.

- **[Clinical]** - Clinical measurements of hip joint motion using goniometer or photographic techniques (Ahlberg et al., 1988; Boone and Azen, 1979; Davis et al., 2007; Gajdosik and Bohannon, 1987; James and Parker, 1989; Johnston and Smidt, 1970; Nonaka et al., 2002; Roach and Miles, 1991; Roaas and Andersson, 1982; Svenningsen et al., 1989).
- **[Reference]** - Reference values of hip joint motion without indication of distribution, from orthopaedic and physical therapy literature (American Academy of Orthopaedic Surgeons, 1965; Cailliet, 1978; Cole, 1971; Daniels and Worthingham, 1972; Green and Heckman, 1994; Hoppenfeld and Hutton, 1976; Japanese Orthopaedic Association, 1995; Kendall et al., 1971; Mohr, 1989; Stuchin, 2008).

- **[Simulation]** - Pure joint motion benchmarks for use in computer simulations (D'Lima et al., 2000; Kessler et al., 2008; Noble et al., 2003; Seki et al., 1998; Sun et al., 2007; Thornberry and Hogan, 2009; Widmer and Zurfluh, 2004; Widmer and Majewski, 2005; Yoshimine, 2005, 2006).

The **[Simulation]** category was excluded from the study as their values for pure joint motion were derived as a basis from which to assess THA procedures in computer simulations, rather than actively measuring the amount of pure joint motion. Therefore, these values are likely to over-estimate the range of motion requirement and are larger in all anatomical planes when compared with the other two categories (Noble et al., 2003).

To be able to derive a prosthetic range of motion benchmark for all anatomical planes, it was required to infer a boundary within which patients would be impingement-free post-THA, during their activities of daily living. It was found that, owing to the ability of subjects to compensate through inter-joint adaptation, many activities of daily living including those at the higher end of the demand scale could be done by THA patients within a tighter mean boundary than many of the defined **[Reference]** values (Davis et al., 2007; Johnston and Smidt, 1970). This will be discussed further in chapter 7. Based on this finding and the elimination of the **[Simulation]** articles, the **[Clinical]** measures were compared further to the **[Reference]** figures.

All **[Reference]** values, excluding the paper by Stuchin (2008), made recommendations for the maximum amount of joint excursion in each of the clinical planes. These recommendations for pure joint motion differ by 5° in the coronal plane to a discrepancy of 20° in the sagittal plane. **[Clinical]** measurements were evaluated for suitability to providing a good comparison with the **[Reference]** figures. Measurements of healthy individuals between the ages 20-70 provide the most stable and realistic sample from which base a range of motion benchmark (James and Parker, 1989; Roach and Miles, 1991). To obtain samples of pure joint motion that can be compared, measurements of healthy male subjects from Europe and North America were used. Four papers satisfied these criteria (Boone and Azen, 1979; Roaas and Andersson, 1982; Roach and Miles, 1991; Svenningsen et al., 1989).

	Mean	Extension	Abduction	Adduction	Internal Rotation	External Rotation
Reference	120°	30°	45°	35°	45°	45°
+1SD	130°	37.5°	55°	40°	52.5°	52.5°
+2SD	140°	45°	65°	45°	60°	60°

Table 4.1: Recommended reference and distribution figures for pure joint motion of the hip.

Two of the presented studies measured pure joint motion using the active method (Boone and Azen, 1979; Roach and Miles, 1991) while the other two studies used the passive method (Roaas and Andersson, 1982; Svenningsen et al., 1989). Passive and active range of motion measurements differ by the way the joint is manipulated during measurement. An active range of motion study is characterised by the examinee moving their joint under their own effort. In a passive range of motion study, it is the examiner that manipulates the limb by applying a force until it is felt the peak amplitude is reached (Gajdosik and Bohannon, 1987). Therefore, active range of motion studies were selected because the measurement of pure joint motion is performed under the motivation of the subject, aligning the method closer to the way activities of daily living are performed. Therefore, the two active range of motion measurement studies were compared with the **[Reference]** values. These studies fell within the 5 – 20° range of the **[Reference]** values in both the coronal and sagittal planes. In the transverse plane, one of the studies fell below the lower limit of the **[Reference]** range (Roach and Miles, 1991). Therefore, based on this alignment between the **[Clinical]** and **[Reference]** values, the articles quoting the higher pure joint motion values within the **[Reference]** group were taken to be the recommended mean pure joint motion values for a healthy population. Distribution was estimated by pooling the standard deviation values from the two active range of motion **[Clinical]** studies for each element of pure joint motion. Table 4.1, provides these benchmark figures.

4.2.2 Activities of daily living

A dislocation event relates in 90% of cases to when a patient's range of motion moves outside the boundary that the THA can accept (Scifert et al., 2001). The direction of dislocation has been traced in studies to particular types of movement or posture (Nadzadi et al., 2003; Pedersen et al., 2005). As well as these risk manoeuvres, there are other movements and postures that a person is likely to assume during the course of their daily activities. These range from high demand postures considered to be advanced activities (Hemmerich et al., 2006; Mulholland and Wyss, 2001). To activities which are less demanding but are essential for a person's mobility and their ability to care for themselves (Hemmerich et al., 2006). Articles relating to activities of daily living from the pool of selected articles were categorised for the purposes of this study, as follows.

- **[Gait]** - Motion analysis studies of particular activities of daily living (Costigan et al., 2002; Hagio et al., 2004; Hemmerich et al., 2006; Johnston and Smidt, 1969, 1970; Kadaba et al., 1990; Ko and Yoon, 2008; Nadzadi et al., 2003; Piazza et al., 2004).
- **[Model]** - Simulation of function with coupled joint motions (Amstutz et al., 1975; Barrack et al., 2001; Burroughs et al., 2001, 2005; Chandler et al., 1982; D'Lima et al., 2000; Jaramaz et al., 1998; Kluess et al., 2007; Krushell et al., 1991; Kummer et al., 1999; Miki et al., 2007; Noble et al., 2003; Sun et al., 2007; Thornberry and Hogan, 2009; Yoshimine, 2005, 2006).
- **[Definition]** - Articles which define activities of daily living (Mulholland and Wyss, 2001; Pedersen et al., 2005; Rowe et al., 2000; Weiss et al., 2002).

In total 31 separate activities of daily living were defined in the above literature. In terms of the **[Model]** category, many of the benchmark motions could be directly or indirectly traced back to the Johnston and Smidt (1970) study (Amstutz et al., 1975; Barrack et al., 2001; D'Lima et al., 2000; Jaramaz et al., 1998; Kluess et al., 2007; Kummer et al., 1999; Miki et al., 2007; Yoshimine, 2005, 2006). Therefore, based on this duplication of data the **[Gait]** group was used to obtain joint angle information for activities of daily living. Data


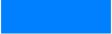







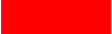





	Code	Description
	FXLG	Sitting on floor cross-legged (Hemmerich et al., 2006).
	KNEEL1	Kneeling with ankles dorsi-flexed (Hemmerich et al., 2006).
	KNEEL2	Kneeling with ankles plantar-flexed (Hemmerich et al., 2006).
	LEVEL	Level walking (Kadaba et al., 1990).
	PIVOT	Standing while turning the upper body away (Nadzadi et al., 2003) & (Ko and Yoon, 2008).
	ROLL	Lying supine, e.g. In bed and rolling over (Ko and Yoon, 2008).
	SQUAT1	Squatting with feet flat (Hemmerich et al., 2006).
	SQUAT2	Squatting balancing on flexed toes (Hemmerich et al., 2006).
	SSL	Stand-sit-stand from a low seat (~40cm high) (Nadzadi et al., 2003) & (Ko and Yoon, 2008).
	SSN	Stand-sit-stand from a normal seat (~46cm high) (Nadzadi et al., 2003) & (Ko and Yoon, 2008).
	STAIR	Ascending and descending stairs (Johnston and Smidt, 1970).
	STOOP	Standing then bending to retrieve object from floor (Nadzadi et al., 2003) & (Ko and Yoon, 2008).
	SWING	Swinging leg back and forth (Ko and Yoon, 2008).
	TIE	Sitting on a normal seat and bending to tie shoes (Nadzadi et al., 2003) & (Johnston and Smidt, 1970).
	XLG	Sitting on a normal seat and crossing legs (Nadzadi et al., 2003) & (Johnston and Smidt, 1970).

Table 4.2: Activities of daily living.

for a total of 15 activities could be obtained from six of these sources (Hemmerich et al., 2006; Johnston and Smidt, 1969, 1970; Kadaba et al., 1990; Ko and Yoon, 2008; Nadzadi et al., 2003). The remaining 3 articles could not be used owing to the data being measured from subjects having undergone THA (Hagio et al., 2004), or data was only presented for a limited number of clinical planes (Costigan et al., 2002; Piazza et al., 2004). Table 4.2, provides details of the 15 activities of daily living, plus a colour and a code for each particular activity. This will be used when the graphical range of motion benchmark is constructed in section 4.3.

The change in joint angles over the movement cycle has led some researchers to divide a manoeuvre into distinct stages, for example in level walking - heel-strike, foot-flat, heel-off and toe-off (Johnston and Smidt, 1969). For the referenced activities of daily living shown in

Table 4.2, the first reference for each activity was used to attain key points throughout the gait cycle. Key points were selected by identifying the points of maximum flexion/extension, abduction/adduction and internal/external rotation and then recording the corresponding joint angles at this point in the other two anatomical planes (Hemmerich et al., 2006; Johnston and Smidt, 1969, 1970; Kadaba et al., 1990; Nadzadi et al., 2003). The full gait cycle was not available for the SWING and ROLL manoeuvres, owing to the manoeuvres having predominance in one anatomical plane. The maximum joint angles were selected in these cases (Ko and Yoon, 2008). The key points were taken from gait cycles which presented the mean of the sample of cohorts measured. Of those activities which had one referenced article, the standard deviation of the manoeuvre could be obtained from that article. Those which had two referenced articles, the standard deviation was obtained from the second reference. The data relating to the ADLs described in Table 4.2 will be presented along with the pure joint motions detailed in Table 4.1 in section 4.3.

4.2.3 Summary

This section has described the process of extracting data from the articles obtained through the systematic search of the literature, described in chapter 3. This data has been used to establish benchmark data for the pure joint motions of flexion/extension, abduction/adduction and internal/external rotation. It has also obtained kinematic data for 15 separate activities of daily living. This data will now be used to construct a graphical representation of hip joint range of motion using the knowledge gained through establishing the theoretical foundation with regard to modelling hip joint motion in chapter 2. There have been a number of considerations which have had to be made in order to arrive at the benchmark data presented in this section. These considerations will be discussed further in section 7.2 of chapter 7.

4.3 Constructing the graphical representation

This section will describe how a graphical representation of the range of motion benchmark was constructed to represent hip joint movement as a continuum. In order to be able to construct this boundary the mathematical concepts with regard to describing human motion presented in chapter 2 will be used. Secondly, the concept of a motion pathway will be introduced. Finally, a mathematical description of the position of the range of motion benchmark will be presented. The constructed range of motion benchmark will then be validated in section 4.4.

4.3.1 Initial representation

The construction of the graphical representation of the range of motion benchmark used the anatomical coordinate frame presented in Figure 2.1 on page 11 as its basis. As defined in section 2.2 of chapter 2 this coordinate frame has the following axis notation.

- X-Axis: Medial/Lateral (Inboard to Outboard).
- Y-Axis: Anterior/Posterior (Front to Rear).
- Z-Axis: Superior/Inferior (Head to Toe).

As discussed in section 2.3, clinical rotations occur in a strict temporal order in a joint coordinate frame. The first rotation (f) occurs around the pelvic x-axis (flexion/extension). The second rotation (a) around a ‘floating-axis’ constructed as the vector cross-product of the pelvic x-axis and the femoral z-axis (abduction/adduction). The third rotation (r) is the internal/external rotation occurring about the femoral z-axis. The ‘floating-axis’ compromises the rotation matrix property of orthogonality, unless the coordinate frames of the pelvis and femur are coincident in the neutral posture. If this is the case, then the second rotation coincides with the y-axis of the femur, producing the rotation matrix detailed in equation 4.1 (Cappozzo et al., 2005; Chezea et al., 2009).

$$\begin{bmatrix} \cos r. \cos a & -\sin r. \cos a & \sin a \\ \sin r. \cos f + \cos r. \sin a. \sin f & \cos r. \cos f - \sin r. \sin a. \sin f & -\cos a. \sin f \\ \sin r. \sin f - \cos r. \sin a. \cos f & \cos r. \sin f + \sin r. \sin a. \cos f & \cos a. \cos f \end{bmatrix} \quad (4.1)$$

Using equation 4.1, when the body is posed in the neutral standing posture the knee centre position would lie directly below the hip centre (Luttgens and Wells, 1982; Rowley and Dent, 1997). Consequently, it would lie on the femoral z-axis and have position vector $\mathbf{p} = (0, 0, -1)$. To visualise the range of motion of the knee, as the hip joint moves, the knee centre position in three-dimensional space for any given manoeuvre would be defined by equation 4.2. Therefore, in three-dimensional space, the clinical rotations of flexion/extension and abduction/adduction define the position of the knee centre, while the internal/external rotation defines the long-axis orientation within that space (Cheng, 2004). This can be proven mathematically. Using the coordinate frame defined in this report, the position of the knee centre, using a standard femoral length, is defined by the position vector (0,0,-466) in the neutral position (Yoshioka and Cooke, 1987). To define the new position of the knee centre based from the joint angle information for a particular activity, this position vector is multiplied with the rotation matrix in equation 4.1. However, as the position vector only has a z-component. To define its position, only the last column of the rotation matrix is relevant, which is not influenced by internal/external rotation as equation 4.2 shows.

knee centre position = $\{[\sin a. - 466]x, [(-\cos a. \sin f). - 466]y, [(\cos a. \cos f). - 466]z\}$ or

$$\begin{bmatrix} \cos r. \cos a & -\sin r. \cos a & \sin a \\ \sin r. \cos f + \cos r. \sin a. \sin f & \cos r. \cos f - \sin r. \sin a. \sin f & -\cos a. \sin f \\ \sin r. \sin f - \cos r. \sin a. \cos f & \cos r. \sin f + \sin r. \sin a. \cos f & \cos a. \cos f \end{bmatrix} \cdot \begin{bmatrix} 0 \\ 0 \\ -466 \end{bmatrix} \quad (4.2)$$

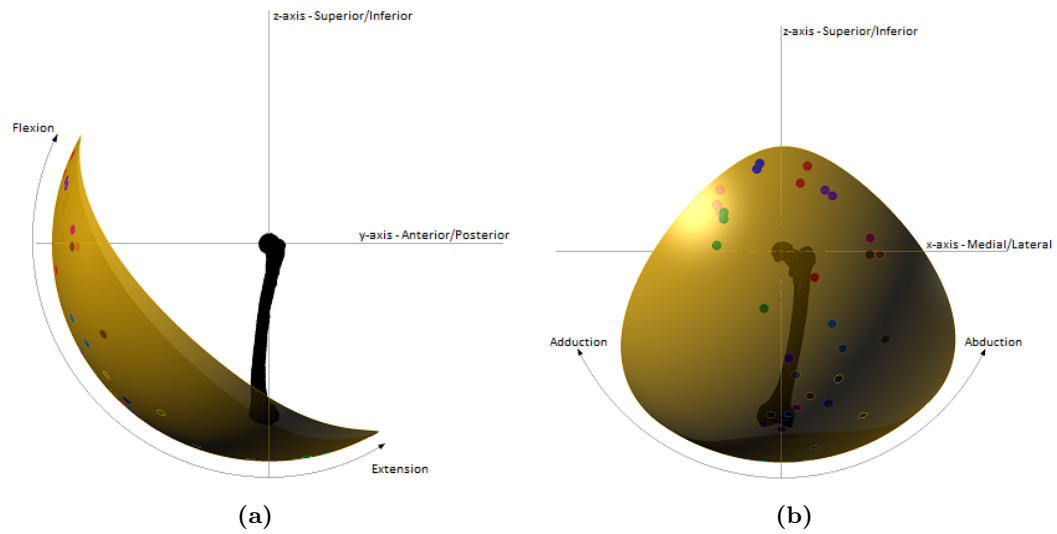


Figure 4.1: Initial three-dimensional range of motion representation (a) view of the initial range of motion in the sagittal plane *and* (b) view in the coronal plane.

An initial range of motion representation was constructed based on the mean reference pure joint motions of flexion/extension and abduction/adduction detailed in Table 4.1. This initial representation is shown in Figure 4.1, which shows the anatomical coordinate frame centred at the hip joint. As it is assumed that there are no translational effects in the hip joint, the position of the knee centre in three-dimensional space will appear as points on the surface of a sphere (Camomilla et al., 2006). To construct the initial boundary, the three-dimensional positions of the knee centre for the reference pure joint motion values of flexion, extension, abduction and adduction defined in Table 4.1 were plotted using equation 4.2 and a curve was interpolated between these values to produce a sphere segment. The knee centre positions correlating to key points in the movement cycle of the 15 activities defined in Table 4.2 were also plotted on the three-dimensional representation using equation 4.2 with the colour code detailed in the Table 4.2.

4.3.2 Final representation

The initial range of motion representation, shown in Figure 4.1, does not consider impingement due to long-axis orientation within the boundary which occurs because of internal/external rotation. To account for the effect of internal/external rotation, the axes of rotation for the researched activities of daily living were calculated. To maintain congruency with the right-hand rule, the researched internal/external rotation joint angles were multiplied by a factor of -1, as this would orientate the femur in the correct spatial context using equation 4.1 for a left hip. The axes of rotation and the rotation about each axis were calculated using equations 4.3 and 4.4 respectively (Cheng et al., 2000; Heading, 1958; Kuipers, 1999). Taking the composite rotation matrix constructed in equation 4.1 as matrix \mathbf{A} and the fixed axis of rotation as \mathbf{V} .

$$Q\mathbf{V} = \left[\mathbf{A} - \mathbf{A}^T \right] \mathbf{V} = \begin{bmatrix} 0 & -q_z & q_y \\ q_z & 0 & -q_x \\ -q_y & q_x & 0 \end{bmatrix} \cdot \begin{bmatrix} v_x \\ v_y \\ v_z \end{bmatrix} = \begin{bmatrix} 0 \\ 0 \\ 0 \end{bmatrix} \quad (4.3)$$

$$\theta = \arccos \frac{\text{Tr}(\mathbf{A}) - 1}{2} \quad (4.4)$$

The angles of the calculated fixed axes of rotation away from the anatomical transverse plane were plotted to see whether there were any similarities between the different phases of the movement cycle for the different activities of daily living. This plot is detailed in Figure 4.2, which shows that 70% of manoeuvres have their rotation axes within 15° of the transverse plane. This shows that flexion/extension and abduction/adduction are the dominant joint rotations for many activities, with the exception of standing while turning the upper body away (PIVOT) and lying supine then rolling over (ROLL). To simulate the effect of daily activities upon the initial three-dimensional range of motion boundary axes of rotation were defined by equation 4.5, based on this finding. These axes have been labelled as the ‘Transverse Plane Rotation Axes’.

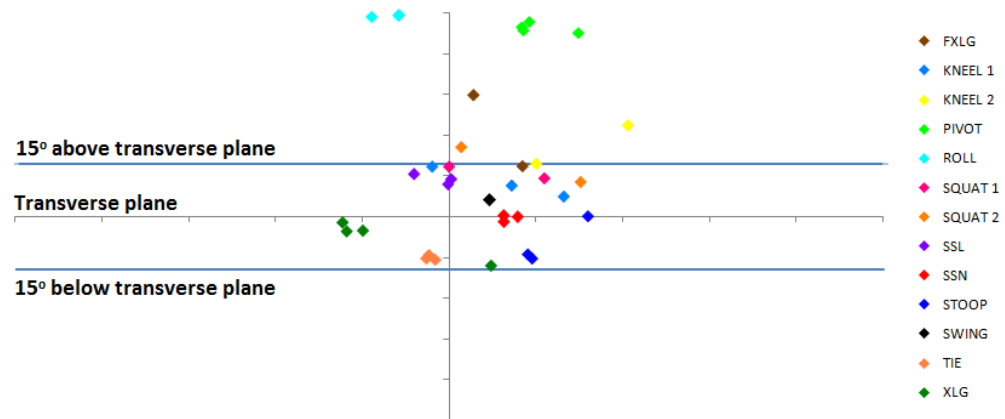


Figure 4.2: Deviation of daily activity fixed axis of rotation away from the transverse plane.

To simulate the effect of daily activities upon the range of motion representation that was shown in Figure 4.1. The knee centre was rotated around calculated axes in the transverse plane, equation 4.5. A visual representation of these rotation axes are shown in the Figure 4.3a. The angle ϕ in equation 4.5 distinguishes individual rotation axes in the transverse plane where ϕ was stepped around in 5° increments producing 72 separate rotations axes in the transverse plane. For each of the calculated rotation axis the knee centre was rotated in 1° (angle γ) increments around the rotation axis until it had reached the edge of the initial three-dimensional range of motion representation, shown in Figure 4.1. This produced a point cloud draped over the initial range of motion representation, shown in Figure 4.3b. For each knee position, Rodrigues' rotational formula was used to construct the composite rotation matrix that was shown in equation 4.1. Rodrigues' formula is shown in equation 4.6 along with how to calculate the constituent joint angles (Murray et al., 1994).

$$\text{Transverse Plane Rotation Axes} = (\cos\phi, \sin\phi, 0) \quad (4.5)$$

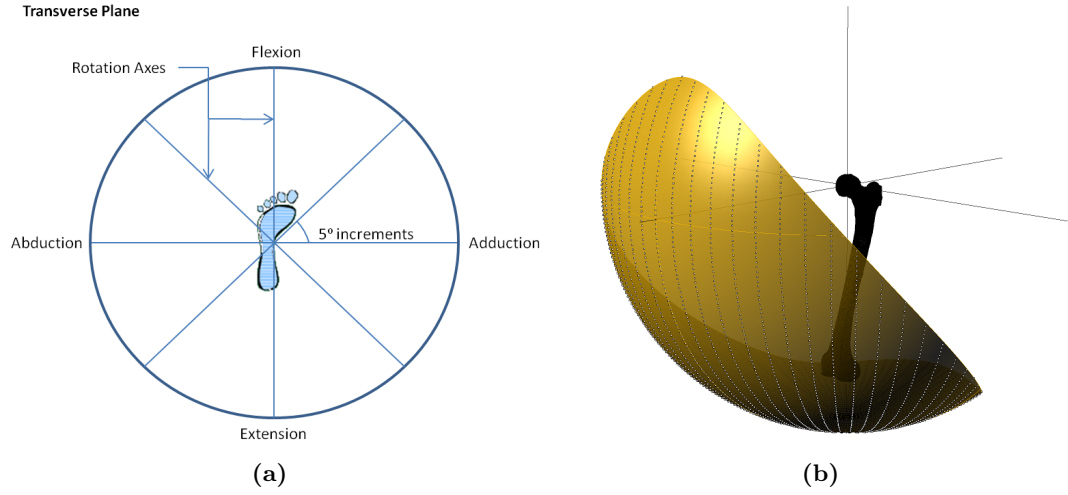


Figure 4.3: Modelling axes of rotation (a) representation of rotation axes in the transverse plane and (b) visual of rotation axes on the initial range of motion representation.

If rotation matrix takes the form:

$$\begin{bmatrix} a_{11} & a_{12} & a_{13} \\ a_{21} & a_{22} & a_{23} \\ a_{31} & a_{32} & a_{33} \end{bmatrix} =$$

$$\begin{bmatrix} v_x^2 + (1 - v_x^2)\cos\gamma & v_x.v_y(1 - \cos\gamma) - v_z.\sin\gamma & v_x.v_z(1 - \cos\gamma) + v_y.\sin\gamma \\ v_x.v_y(1 - \cos\gamma) + v_z.\sin\gamma & v_y^2 + (1 - v_y^2)\cos\gamma & v_y.v_z(1 - \cos\gamma) - v_x.\sin\gamma \\ v_x.v_z(1 - \cos\gamma) - v_y.\sin\gamma & v_y.v_z(1 - \cos\gamma) + v_x.\sin\gamma & v_z^2 + (1 - v_z^2)\cos\gamma \end{bmatrix}$$

Then:

$$\sin a = a_{13}, \quad \cos a = \pm \sqrt{1 - (\sin a)^2}, \quad \cos a = \begin{cases} -\cos a, & \text{if } |\arccos(\cos a)| > \frac{\pi}{2}, \\ +\cos a, & \text{otherwise} \end{cases}$$

$$\cos r = \frac{a_{11}}{\cos a}, \quad \sin r = \frac{-a_{12}}{\cos a}, \quad \cos f = \frac{a_{33}}{\cos a}, \quad \sin f = \frac{-a_{23}}{\cos a}$$

$$\text{flexion/extension} = \text{atan2}(\cos f, \sin f)$$

$$\text{abduction/adduction} = \text{atan2}(\cos a, \sin a)$$

$$\text{internal/external rotation} = \text{atan2}(\cos r, \sin r). - 1 \quad (4.6)$$

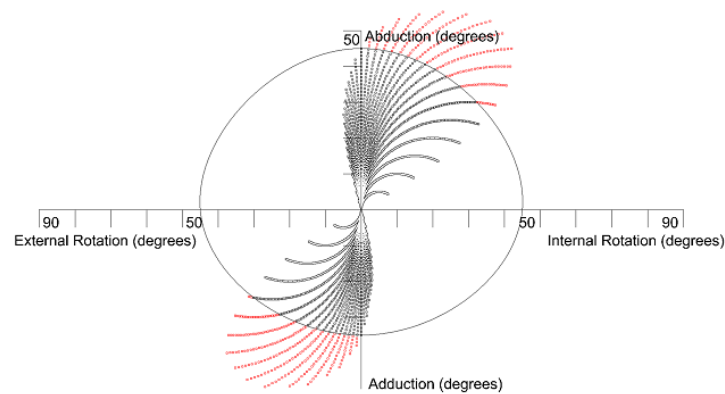


Figure 4.4: Knee centre joint angles in the coronal-transverse plane; impingement shown in red.

The joint angles for all knee centre positions were plotted on two, two-dimensional plots. These plots plotted **(a)** flexion, extension, internal and external rotation and **(b)** abduction, adduction, internal and external rotation. A curve was interpolated between these values to produce a range of motion boundary. Those joint angle positions which breached any of the constructed range of motion boundaries were designated impingement points, as shown in red in Figure 4.4. The Cartesian impinged knee centre positions were then plotted on the initial three-dimensional plot. This produced a range of motion boundary accounting for internal/external rotation, as shown in Figure 4.5. The area in red shows those positions on the initial three-dimensional plot which cause impingement due to internal/external rotation.

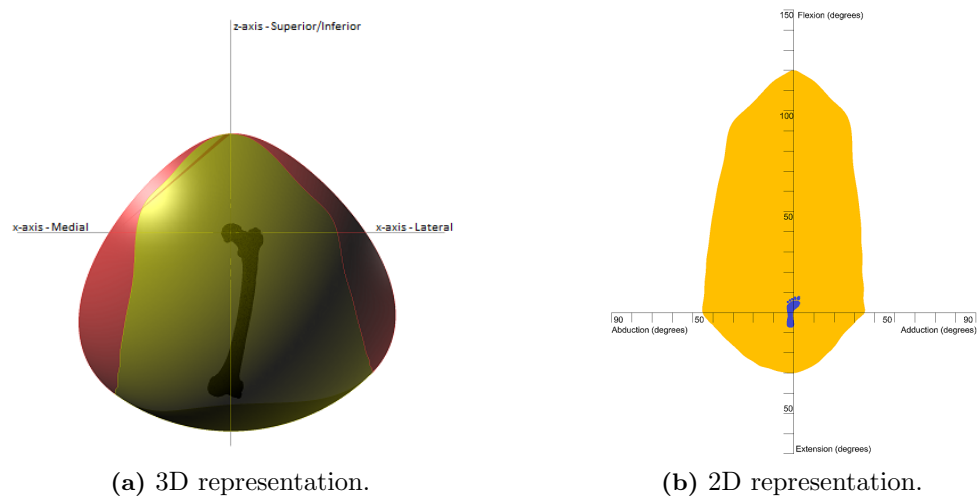


Figure 4.5: Final graphical representation of the range of motion benchmark.

4.3.3 Defining the position of the range of motion benchmark

As well as defining the shape of the range of motion benchmark, its position relative to the anatomical coordinate system needs to be described. This is to allow the position of a graphical representation of a prosthetic range of motion area to be described relative to the range of motion benchmark. To do this, a technique known as moment of inertia analysis was used (Davis, 2002; Fernández, 2005). This method defines a directional axis by constructing a best-fit plane from points taken on the boundary edge of a shape. To define the directional axis the pole to this plane is calculated (Fernández, 2005). The first stage in defining the directional axis was to define the position of the best-fit plane, which is located at the centre of mass of the boundary edge points of the range of motion benchmark, equation 4.7. To define the best-fit plane located at this centroid position, the distance of each point away from the centroid was calculated, equation 4.8, to produce a $3 \times n$ matrix, A . The dot product of $A.A^T$ produced a 3×3 matrix of the sum of squares and cross products of the direction cosines of each of the point vectors on the edge of the range of motion benchmark, equation 4.9 (Davis, 2002). This matrix defines the orientation of the best-fit plane, which minimises the orthogonal distance between each of the boundary edge points and the plane using the Total Least Squares method (Golub and Van Loan, 1980).

$$\begin{pmatrix} \bar{x}, \bar{y}, \bar{z} \end{pmatrix} = \frac{\sum_{n=1}^n x, y, z}{n} \quad (4.7)$$

$$\mathbf{A} = \begin{bmatrix} x_1 - \bar{x} & y_1 - \bar{y} & z_1 - \bar{z} \\ x_1 - \bar{x} & y_1 - \bar{y} & z_1 - \bar{z} \\ \dots & \dots & \dots \\ x_n - \bar{x} & y_n - \bar{y} & z_n - \bar{z} \end{bmatrix} \quad (4.8)$$

If:

$$a_i = \sum x_n - \bar{x}$$

$$b_i = \sum y_n - \bar{y}$$

$$c_i = \sum z_n - \bar{z}$$

$$\text{Then: } \mathbf{A} \cdot \mathbf{A}^T = \begin{bmatrix} \sum a_i^2 & \sum a_i b_i & \sum a_i c_i \\ \sum b_i a_i & \sum b_i^2 & \sum b_i c_i \\ \sum c_i a_i & \sum c_i b_i & \sum c_i^2 \end{bmatrix} \quad (4.9)$$

Matrix $\mathbf{A} \cdot \mathbf{A}^T$ is symmetric and therefore can be solved to find its eigenvalues ($\lambda_1, \lambda_2, \lambda_3$) and their associated eigenvectors (ν_1, ν_2, ν_3). ν_1 corresponds to the orientation of the maximum density of vectors, and lies on the best-fit plane. ν_2 lies in the same plane orthogonal to ν_1 (Fernández, 2005). ν_3 lies orthogonal to the other eigenvectors and is where the moment of inertia to the range of motion boundary edge vectors is at its greatest. This means that the distance between the range of motion boundary vectors and this eigenvector is the maximum possible (Davis, 2002). Hence, ν_3 corresponds to the orientation which contains the minimum density of vectors. Consequently, λ_3 will always be the smallest eigenvalue. ν_3 is the normal vector to the best-fit plane and defines the directional axis for the range of motion benchmark, equation 4.10. Figure 4.6, shows the directional axis for the range of motion benchmark.

$$\text{Range of motion axis} = (0.067x, -0.674y, 0.735z) \quad (4.10)$$

4.3.4 Summary

In this section the hip joint range of motion benchmark data determined in section 4.2 has been used to construct a graphical representation. The data used to construct this boundary was based from the mean reference values for pure joint motion and activities of daily living. This is because due to inter-joint adaptation many daily activities are able to be completed within this defined motion benchmark (Davis et al., 2007; Johnston and Smidt, 1970). This will be considered further in the chapter 7. The range of motion benchmark has been constructed, considering both the mathematical and clinical requirements for reporting joint angles. It has been found that the motions of flexion/extension and abduction/adduction define the position of the knee centre on the surface of a sphere. However, constructing a range of motion boundary using these values does not consider impingement due to internal/external rotation. Many motions are contained within axes that are less than 15° away from the transverse plane. Therefore, the analysis of the activities that a person is likely to undertake has been modelled within this range of motion representation. As well as defining its shape, the direction of the range of motion benchmark has also been defined. This means that two characteristics can be used to evaluate prosthetic range of motion, surface area and position. The following section will now validate the graphical representation of the range of motion benchmark.

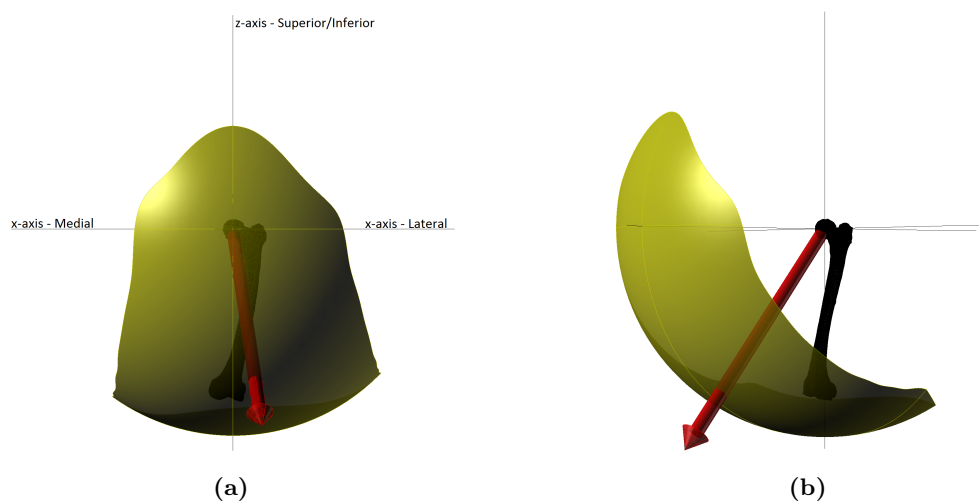


Figure 4.6: The range of motion benchmark directional axis.

4.4 Validation of the range of motion benchmark

In section 3.3.3 of chapter 3, it was described how as well as having a valid and reliable systematic review methodology to establish a hip joint graphical range of motion benchmark. The theoretical foundation which underpins the construction of the graphical representation using the benchmark data also needs to be validated. A methodology analysing the range of motion of 10 patient CT scans was proposed in section 3.3.3 in order to make this evaluation.

To run the range of motion simulations, the pelvic and femoral models first had to be aligned. In chapter 2, the different pelvic and femoral coordinate frames used in motion analysis (section 2.3) and THA (section 2.5) were discussed. In summary, there are two possible pelvic coordinate frames the APP and the TPP, Figures 2.2a and 2.10a respectively. In this experiment, both the APP and TPP landmarks were marked on the 3D pelvic model. The pelvic coordinate frame was defined from the TPP landmarks with the angle between the TPP and APP being measured. The pelvic coordinate frame using the landmarks of the TPP has been described in section 2.3.1 of chapter 2.

According to Wu et al. (2002), the femoral coordinate frame is constructed from the hip joint centre and the two femoral epicondyles. However, this forms a non-orthogonal coordinate frame and does not define the neutral rotation of the femur (Maruyama et al., 2001; Yoshioka and Cooke, 1987). Based on these findings, clinicians use the condylar axis to define the neutral rotation of the femur. Therefore, the posterior aspect of the femoral condyles was used instead of the femoral epicondyles as the basis from which to construct the femoral body segment coordinate frame (Mayr et al., 2007; Murphy et al., 1987). This femoral coordinate frame has been described in section 2.5.2 of chapter 2. This allowed both the pelvic and femoral coordinate frames to be aligned, whereby any joint angle decomposition would follow the matrix decomposition in equation 4.1.

To define the hip joint centre, the femoral head was disarticulated from the body of the femoral 3D model and a point was inserted at each node on the femoral head mesh. A

sphere was fitted to these points and the centre of which was defined as the hip joint centre. It has been argued whether the head of the femur can be approximated to be a sphere. Therefore, the maximum rms distance between the surface of the sphere and the point cloud was recorded. The diameter of the femoral head was also recorded.

With the pelvis and femur aligned, the Rhino VBScript language was then used to rotate the femur around the transverse plane rotation axes, equation 4.5. The femur was rotated around each axis, located at the hip joint centre, until collision occurred between pelvic and femoral model. The angle at which this collision occurred was recorded for each rotation axis and plotted in both two-dimensional and three-dimensional formats for analysis. Also, the three dimensional angle between the benchmark directional range of motion axis and the patient CT directional axes was calculated, shown in Figure 3.10b on page 64.

Patient	TPP-APP Angle	Femoral Head Diameter	Sphere RMS
Patient 1	95.6°	51.8mm	3.53mm
Patient 2	95.0°	47.1mm	1.34mm
Patient 3	94.6°	52.6mm	2.39mm
Patient 4	90.6°	48.1mm	1.50mm
Patient 5	88.4°	50.0mm	1.44mm
Patient 6	93.2°	53.6mm	1.53mm
Patient 7	100.5°	48.3mm	1.45mm
Patient 8	91.2°	50.5mm	1.22mm
Patient 9	99.8°	46.2mm	1.50mm
Patient 10	86.6°	50.4mm	1.35mm
Average	93.6°	49.8mm	1.72mm
σ	4.5°	2.4mm	0.71mm

Table 4.3: Summary of patient characteristics.

4.4.1 Results

Table 4.3, presents the measurement of the angle between the APP and TPP planes, femoral head size and the maximum rms distance between the femoral head surface and the best-fit sphere. The table shows that on average there is a 93.6° angle between the APP and TPP with a σ of 4.5° . The average femoral head size was 49.8mm with an average maximum rms distance between the surface of the femoral head and the constructed best-fit sphere being 1.72mm. The comparison of the experimental results with previous reported data for the discrete motions of flexion, extension, abduction and adduction has been reported in Table 4.4 (Kubiak-Langer et al., 2007; Tannast et al., 2007). There is a small difference with regard to the variation of experimental means as a percentage of the overall variation for the discrete motions of flexion and adduction. There is no more than 2° deviation between the means of the three experimental results for these motions. A small/medium effect was calculated for the motion of abduction with maximum deviation of 8° between the mean value of the current study and the previously reported studies. However, there was a larger difference with regard to extension, with a 20° difference between the mean of the current study and those by Kubiak-Langer et al. (2007) and Tannast et al. (2007).

Result		Kubiak-Langer et al. (2007) PV	Tannast et al. (2007) PV
Flexion	120° ($\sigma=10.2^{\circ}$)	$5*10^{-3}$ (Small)	$3*10^{-3}$ (Small)
Extension	77° ($\sigma=20.1^{\circ}$)	0.15 (Medium)	0.12 (Medium)
Abduction	56° ($\sigma=9.9^{\circ}$)	0.07 (Small/Med)	0.06 (Small/Med)
Adduction	33° ($\sigma=8.8^{\circ}$)	$0.5*10^{-3}$ (Small)	$0.1*10^{-3}$ (Small)

Table 4.4: Comparison of experimental results with previous studies.

4.4.2 Discussion

A two-dimensional plot of the average patient range of motion compared to the constructed range of motion benchmark is shown in Figure 4.7. This plot shows that the average patient range of motion does not encompass the constructed range of motion benchmark in the areas of adduction, abduction combined with flexion and slightly in flexion. These areas have been shown in red in both Figures 4.7 and 4.8. The amount of impingement equates to 0.3% of the surface area of the range of motion benchmark. These impingement points are recognised to be areas within a person's range of motion which suffer from bony impingement (Kubiak-Langer et al., 2007; Tannast et al., 2007; Thornberry and Hogan, 2009). Consequently, this provides confidence that the range of motion benchmark in these areas is correct. In all other areas except for extension and adduction combined with flexion the patient range of motion is slightly more than the range of motion benchmark. This is congruent to the findings of Tannast et al. (2007) and Thornberry and Hogan (2009) who found that bone-on-bone impingement would slightly overestimate the required range of motion because of the absence of soft tissue.

There are two areas where the patient range of motion is significantly larger than the range of motion benchmark. These are in the areas of extension and adduction combined with flexion. It has been found that motion in extension is not limited by bony impingement, rather it is limited by soft tissue tension. Consequently, the patient range of motion in this area can be regarded as clinically non-relevant (Kurtz et al., 2010). Less has been written about the extra motion in adduction combined with flexion. It is hypothesised two reasons could cause this extreme deviation between the patient range of motion and the range of motion benchmark in this area. Firstly, it is not possible to measure true geometrical adduction as a medial rotation in the coronal plane, the opposite leg obstructs the motion. Therefore, measurement of hip joint adduction, follows a diagonal motion as the adducted leg is moved in front of the stationary leg, as shown in Figure 2.3c in section 2.3.1. Therefore, the construction of the range of motion benchmark should have considered the pure joint motion adduction benchmark value of 35° in this diagonal plane

rather than the coronal plane, so that range of motion benchmark aligns with this natural boundary rather than a geometrically constructed one. Secondly, the extra motion in adduction combined with flexion as exhibited by the patient range of motion may not be limited by bony impingement as motion in this location takes the femur into the acetabular notch, permitting extra motion. It is more likely that motion is limited in this area by tension in the adductor muscles. These two hypotheses are a source for extra investigation for the study.

The directional axes presented in the three dimensional plot shows that while the three-dimensional angle between the range of motion benchmark axis (red) and the patient range of motion axis (purple) is 15.4° . The angle in the transverse plane between the two axes is only 3.1° . Consequently, the deviation in the two axes is largely due to the extra motion exhibited in extension and discounting the effect of this clinically non-relevant motion the position of the two range of motion plots align very closely. Thus providing validation for the range of motion benchmark.

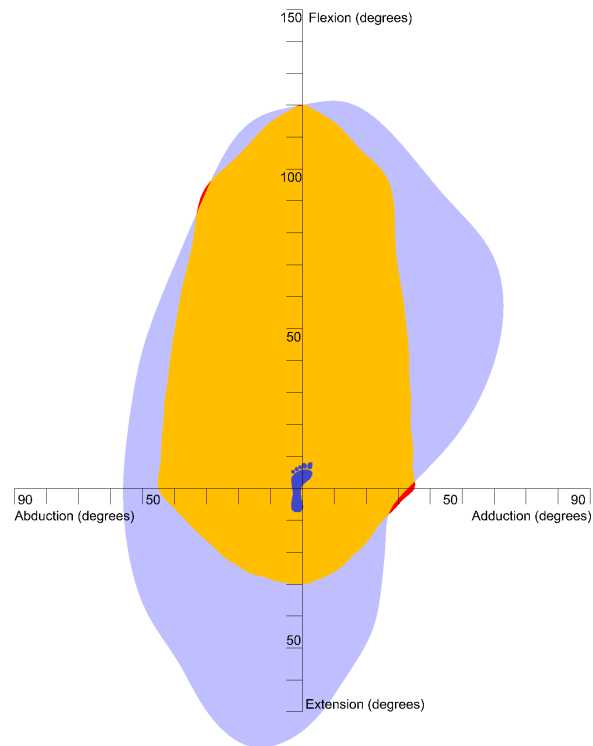


Figure 4.7: Two dimensional plot of patient average range of motion compared to the benchmark.

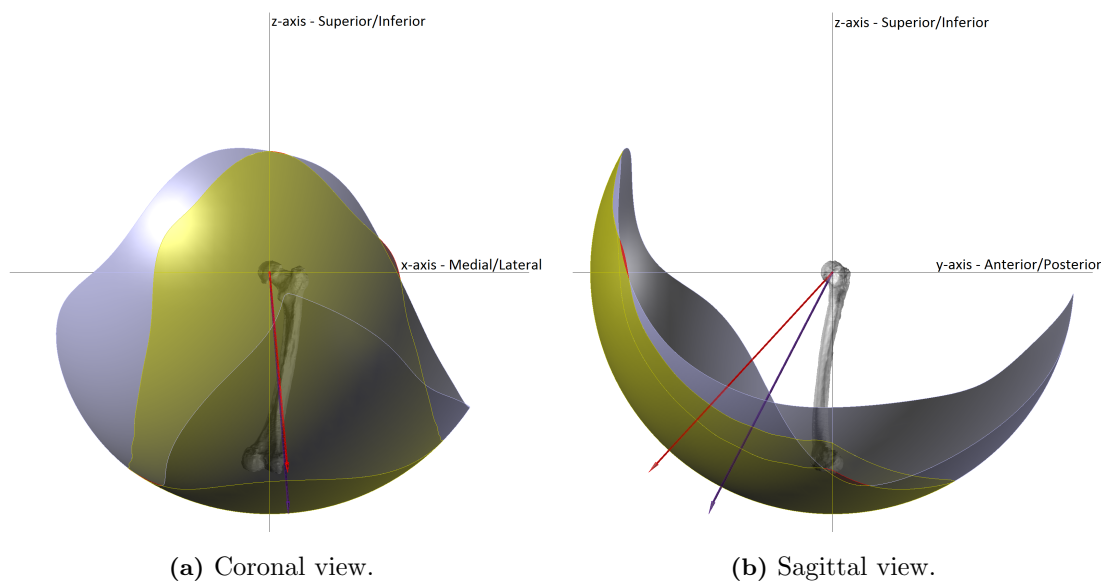


Figure 4.8: Three dimensional plot of patient average range of motion compared to the benchmark.

4.4.3 Summary

In this section the results of the experiment to validate the graphical representation of hip joint range of motion has been presented. The purpose of the experiment was to validate the benchmark data presented in section 4.2 and the theoretical foundation underpinning its construction which was presented in section 4.3.

The experiment had three research objectives - **(1)** to assess the validity of modelling the hip joint as a perfect 'ball and socket' **(2)** to assess the congruence of the pelvic coordinate frames and **(3)** to assess the validity of the graphical representation of the range of motion benchmark. The validation experiment has provided answers to these three objectives and will be discussed in section 7.2.2 of chapter 7. In summary, the modelling assumptions used in the construction of the range of motion benchmark are valid. However, with regard to the experimental boundary the motion in adduction combined with flexion is greater than what the benchmark graphical representation expresses. No activities of daily living have been found in the literature which fall into this area. Therefore, the graphical representation provides a basis from which to assess THA considering all aspects of a person's daily activities.

4.5 Summary

In this chapter, based on the systematic review methodology presented in chapter 3, benchmark data regarding hip joint range of motion was determined. These findings included data relating to both pure joint motion and the activities that a person is likely to undertake during the course of their daily routine. It was found that, owing to the ability of subjects being able to compensate for limited motion in one joint through inter-joint adaption, a minimum permissible range of motion was needed to be established. This was found to be the mean of a population's range of motion (Davis et al., 2007; Johnston and Smidt, 1970). The benchmark data was then taken to construct a graphical representation of hip joint range of motion. This has been constructed considering both the mathematical and clinical requirements for reporting joint angles. As well as defining the shape of the range of motion benchmark, its direction has also been defined. This means that two characteristics of the benchmark can be used for comparison to evaluate prosthetic range of motion, its surface area and its position. Finally, the graphical range of motion benchmark has been validated through analysing the range of motion of patient CT scans. The experiment has validated both the benchmark data produced as a result of the systematic review of the literature and the theoretical foundation with regard to modelling human movement. The purpose of this chapter was to answer the first two research objectives which were detailed in chapter 1 and again at the beginning of this chapter. The extent to which this has been achieved will be discussed further in section 7.2.2 of chapter 7.

Chapter 5

Post-operative assessment using the range of motion benchmark

5.1 Introduction

In chapter 1, it was shown that determining a boundary within which patients would be impingement free would aid surgeons to plan the operative procedure. It would also be able to provide information with regard to the effectiveness of the operative outcome post-THA, in particular its resistance to dislocation. In chapter 4, a graphical representation of the range of motion benchmark was developed and validated. This chapter presents how the range of motion benchmark was implemented with the aim of answering the following research objective.

- To provide an assessment of post-operative outcome using the range of motion benchmark.

The research methodology chapter, in section 3.4, presented a randomised control trial methodology. The results of this experiment are used to analyse the effectiveness of femoral neck modularity in THA. This chapter will describe how the graphical representation of hip joint range of motion was implemented in order to be able to make the assessment.

5.2 Implementation

In section 3.4.3 of chapter 3, a surgical navigation system was described which could be used intra-operatively to measure the orientation of the pelvic acetabular cup and femoral stem. It is this measurement information along with the geometrical specification of the prosthetic components that were used in order to be able calculate the prosthetic range of motion for each patient. This section will describe the measurement protocol for the surgical navigation measurement system. It will detail how this measurement information was used to graphically represent prosthetic range of motion for comparison with the benchmark representation which was constructed in the previous chapter.

5.2.1 Measurement protocol

This section describes the measurement protocol that the surgeons taking part in the randomised controlled trial were required to follow. In the surgical set-up, the patient was positioned in the lateral position (DiGioia et al., 1998). A rigid T-shape three marker array was then fixed to the patient's pelvis on the side being treated, approximately 5cm posterior to the treated ASIS. A Y-shape three-marker array was then fixed to the patient's femur being treated, 5-7cm proximal to the lateral epicondyle. The Kolibri workstation was positioned so that the two arrays were within its field of view, Figure 5.1c. This allowed the local array coordinate frame position and orientation of the patient pelvis and femur to be tracked. To establish the pelvic coordinate frame the landmarks of the APP were palpated using the Brainlab three-marker pointer, Figure 3.9b on page 63. The digitised landmarks were able to be tracked relative to the pelvic array. These landmarks were the treated side and untreated side ASIS and the treated side and untreated side PTUB, which were shown in Figure 2.10a on page 30. The construction of the pelvic coordinate frame using the landmarks of the APP has been described in chapter 2 in section 2.5.1.

Once the pelvic landmarks had been acquired, the surgeon positioned the leg in the anatomical neutral position so that the femoral superior-inferior or mechanical axis was

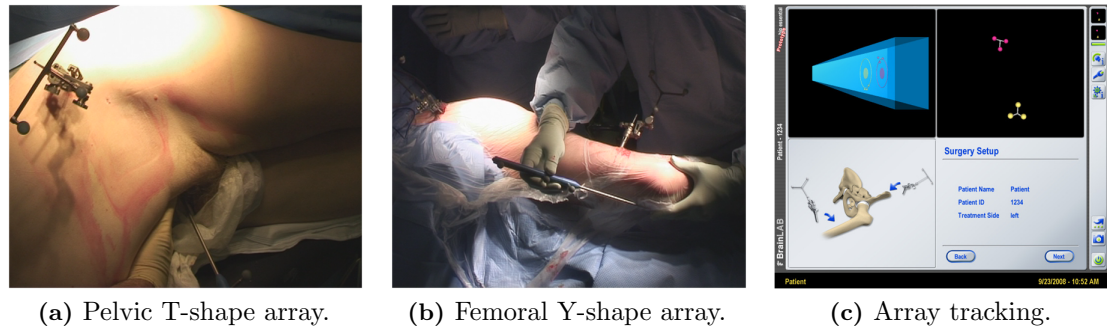


Figure 5.1: The surgical navigation setup.

parallel to the longitudinal axis of the body. This aligned the mechanical axis of the femur, once established, with the superior-inferior z-axis of the pelvis. Prior to incision, the landmarks of femoral medial and lateral epicondyles and the ankle medial and lateral malleolus were palpated to establish the femoral coordinate frame, relative to the femoral Y-shape array, Figure 5.1b. This should be done ideally when the knee is at 90° flexion. Following acquisition, the standard hip replacement procedure commenced. When the femur had been dislocated from the pelvis the surgeon palpated points inside of the pelvic acetabulum to determine the centre of the hip joint. A further landmark, the piriformis fossa of the proximal femur was also registered, shown in Figure 5.2a.

The femoral coordinate frame was constructed with the mechanical z-axis running in the positive direction from the centre of the two femoral epicondyles to the hip joint centre. The x-axis, running in the positive direction from left to right, was defined as the normal to the plane defined by the piriformis fossa, centre of the femoral epicondyles and the centre of the ankle malleoli, the Ankle Epicondyle Piriformis (AEP) Plane, Figure 5.2b. It is necessary to have the knee flexed to have enough non-collinearity between the three points to construct a good plane. The femoral y-axis was perpendicular to the x- and z-axes. The construction of this femoral coordinate system was used as a surrogate for the femoral coordinate system described by Murphy et al. (1987) and be congruent to the figure-of-four axis proposed by Mayr et al. (2007). It aims to define the neutral rotation of the femur (Maruyama et al., 2001; Murphy et al., 1987). The validity of this coordinate frame will be described further in section 5.3.

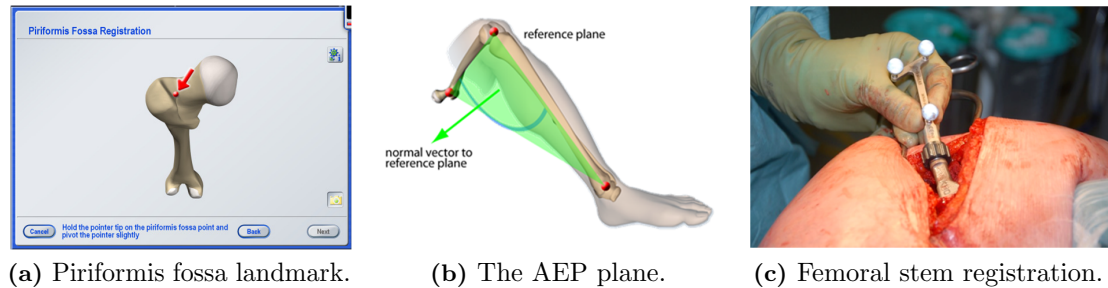


Figure 5.2: Femoral coordinate frame construction and implant registration.

Once the prosthetic components had been inserted, the component specifications were selected in the Hip Essential 5.1.2 software, i.e material selection, shell diameter, etc. The implant positions were registered by the surgeon, with the pelvic and femoral arrays attached. For the acetabular cup the pointer registered five points at the groove between the acetabular shell and liner - the superior rim, anterior rim, posterior rim, inferior rim and posterior inferior rim. The centre of the acetabular system was previously defined as the centre of the acetabulum. The measured position of the opening plane of the acetabular system provided its inclination and anteversion, defined using the operative convention, described in chapter 2 in section 2.4.1 (Murray, 1993).

To register the position of the femoral stem a further three marker array, the antetorsion device, was fitted onto the tapered interface of the proximal femoral stem, shown in Figure 5.2c. The position of the antetorsion device was measured relative to the femoral coordinate frame and provided the anteversion measurement of the femoral neck. Femoral anteversion was measured as the angular difference of femoral x-axis, defined as the normal to the AEP plane, and the neck axis when projected to a plane orthogonal with the mechanical axis. This measurement of anteversion is dependent upon the femoral x-axis defining the neutral rotation of the femur and will be analysed in section 5.3. Stem varus-valgus position in the medullary canal of the femur was not recorded by the software. These prosthetic component positions were used to construct a graphical representation of the prosthetic motion area, discussed in the following section.

5.2.2 Graphical representation of prosthetic range of motion

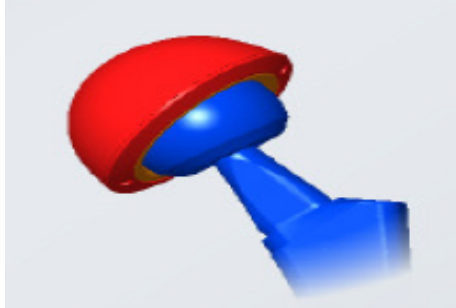


Figure 5.3: Total hip prosthetic position.

The measurements taken in section 5.2.1 allowed the orientation of the pelvic acetabular cup and femoral stem to be defined. The construction of the pelvic and femoral coordinate frames meant that their axes were aligned and coincident with the hip joint centre. Consequently, the acetabular cup and femoral stem were positioned in the correct relative orientation in a orthogonal

Cartesian coordinate frame. These orientation parameters were **(1)** the inclination of the acetabular cup (α) **(2)** the anteversion of the acetabular cup (β) **(3)** the angle between the femoral neck and the transverse plane (a) and **(4)** the version angle of the femoral neck (b). The geometrical product information of the independent variables described in chapter 3 in section 3.4.1 for the control and intervention treatment groups defined the oscillation angle θ . Consequently, all the parameters were defined so that the prosthetic range of motion was able to be calculated.

The measurements taken by the surgeon were used to position the prosthetic components in the correct orientation in the CAD environment, as shown in Figure 5.3. The transverse plane rotation axes defined in the chapter 4 in equation 4.5 were used to calculate the prosthetic range of motion. These axes were the same as those used to define the graphical representation of the range of motion benchmark. Using these axes, the femoral stem was initially rotated around the medial-lateral axis until collision occurred between the neck of the femoral stem and the rim of the acetabular cup. The axis was then stepped around in the transverse plane in $\phi = 15^\circ$ increments stopping at the point where collision occurred between the two prosthetic components. This continued until the axis had stepped back around to the medial-lateral axis. The angle at which collision occurred was recorded for each rotation axis and plotted to produce a graphical representation of the prosthetic range of motion, shown in Figure 5.4a.

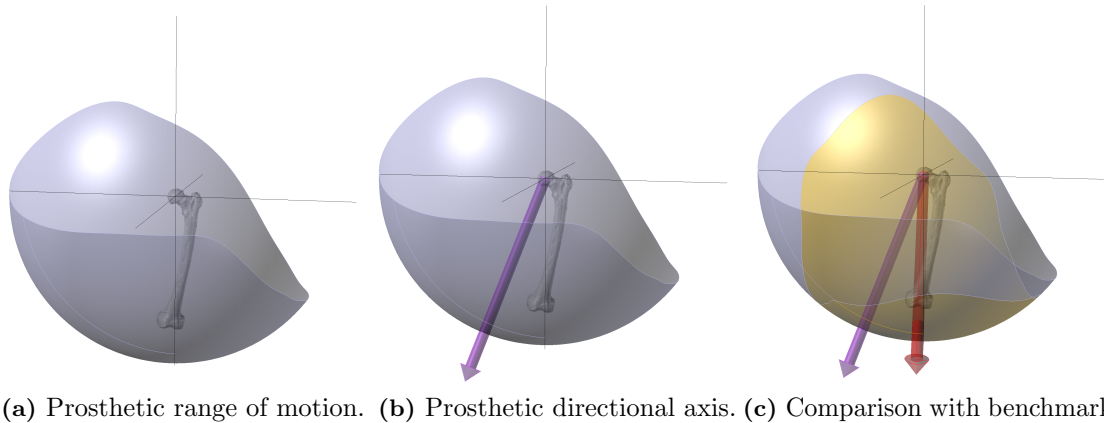


Figure 5.4: Implementing the hip joint graphical range of motion benchmark.

To provide information with regard to the position of the graphical representation of prosthetic range of motion, its directional axis was determined. This was done using the methodology developed in chapter 4 in section 4.3.3. Where a best-fit plane to the boundary edge of the prosthetic range of motion area was calculated and the normal to this plane defined the directional axis for the prosthetic range of motion area, shown in Figure 5.4b. The graphical representation of the hip joint range of motion benchmark could then be overlaid on the prosthetic range of motion area, shown in Figure 5.4c. The outcome measures described in chapter 3 in section 3.4.4 were then able to be calculated. These outcome measures were the three-dimensional angle between the two directional axes, which provided assessment of the position of the prosthetic motion area. The size of the prosthetic motion area, calculated as a percentage of the surface area of the range of motion benchmark. Hence, a prosthetic motion area having an area greater than 100% would be large enough to encompass the range of motion benchmark, providing it was the correct shape and was positioned correctly. If not, there would be impingement within the required range of motion benchmark which was also measured as a percentage of the range of motion benchmark area.

5.2.3 Summary

In this section the method for acquiring intra-operative measurements of prosthetic component orientation has been described. These intra-operative measurements were able to be used with the geometric information of the control and intervention implants to determine the prosthetic range of motion. This prosthetic range of motion has been graphically represented using the same methodology used to develop the graphical range of motion benchmark. Therefore, the two representations can be directly compared to be able to evaluate the size and position of a subject's range of motion post-operatively. This information will be used in chapter 6 to assess the effectiveness of femoral neck modularity with regard to its resistance to dislocation in comparison to an established control. Firstly, it must be assessed whether the prosthetic component orientation was measured without error. There are two concepts which need to be assessed in order to address measurement error, measurement validity and measurement reliability. These will be considered in section 5.3.

5.3 Measurement system assessment

To have an appropriate measurement system it has to be both valid and reliable. To be valid, the measurement tool has to provide the correct measurement for the research concept being observed. To be reliable, the measurement tool or methodology if reapplied should yield the same results. In section 5.2.1, the measurement protocol was outlined, many of the methods with regard to the construction of the body segment coordinate frames and reporting of component position have been applied in previous studies and standardised (DiGioia et al., 1998; Murray, 1993; Wu et al., 2002). However, the construction of the femoral coordinate frame uses the AEP plane, whose normal vector acts as a surrogate for the posterior condylar line used by Murphy et al. (1987) and accepted as standard. Section 5.3.1, presents an experimental methodology to assess the validity of using this alternative to the posterior condylar line, which was not accessible during the surgical procedure, to test measurement reliability. An inter-observer measurement study of the pelvic coordinate frame was conducted and presented in section 5.3.2 to assess measurement reliability.

5.3.1 Measurement validity

In section 5.2.1, it was described how in imageless-navigation the AEP plane is used instead of the condylar axis to define the neutral rotation of the femur. The AEP plane replicates the ‘figure of four’ axis used in non-navigated surgery as a reliable reference to the condylar axis (Mayr et al., 2007). The AEP plane is shown in Figure 5.2b. It is formed by the mid-point of the ankle malleoli, mid-point of the femoral epicondyles and the piriformis fossa. The normal vector to this plane along with the femoral mechanical axis defines the coronal plane of the femur. The pelvic and femoral coordinate frames are required to be aligned to be able to have accurate range of motion simulation and femoral anteversion measurement. Therefore, the constructed medial-lateral axis of the femur should be aligned with the medial-lateral axis of the pelvic coordinate frame. The femoral medial-lateral axis is a line normal to the AEP plane lying in the transverse plane. This alignment will be evaluated within this section.

Materials and methods

To test the validity of alignment between the pelvic and femoral medial-lateral axes, 18 subjects were recruited for a motion analysis experiment using a Vicon MX motion capture system located within The School of Engineering, The University of Warwick. Consent was obtained from all participants for their motion data to be used in the experiment. The Vicon MX motion capture system consists of 12 infra-red cameras located around the laboratory. The cameras track the position of passive marker spheres placed on the subject. The twelve infra-red cameras determine the marker coordinates in a wider field of view compared to the surgical navigation system described in chapter 3. Marker spheres were placed on the subject in the following locations - the medial and lateral ankle malleoli, medial and lateral femoral epicondyles, the pelvic right and left anterior superior iliac spines and the pelvic posterior superior iliac spines.

The angle between the pelvic and femoral axes was measured in the transverse plane, providing a measure of the difference between the pelvic coronal plane and the femoral coronal plane in which the AEP normal vector lies. If minimal deviation was found to exist, then it could be inferred that the normal vector to the AEP plane can reliably define the neutral rotation of the femur.

The first experiment determined the centre of the hip joint. This landmark is estimated based on the motion of the femur relative to the pelvis. It was required to be determined because the landmark of piriformis fossa was not accessible. Therefore, to form the AEP plane an alternative proximal femoral landmark was used as a surrogate, the hip joint centre. To begin the experiment, the subject was asked to stand, positioning themselves so that the centre of their knees were directly below the centre of their hip, defining the neutral posture (Luttgens and Wells, 1982). The subject was then asked to flex, extend, abduct and adduct their femur in the star-arc motion, as recommended by Camomilla et al. (2006). Once complete, the marker trajectories were used to calculate the hip joint centre using the bias compensated least squares estimate of centre of rotation developed by Halvorsen (2003). The hip joint centre was calculated relative to the local pelvic coordinate

frame based from the TPP. The mathematical formulae used to determine the hip joint centre in the first experiment is shown in Appendix A.

In the final experiment, the angle between the pelvic medial-lateral axis and the femoral medial-lateral axis was measured. Again, to start the experiment the subject was asked to stand in the neutral posture. The subject was then asked to flex their hip to approximately 65° and their knee to 90° , ensuring minimal leg adduction or abduction. Once complete, the AEP plane was calculated using the estimated hip joint centre, the mid-point of the two femoral epicondyles and the mid-point of the two ankle malleoli. The AEP plane normal was determined and used to construct the femoral coordinate frame. The angle between the pelvic medial-lateral axis and femoral medial-lateral axis was then measured. This measurement was taken in the transverse plane where the normal vector to the AEP plane is coincident with the femoral medial-lateral axis. Measurement of the minimum angle between the two axes was recorded as well as the angular deviation at 25° , 45° and 65° of hip flexion. The mathematical formulae used to construct the AEP plane and calculate this angle is shown in Appendix B.

To assess whether the normal vector to the AEP plane lies in the coronal plane. It was defined that the mean angle, in the transverse plane, between the medial-lateral axes of the pelvis and femur should be within 2.5° with a $\sigma = 2.5^\circ$. If the results of the experiment met these criteria then the normal vector to the AEP plane can be considered to lie in the coronal plane and be used as a basis from which to measure femoral anteversion.

Results

The measurements in the transverse plane between the pelvic medial-lateral axis and the femoral medial-lateral axis are shown in Table 5.1. The mean difference between the two axes is 0.38° with a $\sigma = 1.06^\circ$. This met the criteria for agreement defined for the study. Table 5.1, also shows how this angle changes over the movement cycle. This Table shows that the angle between the two axes can vary during the movement cycle. The hip flexion angles of 25° and 45° had better agreement between the axes and were less variable than a hip flexion angle of 65° . There was no correlation with regard to hip flexion angle and agreement of the AEP normal vector with the coronal plane.

Subject	Minimum Angle	25° flexion	45° flexion	65° flexion
1	0.002°	0.63°	5.63°	7.08°
2	0.001°	0.06°	2.35°	5.95°
3	-0.003°	2.96°	3.10°	0.74°
4	0.003°	2.91°	2.20°	3.40°
5	0.000°	2.79°	2.95°	1.65°
6	3.936°	6.65°	4.99°	5.59°
7	-0.001°	3.93°	5.10°	7.74°
8	-0.019°	3.53°	0.22°	2.58°
9	0.001°	1.24°	0.03°	1.56°
10	0.672°	4.91°	1.08°	3.08°
11	-0.152°	3.38°	2.98°	3.49°
12	0.001°	4.52°	2.63°	4.44°
13	0.003°	1.65°	2.89°	0.33°
14	-0.001°	1.38°	1.97°	2.97°
15	-0.005	1.60°	2.52°	2.50°
16	-0.003	0.82°	2.95°	6.60°
17	0.029	1.99°	2.83°	1.36°
18	2.357	2.97°	2.77°	5.67°
μ	0.379	2.66°	2.73°	3.71°
σ	1.056	1.68°	1.47°	2.27°

Table 5.1: Gait analysis method: angle between pelvic and femoral medial-lateral axes.

5.3.2 Measurement reliability

For a measurement tool to be reliable there must be confidence that if it is reapplied then the same results would be produced. Therefore, an inter-observer study was chosen to assess measurement reliability as it provides a measure of association between the measurements made by two different observers (Rees, 2001). If a high degree of association between the measurements made by the observers is found then this provides confidence that the measurement tool is able to be reapplied to produce the same results.

Materials and methods

To test inter-observer reliability, two surgeons used the surgical navigation measurement system to measure the APP pelvic landmarks of the patient. Each surgeon measured the APP landmarks once for each patient, for a total of 22 patients. The surgical set-up used was the same as the measurement protocol described in section 5.2.1. The pelvic T-shape and femoral Y-shape arrays were fitted to the patient by the surgeon conducting the operation. The Kolibri workstation was then positioned so that the two arrays were within the field of view. The surgeon not conducting the operation then registered the pelvic landmarks using the Brainlab three-marker pointer. When the first surgeon completed their registration, the pelvic registration step was then repeated by the surgeon conducting the operation. The surgery then proceeded as described in section 5.2.1, using the measurements made by the surgeon conducting the operation. It is regarded due to soft tissue coverage. Surgeon recognition of the pelvic landmarks is the limiting factor in the experimental reliability, rather than the registration of the clearly defined acetabular cup (DiGioia et al., 1998; Kelley and Swank, 2009). The technical report from the Kolibri workstation contained the x, y, z coordinates for both surgeons' measurement of the pelvic landmarks and the reported acetabular cup operative inclination and anteversion made by the surgeon conducting the operation. Based on comparing the two pelvic coordinate systems constructed from the landmark measurements, the operative inclination and anteversion deviation between the two surgeons was compared using the calculation steps detailed in Appendix C

Results

Table 5.2, presents the results for the inter-observer reliability experiment. These results were used to calculate the Pearson correlation coefficient for both operative inclination and anteversion (Rees, 2001). The calculated correlations were $r = 0.93$ and $r = 0.96$ respectively for operative inclination and anteversion. The p-values for both correlations were less than 0.01 which meant that the inter-observer results were not significant to an $\alpha = 0.01$ level.

	1 st assessor inclination	2 nd assessor inclination	1 st assessor anteversion	2 nd assessor anteversion
	36.4°	27.6°	24.5°	30.2°
	46.5°	42.8°	22.6°	24.9°
	43.6°	42.0°	20.1°	18.9°
	26.4°	24.7°	18.8°	24.9°
	35.5°	37.1°	9.5°	12.8°
	32.3°	35.7°	1.2°	-4.6°
	36.4°	32.3°	48.9°	49.7°
	33.8°	31.4°	13.2°	19.1°
	25.1°	25.4°	44.3°	37.1°
	23.4°	22.2°	8.2°	13.7°
	36.0°	38.9°	9.6°	7.9°
	37.8°	40.1°	41.3°	45.2°
	40.1°	36.2°	7.8°	9.5°
	38.8°	37.5°	22.1°	27.5°
	44.8°	43.2°	42.4°	35.7°
	27.0°	28.9°	18.2°	18.0°
	40.7°	41.3°	43.0°	43.8°
	40.3°	35.1°	6.6°	4.7°
	30.6°	28.6°	12.0°	17.9°
	45.0°	45.6°	47.9°	47.0°
	36.1°	36.7°	23.1°	26.8°
	58.5°	55.1°	31.5°	37.2°
\bar{x}	37.1°	35.8°	23.5°	24.9°
σ	8.1°	7.8°	15.0°	14.8°

Table 5.2: Inter-observer results for the surgical navigation measurement system.

5.3.3 Summary of results

The experiments described in this section were conducted to assess whether the normal-vector to the AEP plane aligns with the medial-lateral axis of the pelvic coordinate frame and so accurately define the neutral rotation of the femur providing a reliable measurement of femoral anteversion and prosthetic hip joint range of motion. The inter-observer variability of the surgical navigation system used in this study was also assessed.

The results of the first experiment have shown that the medial-lateral axes of the femoral and pelvic coordinate frames align extremely closely with a mean deviation of 0.38° . This validates that when the posterior aspect of the femoral condyles are not available to construct the condylar axis. The AEP plane can be used to construct a coordinate frame which accurately defines the neutral rotation of the femur. Therefore, the AEP plane provides an accurate measure of femoral anteversion from which to infer prosthetic range of motion. The results of the second experiment show that measurements made by different surgeons have a high degree of association. It can therefore be concluded, that the measurement system used throughout the randomised controlled trial, whose results are described in the following section can be considered both valid and reliable.

5.4 Summary

In this chapter, based on the measurement of prosthetic component orientation and an implant's product geometry a post-operative prosthetic range of motion has been able to be calculated and represented graphically. This has used the same methodology developed for the benchmark graphical representation which was presented in chapter 4. This allows a patient's prosthetic range of motion to be directly compared to the benchmark standard to assess the operative outcome with regard to its resistance to dislocation.

This chapter has also considered the validity and reliability of both the experimental set-up and the navigation system used to measure the prosthetic component orientation. The navigation system has proven to be a valid method of recording the orientation of both the acetabular and femoral component, from which hip joint range of motion is calculated. The surgical navigation measurement system is also very reliable with a high degree of association between the component measurements of different surgeons.

The following chapter will now present the results of the randomised controlled trial described in section 3.4 in chapter 3. This chapter will present the results using the valid and reliable surgical navigation measurement system to assess the effectiveness of femoral neck modularity against an established control.

Chapter 6

Assessment of femoral neck modularity

6.1 Introduction

In chapter 4, a graphical range of motion benchmark was developed. The methodology for representing this benchmark was used to construct a patient's prosthetic motion area using intra-operative measurement. A randomised controlled trial was presented in chapter 3 to assess prosthetic range of motion compared to the developed benchmark. The results are presented in this chapter which were used to answer the following research objectives.

- To assess the effectiveness of femoral neck modularity in limiting prosthetic impingement.
- To evaluate the effectiveness of graphically representing hip joint range of motion in the assessment of operative outcome.

The first objective was split into two sub-objectives. Section 6.2, presents the results used to assess the influence of femoral neck modularity. Section 6.3, provides results related to how effectively it is being used. Finally, section 6.4, presents the results related to how effective the graphical representation is in assessing operative outcome.

6.2 Influence of femoral neck modularity

As stated in section 6.1, to assess the effectiveness of femoral neck modularity in limiting prosthetic dislocation. This research objective was required to be split into two further sub-objectives. This section presents the results which relate to the first sub-objective.

- To evaluate the influence of femoral neck modularity on hip joint range of motion.

In chapter 3, the independent variables which influence the size and position of the graphical representation of prosthetic range of motion were presented. These independent variables included those defined by Yoshimine and Ginbayashi (2002) and implant specific variables. Those defined by Yoshimine and Ginbayashi (2002) concern prosthetic component positioning - inclination of the acetabular cup (α), anteversion of the acetabular cup (β), the angle between the femoral neck and the transverse plane (a) and the version angle of the femoral neck (b). For the control treatment group further implant specific variables were identified as femoral head diameter, femoral head offset, acetabular liner rotation centre, neck offset, neck-shaft angle and stem length. The intervention treatment group implant variables were identified as femoral head diameter, femoral head offset, acetabular liner rotation centre, neck length and femoral neck modularity.

A full-factorial analysis was chosen to analyse the influence of femoral neck modularity on hip joint range of motion in relation to the other independent variables described. First, these independent variables were required to be screened to identify the main factors which influence prosthetic hip joint range of motion. Section 6.2.1 presents further definition with regard to the experimental independent variables. Section 6.2.2 presents the results of the screening experiment and section 6.2.3 the results of the full-factorial experiment.

	Cup Inclination		Cup Anteversion		Stem Version	
	Control	Intervention	Control	Intervention	Control	Intervention
Mean	36.7°	38.0°	23.1°	22.8°	8.9°	5.2°
S.D.	7.7°	6.7°	14.3°	15.2°	14.5°	13.0°
F-Test (p-value)	0.1687		0.3500		0.2325	
t-Test (p-value)	0.3729		0.9155		0.1853	

Table 6.1: Acetabular cup and femoral stem orientation.

6.2.1 Definition of independent variables

To screen for the main factors which influence prosthetic range of motion. A systematic fractional replicate design was chosen to be the suitable analysis method (Cotter, 1979). This method has been described in chapter 3 in section 3.4.4. To do this analysis, the high (+) and low (-) values for each of the independent variables had to be defined. These high and low values would interact to change the implant oscillation angle by altering the head-neck ratio or by changing the opening angle of the acetabular cup. The independent variables may also change the position of the primary arc of movement by altering the relative orientation between the acetabular cup and femoral neck. Those variables which were associated with the component orientation are presented in Table 6.1. This table details the acetabular cup operative inclination and anteversion and femoral version mean and standard deviation values for the two treatment groups. Due to the influence of femoral neck modularity upon femoral version, the intervention group results were reprocessed using straight necks to determine femoral stem version. Table 6.1, shows no significant difference in the component placement between the two treatment groups. Component positions for both treatment groups were combined and the high and low component positions were defined as **Mean** \pm **2 σ** . As well as the independent variables that were associated with component orientation, there were implant specific variables. Table 6.2 provides the high-low values for both treatment groups.

Control group high-low values					
Head Diameter	Rotation Centre	Head Offset	Neck Offset	Neck Angle	Stem Length
36mm	0mm	+3.5mm	High Offset	125°	Size 9
28mm	+2mm	-3.5mm	Std Offset	135°	Size 20

Intervention group high-low values					
Head Diameter	Rotation Centre	Head Offset	Neck Offset	Ante/Retro	Varus/Valgus
36mm	0mm	+3.5mm	Long Neck	15° Ante	15° Varus
28mm	+1mm	-3.5mm	Short Neck	15° Retro	15° Valgus

Table 6.2: Prosthetic high-low values.

6.2.2 Screening results

The results of the systematic fractional replicate design experiments are provided in Tables 6.3 and 6.4 for the control group and in Tables 6.5 - 6.8 for the intervention group. Two separate screening tests were required for the intervention group as it was not possible to combine the maximum 15° ante-retroverted neck with the maximum 15° varus-valgus options.

The outcome measures for the screening experiments were defined in section 3.4.4 in chapter 3. The first outcome measure was defined as the size of the prosthetic motion area, measured by its surface area as a percentage of the surface area of the range of motion benchmark. The second outcome measure was defined as the position of the prosthetic motion area as measured by the three dimensional angle between the prosthetic motion area directional axis and the directional axis of the range of motion benchmark. These outcome measures were shown in Figure 3.10 in section 3.4.4.

The initial results for the control treatment group show that rotation centre has the most significant influence upon the size of the prosthetic range of motion area, as measured by M . The orientation of the prosthetic components has the most influence upon the position of the prosthetic motion area. Higher values of C_e indicate interaction between the independent variables. There is evidence of interaction between component positioning and neck-shaft angle with regard to the positioning of the prosthetic motion area. For both outcome measures the variables of femoral head offset, neck offset and stem length have low values for both C_o and C_e , indicating that they are not main factors and have very limited interactive effect. Therefore, these factors were screened from the full factorial experiment and set at their economic values.

The initial results for the intervention treatment group showed evidence of a strong degree of interaction between the modular femoral neck and component positioning, both in ante-retroversion (Tables 6.5 and 6.6) and varus-valgus (Tables 6.7 and 6.8). This is shown by component positioning and the modular options having high and near equal C_e values. The estimated effect of the rotation centre as measured by $2C_o$ upon the size of

the prosthetic motion area was half compared to its equivalent in the control group. There was also an anomaly with regard to the influence of femoral head diameter on the size of the prosthetic motion area between the experimental results using the varus-valgus necks compared with those using the ante-retroverted necks. The estimated effect was three times greater on the prosthetic motion area when using varus-valgus necks and requires further investigation with a full factorial analysis in section 6.2.3. The main factors were identified as component positioning, rotation centre, head diameter and femoral neck modularity. The other factors were screened from the full factorial experiment and set at their economic values. However, it was noted that femoral head offset had a greater influence over the size of the prosthetic motion area in the intervention treatment group in comparison to the control treatment group.

	Prosthetic Area		
	C_o	C_e	M
Rot. Centre	13.84%	-0.56%	14.41%
Position	-4.68%	-2.16%	6.84%
Head Diameter	3.71%	2.98%	6.69%
Neck Angle	1.20%	-1.81%	3.01%
Head Offset	2.71%	0.18%	2.89%
Neck Offset	2.14%	0.76%	2.89%
Stem Length	0.76%	-0.46%	1.21%

Table 6.3: Control group screening results - prosthetic motion area.

	Angle Deviation		
	C_o	C_e	M
Position	-19.6°	-2.5°	22.1°
Neck Angle	-0.2°	-3.1°	3.3°
Rot. Centre	-1.2°	-1.0°	2.2°
Head Diameter	-0.3°	-0.8°	1.1°
Stem Length	-0.3°	-0.7°	1.0°
Head Offset	-0.6°	-0.4°	1.0°
Neck Offset	-0.5°	-0.5°	1.0°

Table 6.4: Control group screening results - prosthetic angle deviation.

	Prosthetic Area		
	C_o	C_e	M
Ante-Retro	-16.6%	-19.6%	36.2%
Position	-6.4%	-19.9%	26.3%
Rot. Centre	6.2%	-2.9%	9.1%
Head Offset	2.0%	-4.3%	6.3%
Head Diameter	2.8%	-1.6%	4.4%
Neck Length	1.1%	-0.8%	2.0%

Table 6.5: Intervention group ante-retroverted screening results - prosthetic motion area.

	Angle Deviation		
	C_o	C_e	M
Position	-11.9°	10.9°	22.8°
Ante-Retro	-2.0°	10.0°	12.0°
Head Diameter	1.2°	1.2°	2.4°
Head Offset	0.8°	1.0°	1.8°
Rot. Centre	0.4°	-0.3°	0.7°
Neck Length	0.4°	-0.2°	0.6°

Table 6.6: Intervention group ante-retroverted screening results - prosthetic angle deviation.

	Prosthetic Area		
	C_o	C_e	M
Position	-7.4%	6.6%	14.0%
Head Diameter	7.4%	-2.8%	10.2%
Rot. Centre	7.7%	-1.9%	9.6%
Varus-Valgus	3.2%	-4.5%	7.7%
Head Offset	4.1%	-1.4%	5.5%
Neck Length	1.7%	-0.8%	2.5%

Table 6.7: Intervention group varus-valgus screening results - prosthetic motion area.

	Angle Deviation		
	C_o	C_e	M
Position	-14.5°	-5.7°	20.2°
Varus-Valgus	-0.4°	-6.5°	6.9°
Head Diameter	-1.1°	-1.0°	2.1°
Rot. Centre	-0.8°	-0.8°	1.7°
Head Offset	-0.4°	-0.5°	0.9°
Neck Length	0.2°	0.2°	0.5°

Table 6.8: Intervention group varus-valgus screening results - prosthetic angle deviation.

6.2.3 Full factorial results

The full factorial single replicate experiment analysed the main factors identified in section 6.2.2. For the control group, these were identified as acetabular cup rotation centre, femoral head diameter which when altered changes the femoral head-neck ratio, component positioning and femoral neck-shaft angle. This produced a 2^4 factorial design with four main effects, six two-factor interactions, four three-factor interactions and one four-factor interaction. The percentage contribution of the main effects and their interactions are shown in Figure 6.1. The factorial analysis shows that rotation centre and head diameter are the main factors which influence the size of the prosthetic motion area. There is very little interaction, only the interaction between component positioning and the neck-shaft angle contributes greater than 1%. The dominant factor which influences the position of the prosthetic motion area is component positioning, while neck-shaft angle and its interaction with component positioning have a limited effect.

For the intervention group the main factors identified from the screening analysis were component positioning, rotation centre, head diameter and modular femoral neck design. Initially, to identify any interaction between neck ante-retroversion with neck varus-valgus, a full factorial using the AR/VV necks was used. These necks are shown in Figure 2.13 on page 36. They combine 4.5° of anteversion or retroversion with 6° of varus or valgus. The maximum level of 15° of pure ante-retroversion or varus-valgus cannot be combined.

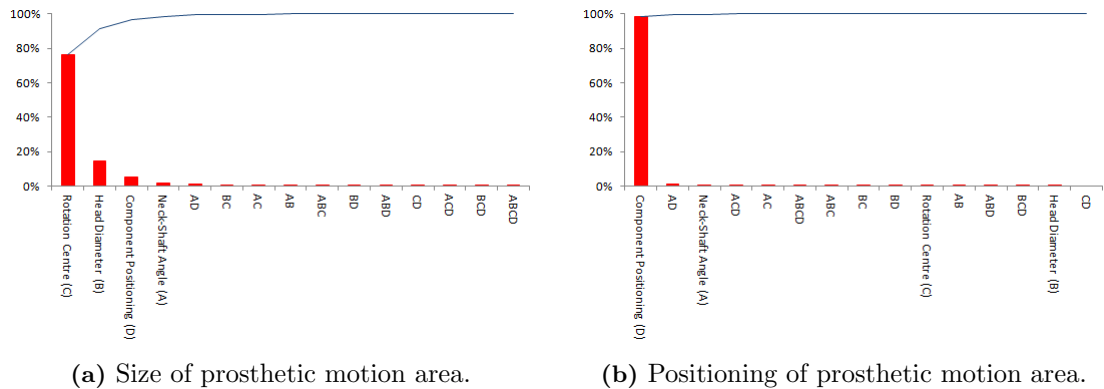


Figure 6.1: Percentage contribution of the control group independent variables.

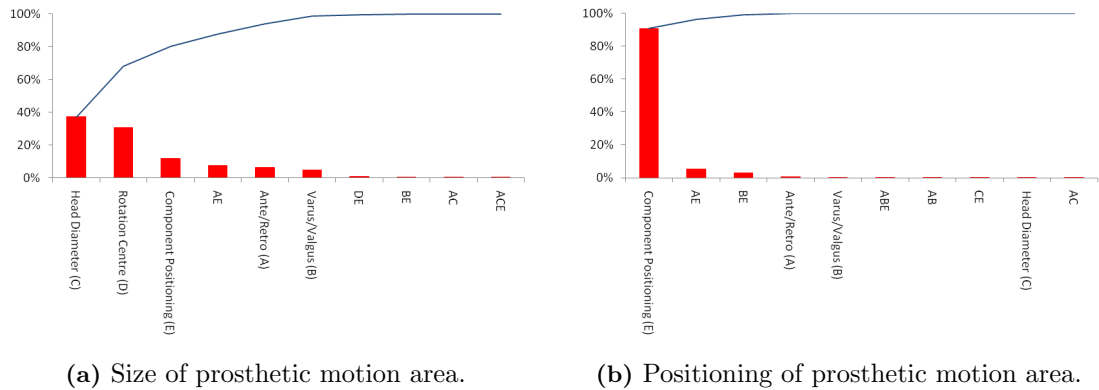


Figure 6.2: Percentage contribution of the intervention group independent variables.

This produced a 2^5 factorial design with five main effects, ten two-factor interactions, ten three-factor interactions, five four-factor interactions and one five-factor interaction. The percentage contribution of the top ten main effects or interactions are shown in Figure 6.2 for both the size and position of the prosthetic motion area. The results show that rotation centre and head diameter are the main factors which influence the size of the prosthetic motion area. Although, component positioning, neck ante-retroversion, neck varus-valgus and the interaction between component positioning and neck ante-retroversion total to a 20% influence on the size of the prosthetic motion area. Analysing the position of the prosthetic motion area, component positioning is the dominant factor influencing its positioning, although the interaction between component positioning and femoral neck modularity has a limited influence. Further, there is no interactive effect between neck ante-retroversion and neck varus-valgus.

Based on the results of the intervention treatment group full factorial experiment showing no interaction between femoral neck ante-retroversion with neck varus-valgus. Two further factorial studies were conducted, one with maximum neck ante-retroversion and one with maximum neck varus-valgus. For these tests, the factors of rotation centre and head diameter were merged into a single factor. This was done as both factors had no interactive effects and their high and low values had respective positive and negative effects on the size of the prosthetic motion area and did not influence the position of the prosthetic motion area. These factors were combined, into a head/rotation centre group with a high

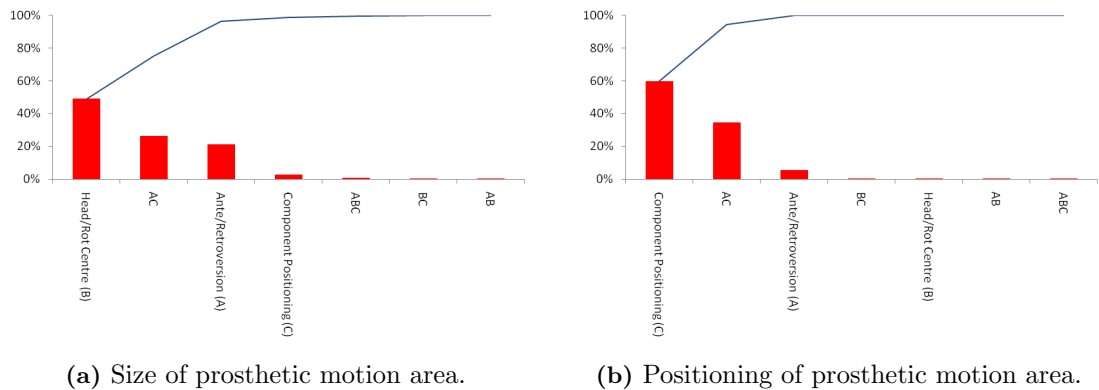


Figure 6.3: Percentage contribution of the intervention group independent variables using only neck ante-retroversion.

value of a 36mm diameter femoral head with a 0mm rotation centre. The low value was a 28mm femoral head with a +2mm rotation centre. This produced a 2^3 factorial design with three main effects, three two-factor interactions and one three-factor interaction. The percentage contribution of the main effects and their interactions are shown in Figure 6.3 for the ante-retroverted neck and Figure 6.4 for the varus-valgus neck.

The results using the ante-retroverted neck show that neck version has significant interaction with component positioning affecting both the size and position of the prosthetic motion area. Neck varus-valgus also interacts with component positioning to alter the position of the prosthetic motion area and independently is the second most important variable influencing the size of the prosthetic motion area.

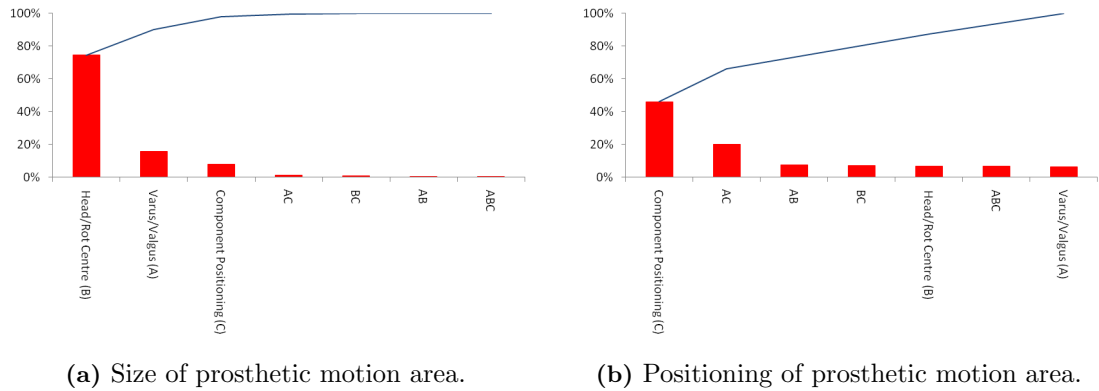


Figure 6.4: Percentage contribution of the intervention group independent variables using only neck varus-valgus.

6.3 Effectiveness of femoral neck modularity

The results presented in section 6.2 have shown that femoral neck modularity influences both the size and position of the prosthetic range of motion area. This section aims to provide results which assess whether this influence is being effectively used to answer the second research sub-objective.

- To assess if femoral neck modularity is being effectively used to relieve impingement.

In chapter 3, section 3.4.4 presented two outcome measures. The first was defined as the propensity to impinge. This measured whether the prosthetic motion area was large enough and well positioned enough to encompass the graphical range of motion benchmark, shown in Figure 3.10 on page 64. If so, then it could be inferred that the post-operative outcome for that particular patient would be impingement free. This outcome measure was used to assess if the intervention treatment group with the benefit of femoral neck modularity provided a significant difference in the propensity to impinge in comparison to the control treatment group.

The second outcome measure was defined as impingement severity. This measured the degree of impingement if the prosthetic range of motion area was not large enough or well positioned enough to encompass the graphical range of motion benchmark. This outcome measure assessed, if impingement did occur, whether the intervention group provided a significant difference in the severity of impingement in comparison to the control treatment group. Finally, the outcome measure of propensity to impinge was also used to assess whether the ideal neck choice was made by the surgeon in the intervention treatment group. These three measures were used to assess whether femoral neck modularity was being effectively used in the clinical setting. This section presents the results of this experiment.

6.3.1 Clinical trial results

In chapter 3, an estimated sample size for each treatment group was determined. To accommodate for losses during the study, 61 patients were recruited for each treatment group. There were a total of 25 losses during the clinical trial representing a figure of 20.5%. Reasons for these losses included navigation failure, lack of navigation availability, a patient wishing to withdraw from the study and conversion from uncemented to cemented implants. Therefore, the control treatment group had 49 patients with 48 patients in the intervention treatment group. The results of the clinical trial, using the actual components that were implanted into the patients, shows that there was no significant difference in the propensity to impinge between the control and intervention groups, Table 6.9.

In chapter 3, impingement severity was defined as the size of the impingement area as a percentage of the graphical range of motion benchmark. Preceding the analysis, a Shapiro-Wilk test was conducted on the distribution of impingement area for the two cohorts and the results showed evidence of non-normality (Rees, 2001). Therefore, the canonical transformation of the impingement area was taken, which was its square root. The Shapiro-Wilk test, in this form, showed no evidence of non-normality in its distribution. Consequently, assessment of difference in the variance and mean of the two cohort distributions was done using this canonical transformation. The results of those patients who had evidence of impingement shows a significant difference in the mean impingement area between the two cohorts with the intervention group having a lesser degree of impingement as compared to the control treatment group, Table 6.10.

	Control	Intervention	Total
Impinged	19	22	41
No Impingement	30	26	56
Total	49	48	97

p-value = 0.310

Table 6.9: Clinical trial result - propensity to impinge.

	Control	Intervention
Mean impinged area	9.3%	4.3%
Standard deviation	6.7%	3.7%
F-Test p-value (1-tail)	0.069	
t-Test p-value (2-tail)	0.020	

Table 6.10: Clinical trial result - impingement severity.

It was noted that differences in the other independent variables could contribute to a significant difference between the control and intervention groups with regard to impingement severity. It was shown in Table 6.1, that there were no significant differences between the acetabular cup inclination, anteversion and femoral stem version values of the two treatment groups. To assess the significance of having a modular femoral neck, all the modular necks in the intervention group were swapped post-operatively in the computer simulation with straight necks. Tables 6.11 and 6.12 analyses impingement propensity and severity between the control group and the non-modular intervention group. The results show that there would have been four more cases of impingement if a straight neck was consistently used in the intervention treatment group. Also, the severity of impingement between the control and the non-modular intervention is not significant, although there is a significant difference between their variances due to the greater amount of impinged cases in the non-modular intervention from which to calculate the F-statistic.

In the intervention group, to assess whether the most ideal modular femoral neck had been chosen in each case. Those 22 cases which had evidence of impingement were reprocessed post-operatively with alternative neck choices. Table 6.13, compares the actual choice of modular neck with the most ideal choice. Table 6.14, provides the propensity to impinge statistic between the control treatment group and the idealised modular neck intervention group. The results show that if the ideal neck was chosen in those cases that impinged, then this would have created a significant difference in the propensity to impinge when compared to the control group.

	Control	Intervention	Total
Impinged	19	26	45
No Impingement	30	22	52
	49	48	97

p-value = 0.094

Table 6.11: Non-modular intervention result - propensity to impinge.

	Control	Intervention
Mean impinged area	9.3%	6.0%
Standard deviation	6.7%	4.0%
F-Test p-value (1-tail)	0.038	
t-Test p-value (2-tail)	0.202	

Table 6.12: Non-modular intervention result - impingement severity.

	Ante (15°)	Ante (8°)	Retro (15°)	Retro (8°)	Retro & Varus	Retro & Valgus	Neutral
Actual	5	4	0	1	0	0	8
Ideal	8	2	1	0	0	0	1
	Varus (15°)	Varus (8°)	Valgus (15°)	Valgus (8°)	Ante & Varus	Ante & Valgus	
Actual	0	0	0	0	3	1	
Ideal	6	4	0	0	0	0	

Table 6.13: Intervention treatment group - modular neck choice.

	Control	Intervention	Total
Impinged	19	9	28
No Impingement	30	39	69
	49	48	97

p-value = 0.025

Table 6.14: Ideal modular neck choice result - propensity to impinge.

6.4 Effectiveness of range of motion benchmark

The final research objective for this study presented at the beginning of this chapter required an evaluation of the effectiveness of the graphical representation of hip joint range of motion in assessing operative outcome. It was determined in chapter 3, that modelling range of motion using the methodology applied in this study was required to be sensitive to changes in the operative parameters for it to be effective. The factorial experiments presented in section 6.2, provided the first assessment of the sensitivity of the prosthetic motion area. It was shown that changing the value of each of the independent variables defined in this study between their high and low values resulted in size and/or position of the prosthetic motion area changing.

A second measurement was used to evaluate how sensitive the graphical representation of prosthetic motion was to changes in the operative parameters. To do this, the operative parameter of combined version was measured and compared with the size and position of the prosthetic motion area. Table 6.15, provides the combined version values for the control and intervention treatment groups. The results show that there is a non-significant difference in the distribution between the combined anteversion values of the control and intervention treatment groups. Analysing the size and position of the prosthetic motion area, Tables 6.16 and 6.17 shows a significant difference in distribution of the size and position of the prosthetic motion area. Therefore, a significant difference in the prosthetic range of motion area is not caused by a significant difference with regard to the main independent variable being assessed. Consequently, a significant difference in the output measure does not correlate with a significant difference with regard to the input parameters. A full assessment of the effectiveness of the range of motion benchmark will be discussed in more detail in chapter 7 in section 7.2.5.

	Control	Intervention
Mean version	35.0°	33.9°
Standard deviation	22.3°	18.5°
F-Test p-value (1-tail)	0.097	
t-Test p-value (2-tail)	0.398	

Table 6.15: Clinical trial result - combined version.

	Control	Intervention
Mean prosthetic area	196%	193%
Standard deviation	24%	17%
F-Test p-value (1-tail)	0.018	
t-Test p-value (2-tail)	0.524	

Table 6.16: Clinical trial result - size of prosthetic motion area.

	Control	Intervention
Mean angle deviation	20.9°	18.2°
Standard deviation	13.3%	9.6%
F-Test p-value (1-tail)	0.014	
t-Test p-value (2-tail)	0.249	

Table 6.17: Clinical trial result - position of prosthetic motion area.

6.5 Summary

In this chapter, the graphical representation of hip joint range of motion was used to assess the effectiveness of femoral neck modularity using the randomised control trial experimental methodology presented in chapter 3. The benchmark requirement for the graphical representation was developed in chapter 4 and the method of inferring prosthetic motion was presented in chapter 5. The results presented have shown that having a modular femoral neck provides the surgeon with the opportunity to significantly influence both the size and position of the prosthetic motion area to improve range of motion until impingement. However, the result of the randomised control trial has shown that the technology is not being as effectively used as it potentially could be. At present, surgeons are able to use femoral neck modularity to reduce the severity of impingement when it does occur. However, they cannot use the technology to significantly reduce the propensity to impinge and thus improve the implant's resistance to dislocation.

The graphical representation of hip joint range of motion developed in this study has shown that it is sensitive to changes in the operative parameters. However, due to the number of independent variables in the study a significant difference in one input parameter may not result in a significant difference in the outcome measures defined for this study using the graphical representation of hip joint range of motion. The results presented in this chapter will now be discussed in more detail in the following chapter.

Chapter 7

Discussion

7.1 Introduction

The research that has been conducted as part of this study to construct a graphical representation of hip joint range of motion to assess operative outcome in total hip arthroplasty will be brought together in this chapter. The aim of bringing together the themes of research is to assess the study's fulfilment of its research question.

“How can range of motion be graphically represented and modelled physiologically to assess resistance to dislocation in total hip arthroplasty?”

This research question was split into a series of research objectives which were required to be achieved during the study. The following section will assess each research objective in turn. This evaluation allows the extent to which the study has answered the overall research question to be determined. Further, an analysis with regard to the innovation and application contained within the study will be conveyed. Finally, this chapter will present the limitations of the research and the further work which has been conducted as a result of the research contained within this study.

7.2 Research objectives

This section summarises the findings in relation to each of the research objectives.

7.2.1 Establishing a prosthetic range of motion benchmark

A benchmark requirement for hip joint range of motion had to be established for the first research objective. To do this, it was necessary to obtain data from the biomechanical and clinical field to develop an evidence based benchmark. A systematic review methodology was chosen to obtain kinematic data for hip joint range of motion from experimental studies. This methodology provided the opportunity to combine and analyse information from independent studies allowing for more precise estimates of the required range of motion.

There were two types of motion data obtained through the systematic search of the literature, pure joint motion and activities of daily living. To obtain benchmark data for these two types of motions, studies of healthy male subjects from Europe and North America between 20-70 years of age were selected. Selection criteria were partly because of convenience due to the limited number of female studies or studies from other geographical locations. Selection criteria which was not based on convenience was the requirement for measurements to be drawn from a healthy population within the age group defined. There was strong correlation amongst the studies that commented upon the effect of age upon range of motion (Boone and Azen, 1979; James and Parker, 1989; Nonaka et al., 2002; Roach and Miles, 1991; Svenningsen et al., 1989). Broadly, these studies agreed that there is a significant reduction in range of motion during the first 20 years of life. Then it is not until patients reach their 70th year that range of motion undergoes a marked reduction. Consequently, measurement of individuals within the 20-70 age range provided the most stable and realistic sample from which to base a range of motion benchmark.

Selecting studies which only used healthy subjects was based on the reasoning that the range of motion of a patient after total hip arthroplasty would be more restricted than that of a healthy individual. Therefore, a range of motion benchmark based on data from

a healthy population would provide an ideal impingement free range of motion for patients post-THA. The study of Miki et al. (2007) supports this reasoning. This study measured range of motion in patients post-THA to examine whether a benchmark based on the range of motion of a healthy population was valid. The measured maximum prosthetic range of motion was within 10° and generally less than the mean benchmark pure joint motion data presented in Table 4.1 on page 74. Therefore, the pure joint motion benchmark average or mean provide a realistic minimum requirement to be achieved post-THA.

The data presented in Table 4.1 on page 74 with regard to pure joint motion and the motion data obtained for the activities of daily living defined in Table 4.2 on page 76 showed an empirical relationship upon which other studies have commented. Fourteen of the fifteen activities of daily living had lower peak amplitudes of flexion/extension, abduction/adduction and internal/external rotation than the mean benchmark of pure joint motions established in Table 4.1. This relationship is supported by both the studies of Davis et al. (2007) and Johnston and Smidt (1970) who both found ability to perform activities of daily living was positively correlated with achieving a certain amount of pure joint motion. Consequently, the high variability in the measurement of joint motion during activities of daily living is associated with the variability of how each individual performs the manoeuvre (Hemmerich et al., 2006; Johnston and Smidt, 1970). This variability has been found to be caused by inter-joint adaptation between the hip, knee and ankle (Mulholland and Wyss, 2001; Nonaka et al., 2002; Perron et al., 2000).

Inter-joint adaptation and the association of activities of daily living being successfully achieved within a defined range of pure joint motion meant that a functional limit was required to be placed on the range of motion benchmark. This was selected to be the mean values of both pure joint motion and activities of daily living, based on their correlation with previous studies which have shown functional success within a limited range of motion (Davis et al., 2007; Johnston and Smidt, 1970; Miki et al., 2007).

This section has discussed the basis on which healthy subjects within the 20-70 age range were selected to provide the benchmark data for range of motion of the hip joint. How the

range of motion benchmark can be generalised needs to be considered especially with regard to gender and ethnicity. This is because the range of motion benchmark has mainly used data from male subjects in its construction. Considering ethnicity, the gait analysis studies presented in this chapter do not support the case for ethnicity having an effect on joint mobility. Although, there may be a greater demand from asian and middle eastern cultures to perform high excursion manoeuvres, such as kneeling and squatting (Mulholland and Wyss, 2001; Hemmerich et al., 2006). These manoeuvres have been incorporated within the range of motion benchmark and do not exceed the pure joint motion values derived from measurements of mainly European or American subjects.

The need for having an alternative range of motion benchmark based on gender is unclear. Data from level-walking studies shows that females have in the region of 4 – 5° greater motion (Alton et al., 1998; Benedetti et al., 2007; Boyer et al., 2008; Cho et al., 2004; DeVita and Hortobagyi, 2000; Judge et al., 1996; Hurd et al., 2004; Kadaba et al., 1990; Kerrigan et al., 1998a, b) and similar results were found in a limited number of studies measuring higher demand sporting activities (Ferber et al., 2003; Pollard et al., 2004). It is unknown whether this difference transfers across all activities to indicate whether females have greater joint mobility or whether, similar to age, joint excursion is dependent upon other factors such as neurological and muscle interactions. However, at present not enough information is available to justify having a separate range of motion benchmark dependent upon age, ethnicity or gender.

7.2.2 Graphical representation of the range of motion benchmark

The second research objective required the established range of motion benchmark to be represented graphically. To do this, it was necessary to use the theoretical foundation regarding modelling motion of the hip joint, presented in chapter 2. This theoretical foundation highlighted certain incongruence's between the modelling of hip joint motion used in gait analysis and clinically in total hip arthroplasty. These mainly concerned the landmarks from which the femoral and pelvic coordinate frames are based. The issue with the femoral coordinate system concerned the accessibility of the posterior aspects of the femoral condyles which form the condylar axis and define the neutral rotation of the femur (Maruyama et al., 2001). Regarding the pelvis, there are two differing coordinate frames, the TPP recommended for gait analysis studies and the APP used in clinical situations. These angles differ by a tilt angle measured in the sagittal plane. Further, there is the assumption that the hip joint can be modelled as a perfect 'ball and socket'.

The studies contained within the systematic search of the literature utilised different coordinate frames including orthogonal and non-orthogonal alignments and those which used the landmarks of the TPP and others the APP. Therefore, for a realistic graphical representation to be produced, agreement between these differing coordinate frames was required.

Considering the assumption of perfect 'ball and socket' behaviour. The validation study presented in chapter 4 measured the maximum rms distance from the surface of a femoral head to a constructed best-fit sphere, whose centre approximated the hip joint centre. This was measured in ten patient CT scans and the results were presented in Table 4.3. On average this distance was 1.72mm. This means, if motion of the femur follows the contour between the acetabulum and the femoral head there would be a translation of the hip joint centre of approximately 3.5mm. Modelling this effect in flexion, the largest range of motion, this translation represented 0.1° difference when compared with modelling the joint with a single kinematic centre of rotation. Consequently, the hip can be considered to be modelled as a 'ball and socket' joint.

The validation study presented in chapter 4 also measured the tilt angle between the pelvic TPP and APP planes. This experimental study found a mean difference of 93.6° . This measurement provides support for the study of Dandachli et al. (2006) that the TPP-APP relationship is approximately orthogonal. The effect of modelling this difference on range of motion was assessed. It was found that for each degree above or below 90° reduced or increased the amount of flexion by the same amount. Therefore, the two pelvic coordinate frames could be considered orthogonal with any degree of non-orthogonality causing on average a 3.6° difference between range of motion measurements.

The alignment between the orthogonal femoral coordinate frame using the condylar axis defined by Murphy et al. (1987) and the non-orthogonal coordinate frame using the transepicondylar axis defined by Wu et al. (2002) depended upon whether the condylar axis is congruent to the medial-lateral axis of the pelvis and relate consistently to the transepicondylar axis. A further study, presented in Turley et al. (2012), measured the angle between the transepicondylar axis and the medial-lateral axis in two scenarios. The first where the condylar axis could be determined and aligned with the pelvic medial-lateral axis. The second where the condylar axis was not accessible, but the subject was able to pose in the anatomical standing neutral posture. There was found to be no significant difference in the measured angle between the two axes in the two measurements. Therefore, this shows that the condylar axis can reliably determine the neutral rotation of the femur when a person is posed in the anatomical posture.

The alignment of the pelvic and femoral coordinate frames show congruence between the methods adopted by the clinical community and those used in gait analysis. Further, evidence of the condylar axis defining the neutral rotation of the femur meant that the graphical representation of hip joint motion could use an orthogonal reference frame. Therefore, in the neutral position the femoral and pelvic coordinate frames were aligned and coincident at the hip joint centre. Motion of the femur could then be represented as a point rotation about orthogonal anatomical axes (Kuipers, 1999). This alignment permitted a three dimensional representation of hip joint motion to be produced.

The development of a graphical representation was required to build upon the theoretical foundation with regard to modelling of hip joint motion. This was because in order to have a representative three-dimensional range of motion benchmark, impingement due to internal/external rotation was required to be incorporated. It was found that the axes of rotation of 70% of the key phases of the 15 activities of daily living were within 15° of the transverse plane. Of those activities that did not lie within this range, many were lower demand activities whose axes of rotation are difficult to define (Woltring, 1991). However, the PIVOT and ROLL manoeuvres were not contained within this boundary, this will be considered further in section 7.5. Consequently, the developed graphical representation can be considered representative of 13 out of the 15 key activities of daily living.

The developed graphical representation was validated using patient CT scans in chapter 4. Table 4.4, presented the comparison of the discrete measurements made in the validation experiment with previous studies by Kubiak-Langer et al. (2007) and Tannast et al. (2007). The results in flexion, abduction and adduction were validated by these measurements. However, there was a significant difference with regard to extension. The experimental results in extension agreed with the average reported by Kurtz et al. (2010) of 78° . The agreement with previous studies shows that the constructed range of motion boundary is valid. However, certain motions such as those in extension are not limited by bony impingement and cannot be assessed using CT scans. A further such site was the motion of flexion combined with adduction. This will be considered further in section 7.5.

The results of the validation experiment presented in Figure 4.7 reveal the possible sites for bony impingement. These areas include motions in adduction, flexion and also abduction combined with flexion. The later possible impingement site highlights the need to represent range of motion as a continuum. It is possible for discrete measurements to miss impingement in these highlighted risk areas. This demonstrates a key benefit that the graphical representation of hip joint range of motion can provide.

7.2.3 Assessment of post-operative outcome using the graphical representation

The third research objective required the range of motion benchmark to be implemented within the surgical field to assess the effectiveness of femoral neck modularity. The development of the graphical representation based on the range of motion benchmark data defined two characteristics. Firstly, its size and shape in terms of its surface area and secondly its position as defined by its directional axis, shown in Figure 4.6 on page 87. The experimental validation of the graphical range of motion benchmark showed that these two characteristics were able to be used to evaluate range of motion outcome.

The modelling techniques and outcome measures developed for graphical range of motion benchmark were able to be used to develop a graphical representation of prosthetic range of motion. This representation was based from intra-operative measurements of patient prosthetic component orientation and the geometric information regarding the hip implant. This information was able to be used to place the prosthetic components in their anatomical orientation relative to an aligned pelvic and femoral coordinate frame when posed in the anatomical neutral position. The method of modelling hip joint range of motion produced a prosthetic range of motion representation which could be directly compared against the benchmark representation, using the outcome measures defined in the previous paragraph and any source of impingement identified.

A range of the different prosthetic range of motion outcomes have been shown in Figure 7.1. The different outcomes show the irregular nature of the prosthetic range of motion area. Figure 7.1, also shows the various different locations of impingement which occur in coupled motions of flexion/extension, abduction/adduction and internal/external rotation. This complexity, demonstrates the need for the having a graphical evaluation of range of motion and how prosthetic impingement can no longer be represented by simplified methods (Nikou et al., 1998).

7.2.4 Assessment of femoral neck modularity

The fourth research objective required an assessment of femoral neck modularity in limiting prosthetic dislocation. The graphical representation of both the required benchmark and prosthetic range of motion was used for this evaluation using the outcome measures described in the previous section. Femoral neck modularity was discussed in chapter 2, where previous studies found modularity was useful to the surgeon in adjusting intra-operative parameters to restore hip joint biomechanics and range of motion. However, these studies did not evaluate femoral neck modularity against an established control. A total of 49 control and 48 intervention treatment group patients were analysed using the graphical representation. To be able to fully assess the effectiveness of femoral neck modularity the research objective was broken down into two sub-objectives.

Influence of femoral neck modularity

The results for the experiment to evaluate the influence of femoral neck modularity on hip joint range of motion were presented in chapter 6. The results of this experiment showed in both the control and the intervention treatment groups, independent variables associated with the offset and the length of the femoral neck and head had a minimal effect upon the prosthetic range of motion. There was also further commonality with regard

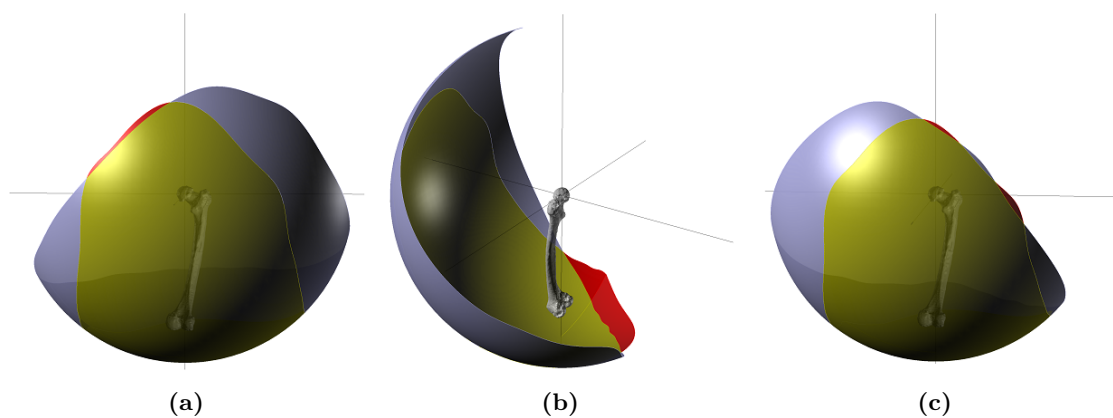


Figure 7.1: Examples of areas of impingement in prosthetic motion.

to the main factors which influence the size of the prosthetic motion area. This outcome measure is predominantly influenced by the depth of the rotation centre of the acetabular liner and the femoral head diameter. While the position of the prosthetic motion area is influenced by the orientation of the prosthetic components. In the control group, other than these factors there is very little opportunity to influence the range of motion until impingement. However, the results show in the intervention group that alteration, to a large enough degree, of the neck-shaft angle and version angle of the femoral neck through modularity can significantly influence both the size and position of the prosthetic motion area to improve range of motion until impingement.

Analysis of femoral neck-shaft angle or varus-valgus in both the control and intervention groups and femoral neck ante-retroversion in the intervention group provided insight with regard to the degree of influence of femoral neck modularity. Femoral neck varus-valgus alters the neck-shaft angle of the femoral stem and has mainly been reported to be an aid in limb length restoration to improve joint stability (Toni et al., 2001). However, Widmer and Majewski (2005) also considered its effect upon altering the degree of prosthetic range of motion. For the control group, the 10° difference in neck-shaft angle of the femoral stems offered, resulted in a negligible effect upon range of motion, shown in Figure 6.1. In the intervention treatment group, due to the high and low values of femoral neck ante-retroversion and varus-valgus not being able to be combined, the factorial analysis of the intervention group consisted of three parts. The first part analysed the interaction between femoral neck ante-retroversion and varus-valgus in the AR/VV necks which combine 4.5° of anteversion (+) or retroversion (-) with 6° of varus (+) or valgus (-). Similar to the control group, the results of the first factorial experiment, presented in Figure 6.2, showed that given the limited adjustment in neck ante-retroversion and varus-valgus for the AR/VV modular necks. These modular necks have a limited effect upon the size and position of the prosthetic motion area. Further, there is no interaction between femoral neck ante-retroversion with neck varus-valgus.

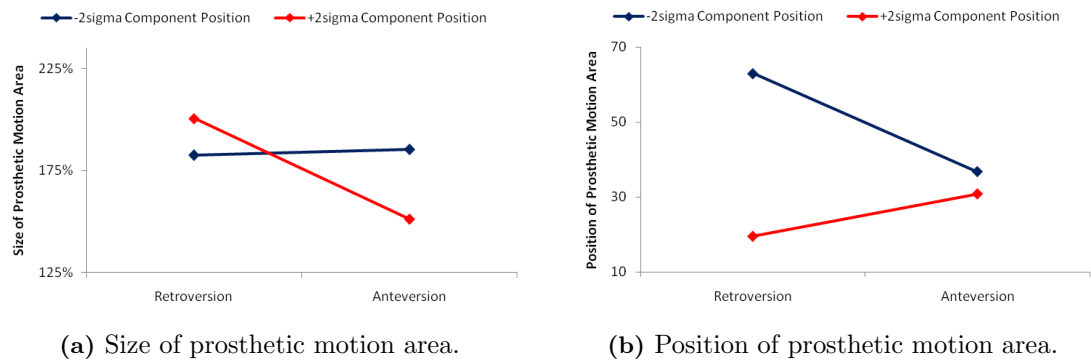


Figure 7.2: Interaction plots: modular neck version and component positioning.

The following two factorial experiments, considered the effect of setting modular neck anteversion (+) and retroversion (-) at their maximum 15° in the first experiment and varus (+) and valgus (-) at their maximum 15° in the second experiment. The results presented in Figures 6.3 and 6.4, show that these femoral neck options have a significant effect upon both the size of the prosthetic motion area and its position. This effect is visualised in Figure 7.2 for modular neck ante-retroversion and Figure 7.3 for modular neck varus-valgus. Modular femoral neck ante-retroversion has significant interaction with component positioning, as shown in Figure 7.2. In this figure, the $+2\sigma$ component position consisted of a high acetabular cup inclination with a high degree of combined version. The -2σ component position consisted of a low acetabular cup inclination and combined retroversion. The retroverted neck is effective at improving the position and size of the prosthetic motion area for component orientations which have a high degree of combined version to bring the primary arc of movement closer to the physiological requirement. While the anteverted neck is effective in improving the position of the prosthetic motion area with component orientations which have a low degree of combined version. This analysis shows that given a certain orientation femoral neck modularity is able to significantly improve a patient's range of motion until impingement. However, given their effect, if the wrong neck choice is made then this can have very negative consequences. A further point is that for implants with significant combined retroversion the 15° anteverted neck may not be effective enough to align the prosthetic motion area to where it is required physiologically.

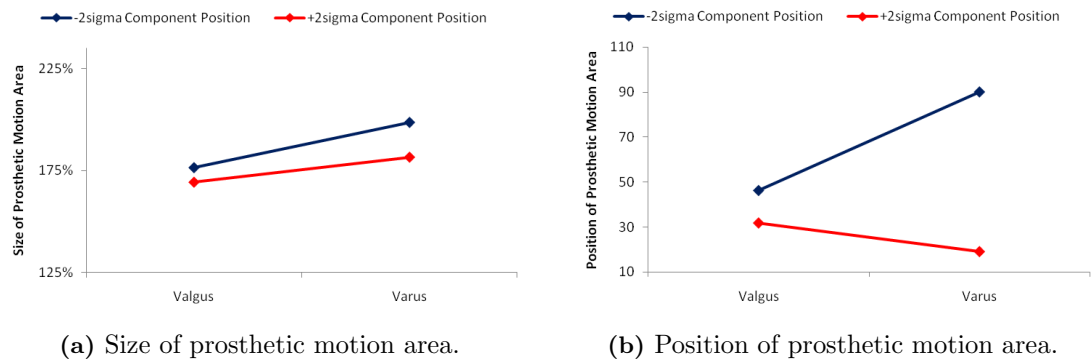


Figure 7.3: Interaction plots: modular neck-shaft angle and component positioning.

Varus-valgus modular necks adjust the neck-shaft angle from varus (120°) to valgus (150°). In the experiment a large degree of neck varus had the effect of increasing the size of the prosthetic motion area. It achieves this by reducing the angle between the femoral neck axis and the transverse plane, which allows for a greater degree of flexion, extension and adduction. However, this comes at a cost, a reduced amount of abduction which is why varus necks have a negative effect with regard to the positioning of the prosthetic motion area with low acetabular cup inclinations, as show in Figure 7.3b. This is because a varus neck combined with a low acetabular cup inclination closes the angle between the opening plane of the acetabular cup and femoral neck. However, in contrast with high cup inclination a varus neck is able to have a positive effect at aligning the prosthetic motion area with the benchmark requirement.

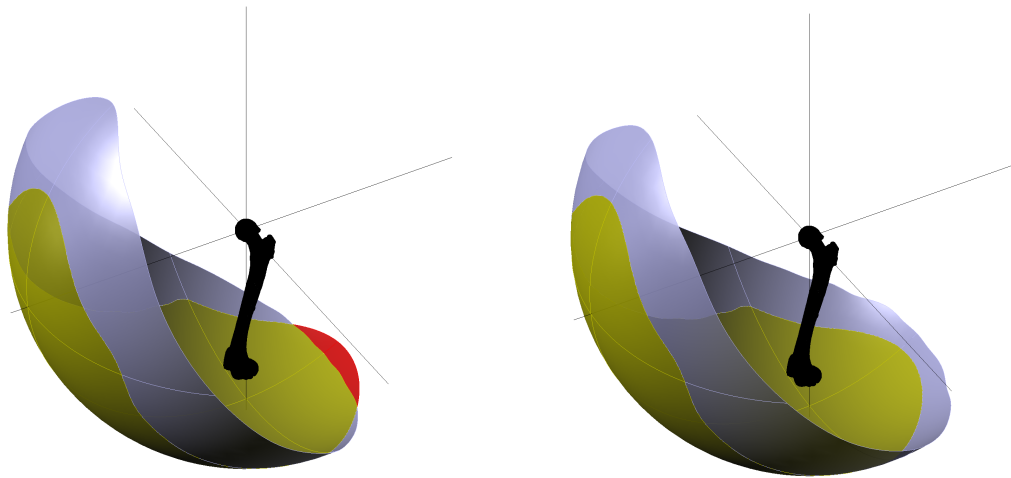
The factorial analysis used in this study has found that femoral neck modularity is one of the main factors which can significantly alter the size and position of the prosthetic range of motion area. Indeed, the control without this feature, once the acetabular and femoral stem orientations are fixed has no further option to alter the position of the prosthetic range of motion area. This highlights the potential advantage of femoral neck modularity.

Effectiveness of femoral neck modularity

The results of the randomised controlled trial to assess if femoral neck modularity is being effectively used to relieve impingement were presented in chapter 6. The factorial analysis showed that femoral neck modularity could significantly alter both the size and position of the prosthetic motion area. However, the results of the randomised controlled trial have shown that this potential is not being maximised in the clinical setting. This is shown by there being no significant difference between the propensity to impinge between the control and intervention treatment groups as shown in Table 6.9. This effectiveness is limited by knowledge of which is the best modular neck to select. Table 6.14, shows that if the ideal neck was chosen by the surgeon then this would have resulted in significant difference in the propensity to impinge favouring the intervention group. However, surgeons were able to use femoral neck modularity to significantly reduce impingement severity, as shown in Table 6.10.

To analyse further the results of the randomised controlled trial the neck choice made by the surgeons in the intervention treatment group were analysed. This analysis revealed that on thirteen occasions a straight neck was used, thirteen AR/VV necks were used, nine 8° varus-valgus necks, eight 8° ante-retroverted necks and five 15° ante-retroverted necks. The factorial analysis highlighted the limited effect with which the AR/VV neck options had upon the range of motion until impingement. Therefore, 26 of the 48 patients did not have their range of motion altered by the femoral neck modularity in the intervention group. Further, by swapping all modular necks in the intervention group for straight necks only resulted in four more cases of impingement. Consequently, the modular neck selection made in the study had little influence on the propensity of a THA to impinge.

In cases where impingement did occur, it was found that the intervention group was able to significantly reduce impingement severity. Analysing the neck choice in these impinging cases, reveals that all of the 15° ante-retroverted necks used in the trial were contained within the impingement group. It was the use of these necks that caused the most significant reduction in the impingement area, although not enough to prevent impingement entirely.



(a) Clinical trial impinged case - straight neck. (b) Post trial correction - 8° retroverted neck.

Figure 7.4: Example of the effect of modular neck choice.

This indicates that in cases of gross mal-orientation of the prosthetic components it is easier to make the right neck choice. However, the degree of modularity in these grossly mal-orientated cases is not enough to prevent impingement, just to reduce its severity. This supports the findings of Sakai et al. (2000; 2002), who found there was a practical limit to the extent that a modular neck system can aid post-operative outcome.

The neck choice of the 22 impinged cases in the intervention group were analysed further. This impinged group contained eight straight necks and four AR/VV necks. In these twelve cases, if an anteverted or a varus neck was chosen, then there would be no evidence of impingement. Figure 7.4, provides an example of one of these corrected cases. Analysing this with the ideal neck choice presented in Table 6.13. The overall summary of the ideal neck choice is as follows - 22 non-impinged cases not requiring femoral neck modularity, 17 non-impinged cases requiring a non-straight, non-AR/VV neck to avoid impingement and 9 impinged cases where significant neck anteversion or neck varus is required to reduce the severity of impingement to 1.9% on average. In this distribution of cases, as Table 6.14 shows, modularity would make both a significant difference in the propensity to impinge and when impingement does occur the impingement severity.

The factorial analysis and the post clinical trial analysis have shown that femoral neck modularity has the potential to make a significant difference to the outcome of THA procedures with regard to range of motion until impingement. However, there are two factors which have been shown to inhibit its use in practice, the limited effect of the AR/VV modular neck and knowledge of which is the best neck to select. It is only in cases of gross mal-orientation that the surgeon is able to recognise and correct as far as practically possible the extent of this mis-alignment through the use of neck modularity. Therefore, the surgeon needs further knowledge with regard to the relative position of the acetabular cup and femoral stem to be able to make the appropriate modular neck choice.

7.2.5 Effectiveness of graphically representing hip joint range of motion

The results presented in chapter 6 were also used to evaluate the effectiveness of graphically representing hip joint range of motion to assess operative outcome. It was found that the outcome measures regarding the size and position of the prosthetic motion area were sensitive to changes in the operative parameters. This case was shown in the factorial experiment evaluating the influence of femoral neck modularity. In this experiment, changing the value of each of the independent variables defined in this study between their high and low values resulted in size and/or position of the prosthetic motion area changing. However, a significant difference in the output measures may not correlate with a significant difference with regard to the input parameters. This was found by evaluating the combined version of the femoral neck with the size and position of the prosthetic motion area in the control and intervention treatment groups. There was a non-significant difference in combined version but a significant difference measured in the average size and position of the prosthetic motion areas in the control and intervention groups. It is hypothesised that this could be a consequence of more than one independent variable affecting the size and position of the prosthetic motion area for it to be able to detect a significant difference in any particular one.

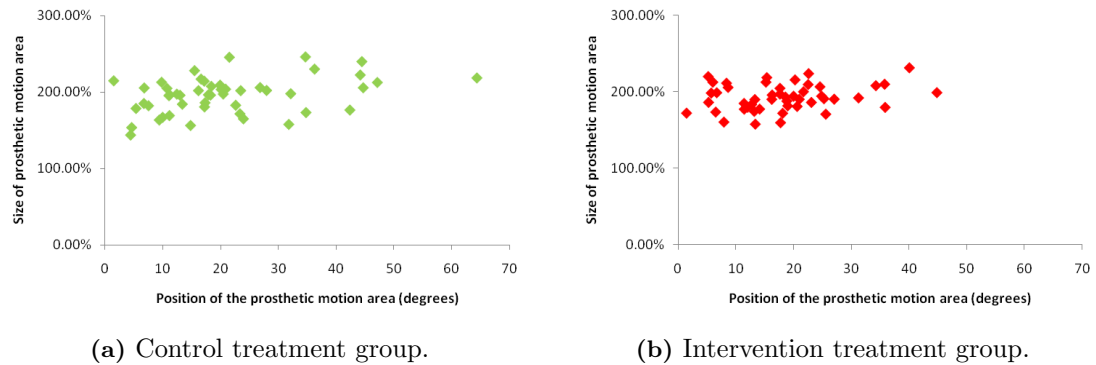


Figure 7.5: Plot of the size of the prosthetic motion area compared to its position.

A further analysis of the independent variables identified two factors to be different. The depth of the acetabular liner rotation centre and the presence in the intervention group of femoral neck modularity. It was found that the depth of the acetabular liner rotation centre influences the size of the prosthetic motion area but not the position of the prosthetic motion area. There was a greater choice in acetabular liner options in the control group. This showed up in the comparison of the size of the prosthetic motion area between the control and intervention groups, where the control had a significantly wider distribution. This is shown in Figure 7.5, where the size of the prosthetic motion area is plotted against its position. The control group has a wider spread in the y-axis which plots the size of the prosthetic area.

The second difference in the independent variables was the presence of femoral neck modularity in the intervention group. It was found that the only factors which significantly influenced the position of the prosthetic motion area, was component positioning and femoral neck modularity. Examining prosthetic component positioning, there was found to be no difference in relation to the mean and distribution of acetabular cup inclination, anteversion and stem version between treatment groups. Therefore, the only factor which created a significant difference in the position of the prosthetic motion area was femoral neck modularity. Table 6.17, shows that the intervention group has a significantly tighter distribution than the control group with regard to the position of the prosthetic motion area. This is again demonstrated in Figure 7.5, where comparing the x-axes of the two

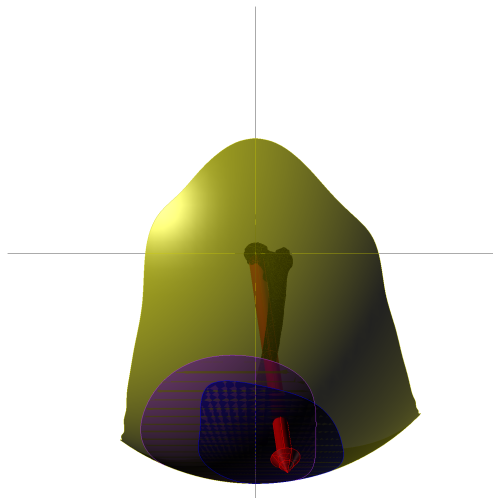


Figure 7.6: Distribution of control (purple) and intervention (blue) directional axes.

plots, the intervention group has a much tighter spread with regard to its position. This tighter dispersion of prosthetic area position is visualised in Figure 7.6, where the blue area is the distribution of the prosthetic motion directional axes for the 48 intervention cases, while the purple area is the distribution of the 49 control cases. It is evident that the intervention group is slightly better positioned and more closely clustered around the directional axis of the range of motion benchmark, indicating its more reliable positioning.

For an output measure to be effective, it is required to be sensitive enough to identify changes in the input variables that are required to be measured (Saltelli et al., 2000). This study has identified key differences between the control and intervention groups using a graphical representation of hip joint range of motion. These differences have been found to correlate back to key differences in the input variables. This shows that the assessment of THA outcome using a graphical representation has been effective. Further, as well as assessing the effectiveness of femoral neck modularity it has also been used to identify further issues, which could be used to aid operative outcome. This includes the significance of acetabular liner rotation centre. In the literature, much has been written about increasing the head-neck ratio by having larger diameter heads to maximise range of motion (Kluess et al., 2007; Yoshimine and Ginbayashi, 2002). This study has shown that this ratio can also be increased by reducing acetabular liner rotation centre.

7.3 Research question

The research that has been conducted during this study has been used to build upon the theoretical foundation in order to be able to answer the following research question.

“How can range of motion be graphically represented and modelled physiologically to assess resistance to dislocation in total hip arthroplasty?”

The related findings of the research objectives presented in the previous section have been able to answer the research question. The principal results have found that the method of modelling the motion of the hip joint presented in the theoretical foundation was able to be used to construct a graphical representation of hip joint range of motion. This modelling approach required both motion data to determine the benchmark range of motion requirement and intra-operative measurement of prosthetic component orientation. Both datasets were then able to be graphically represented and directly compared to identify motion areas which pose risk of impingement and consequently dislocation. This approach was used in a randomised controlled trial to assess the resistance to dislocation of a THA technology, femoral neck modularity. Consequently, the study has achieved all of its set research objectives and answered the set research question.

The findings related to answering the research question and objectives have also had business benefit for a number of companies involved in the study. For Brainlab and Nikon Metrology, the establishment of a graphical representation of range of motion has allowed these companies to improve or incorporate the dynamic motion of the hip joint into their surgical navigation (Brainlab) or motion tracking systems (Nikon Metrology). The findings have also impacted Wright Medical Technology who manufactured the modular neck implant used in the study. The analysis of femoral neck modularity has allowed the current limitations with regard to the technology to be identified. It has also identified which modular necks are not effective at improving the range of motion until impingement. This will allow Wright Medical Technology to rationalise its modular neck options and provide better guidance about how to make the correct femoral neck choice.

7.4 Innovation

The Engineering Doctorate is aimed at developing individuals who can not only innovate but who can implement that innovation. The major aim of the Engineering Doctorate is to develop engineers who are capable of demonstrating innovation in the application of knowledge to an engineering business. In chapter 1, it was stated that only one previous study has attempted to graphically represent a range of motion boundary as a continuum (Thornberry and Hogan, 2009). This graphical representation is shown along with representation constructed in this study in Figure 7.7.

The representations have used two different approaches with regard to modelling hip joint range of motion. The Thornberry and Hogan (2009) approach uses joint angles, similar to the two-dimensional representation shown in Figure 4.7 on page 93. In contrast, the three-dimensional representation constructed in this study uses Cartesian coordinates. This approach allows the motion of the femur to be tracked anatomically for a simpler interpretation. However, both methods reveal the complex motion of the hip joint and justify having an evaluation of operative outcome based on a graphical continuum.

The further innovations that this study has made, in addition to the different interpretation of graphically representing hip motion, have been the development of the benchmark requirement. In the Thornberry and Hogan (2009) study, only one cadaver was used to

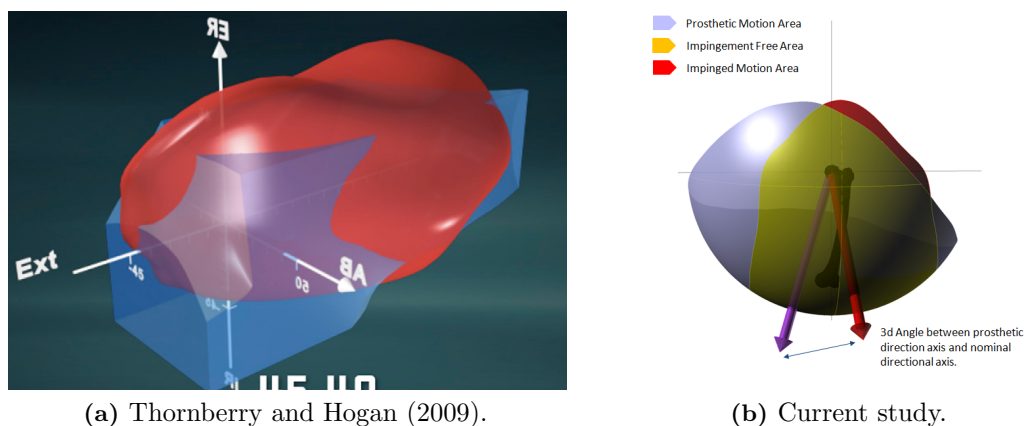


Figure 7.7: Comparison of the graphical representations of hip joint motion.

establish a benchmark requirement, which only considered bone-on-bone impingement. The benchmark requirement established in this study has used the activities that a person is likely to undertake in their daily activities as its basis. Further, it has also considered the axes of rotation of these activities so that a representative range of motion requirement was able to be established considering not only bony impingement, but those restrictions associated with soft-tissues and limitations in secondary joint motion.

In Thornberry and Hogan (2009), the author discusses the potential of navigation and simulation technologies in improving the understanding of normal and abnormal kinematics of the hip as well as the process capability of total hip arthroplasty. The outcome measures developed in this study make the biggest contribution to knowledge in this area. Evaluation of hip joint motion and the process capability of a total hip arthroplasty series can now be evaluated using two different measures, the size and position of the prosthetic motion area. These outcome measures have been able to be applied to evaluate the capability of two different implant types and have used statistical techniques to highlight the potential of femoral neck modularity and its current limitations. This has allowed the intra-operative surgical technique to be evaluated as a manufacturing system to highlight quality improvements to benefit future THA patients.

7.5 Research limitations

The foundation from which this study is built is the assumption that maximising range of motion to impingement improves resistance to dislocation. There have been a number of studies and clinical observations which support this assumption. Firstly, it has been found that a successful THA is dependent upon obtaining joint stability and achieving ideal range of motion (Duwelius et al., 2010). Secondly, many patients that suffer dislocation have evidence of impingement which occurs when the neck of the femoral component contacts with the rim of the acetabular cup (Scifert et al., 2001). This contact is the result of the required motion of the patient moving outside the range that the THA can accept. Finally, it has been found that post-THA range of motion correlates positively with hip function as measured by clinicians (Davis et al., 2007). Consequently, the theoretical basis from which this study is built can be considered valid. However, there are limitations within the study that need to be considered. These limitations have been detailed.

Is there a trade-off between joint stability and range of motion - In the review of the literature it was acknowledged that successful THA outcome was dependent upon two factors, joint stability and range of motion until impingement. This study has evaluated thoroughly the range of motion until impingement. However, joint stability has not been directly assessed. The factorial analysis found that femoral offset and a small 10° adjustment in the neck-shaft angle has minimal effect upon the range of motion until impingement. Therefore, these factors can be considered purely for controlling joint stability. In contrast, femoral neck version and significant adjustment, greater than 10° , in the neck-shaft angle has been found to be important in influencing the range of motion until impingement. Therefore, further research is required into how these factors influence joint stability and whether there is a trade-off with range of motion until impingement in their adjustment.

Femoral neck integrity - The review of the literature presented in chapter 2 highlighted concerns in both the clinical and engineering community with regard to the integrity of the modular femoral neck. The failure rate for the modular femoral necks used in the

study is 0.027% (Traina et al., 2009a). However, the Australian National Joint Registry has found that another modular stem has a five year cumulative revision rate of 11% (National Joint Replactment Registry). Although, it is not clear whether this is a problem with the stem design or due to the presence of a modular femoral neck. This study found that in the intervention treatment group 54% of the cohort would have benefited from femoral neck modularity. This represents a significant potential for the technology which should be considered in the context of its acknowledged failure rate.

Effect of diagonal adduction on the graphical range of motion benchmark - In the validation of the graphical representation of the hip joint range of motion benchmark in chapter 4. The CT experimental analysis showed that there was an increased amount of motion in flexion combined with abduction when compared with the constructed graphical representation, shown in Figure 4.7 on page 93. A reason for this is that it is not possible to measure true geometrical adduction in a patient, as the opposite leg obstructs the motion. Instead anatomical adduction follows a diagonal motion, as shown in Figure 2.3c on page 14. Consequently, this represents a gap in knowledge for further work with regard to the modelling of the graphical range of motion benchmark. Further, how the extra motion in this area is limited by soft tissue needs to be understood.

Modelling of the PIVOT and ROLL manoeuvres - The constructed graphical representation of hip joint range of motion is only representative of 13 out of the 15 activities of daily living researched. The manoeuvres that it is not considered to be representative of are the PIVOT and ROLL manoeuvres. These activities have been described in Table 4.2. Analysing these two activities, their axes of rotation occur not within 15° of the transverse plane but rather have near vertical rotation axes in the superior-inferior direction. Further, these movements concern pelvic rather than femoral movement and represent a limitation with regard to the modelling assumptions presented in chapter 2. In modelling the hip joint the pelvis is considered fixed with the femur moving about it. This modelling assumption is valid for the 13 activities of daily living from which the graphical benchmark is constructed. However, it is not valid for

the PIVOT and ROLL manoeuvres. Further research is required in modelling pelvic movement and its relation to THA outcome. As well as the limitations highlighted there are issues with the alignment of the pelvis with the whole body, discussed in chapter 2.

Confounding of independent variables - The randomised controlled trial design presented in chapter 3 outlined that as well as femoral neck modularity there were other differences between non-modular neck control treatment group and the modular neck intervention. A notable difference between the two treatment groups was the depth of the acetabular liner rotation centre which affects its opening angle and consequently oscillation angle. These variables could have a confounding effect upon the experimental results. However, by using the surgical navigation measurement system, this allowed the effects of these different variables to be isolated to a certain degree. Consequently, this allowed the effect of femoral neck modularity to be assessed against a proven non-modular control. A better assessment of femoral neck modularity would have been achieved if the same implant type was used in both groups but only in the modular neck intervention could a non-straight neck choice be made.

The research limitations highlighted in this section would allow further definition with regard to the range of motion requirement for total hip arthroplasty. This further knowledge could then be incorporated into the graphical representation of the range of motion benchmark to improve assessment of operative outcome further still. The research conducted so far has highlighted the importance of modelling hip joint motion as a continuum and highlighted both its complexity and also impingement sites which cannot be detected through discrete tests. Consequently, further research will build upon the current research to define the continuum of hip joint motion in greater detail.

7.6 Further innovation

Throughout the study the importance of the five factors defined by Yoshimine and Ginbayashi (2002) upon post-operative range of motion have been demonstrated. These five factors are **(1)** the oscillation angle (θ) **(2)** the inclination of the acetabular cup (α) **(3)** the anteversion of the acetabular cup (β) **(4)** the angle between the femoral neck and the transverse plane (a) and **(5)** the version angle of the femoral neck (b). The oscillation angle (θ), determines the amount of movement that a THA can achieve and is dependent upon the design of the THA prosthetic components (Kluess et al., 2007; Yoshimine and Ginbayashi, 2002). The other four factors dictate the orientation of the prosthetic components and are dependent upon the skill of the surgeon. It has been shown in section 7.2.4, that it is only in cases of gross mal-orientation that surgeons are able to recognise and correct as far as practically possible component mal-alignment through the use of neck modularity. Consequently, there is a requirement for a surgical aid to help surgeons assess component orientation to be able to select the best femoral neck option. The medical device presented in this section has been filed for patent (Turley and Griffin, 2012).

To control for prosthetic component placement intra-operatively surgeons have had the option of using surgical navigation, which can track the position of the pelvis and femur in space and fit the prosthetic components relative to these known positions (Kelley and Swank, 2009). This is an expensive and time consuming option for the surgeon (Huo et al., 2008). Consequently, the vast majority of surgeries are performed without the use of navigation. Considering these constraints, a trial femoral head was designed. This femoral head design uses markings on its surface to provide feedback to the surgeon, allowing them to assess whether or not they have achieved the correct prosthetic orientation to enable a patient to fulfil their daily activities without risk of dislocation.

The prosthetic orientation variables defined by Yoshimine and Ginbayashi (2002) can be expressed using a number of different conventions (Murray, 1993). However, if the anatomical convention is used, then both acetabular cup anteversion (β) and femoral neck version (b) are measured in the transverse plane, while acetabular cup inclination (α) and

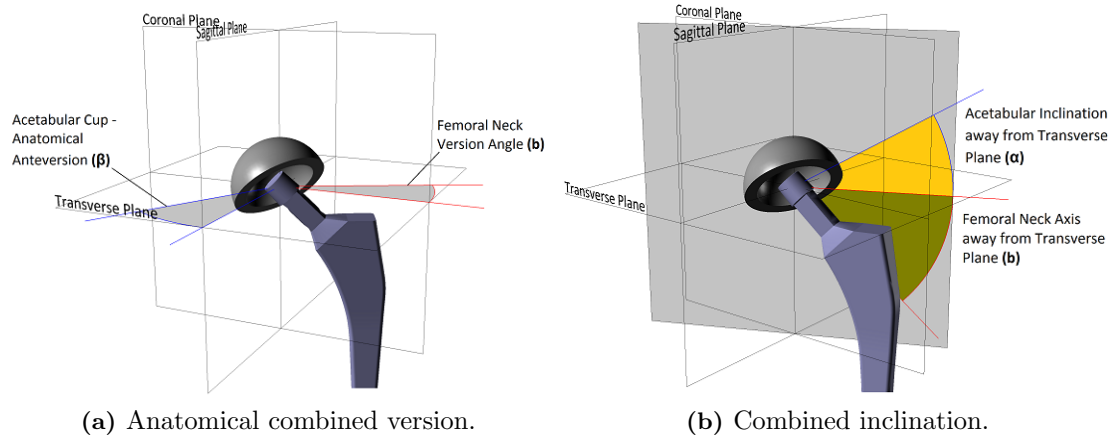


Figure 7.8: Illustration of acetabular cup and femoral stem orientations.

femoral neck angle to the transverse plane (a) are measured as an angle from the transverse plane, shown in Figure 7.8. Therefore, the variables (α) and (a) and the variables (β) and (b) have a simple additive property. This simple additive property is exploited in the design to test for combined version and combined inclination.

The trial femoral head design consisted of an outer part to measure combined version and an inner part to measure combined inclination. These two parts and the final assembly are shown in Figure 7.9. The inner part has one rotational degree of freedom. This is so that when the trial femoral head is located onto the femoral neck, the neck angle away from the transverse plane (a) does not affect the measurement of combined version. Therefore, when the head is correctly fitted to the neck, any change in the femoral neck version angle (b) will rotate the head about the superior-inferior axis in the transverse plane. This means that the position of the outer part of the femoral head is only affected by one factor, femoral neck version (b) which allows combined version to be determined when the femoral head is located in the acetabular cup. Combined version can then be measured as the addition of acetabular cup anteversion (β) as measured from the sagittal plane plus femoral neck version (b) as measured from the coronal plane.

As stated at the beginning of the section acetabular cup inclination (α) and femoral neck angle away from the transverse plane (a) are additive in a plane. However, this plane does not lie in any of the anatomical planes. This is because when considering rotations

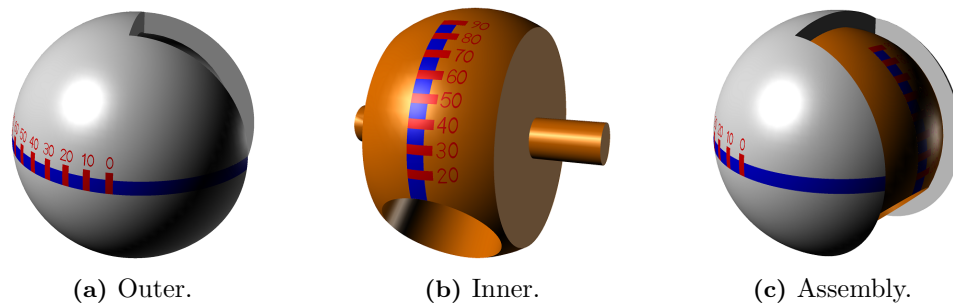


Figure 7.9: The trial femoral head.

mathematically, they are non-commutative, which means they follow a strict temporal order, i.e. a sequence (Kuipers, 1999). Therefore, the femoral and acetabular version takes the acetabular axis and femoral neck axis away from the coronal plane (Murray, 1993; Yoshimine and Ginbayashi, 2002). Consequently, a new plane has to be defined, the femoral neck plane, which is the plane in which the femoral neck axis lies, as shown in grey in Figure 7.8b. This is the plane in which the femoral neck angle away from the transverse plane (α) is measured. Therefore, if acetabular cup inclination (α) is also measured in this plane then (α) and (α) would have the same additive property as (β) and (b) in the combined version measurement.

The inner part of the femoral head has one rotational degree of freedom. This was done so that when the trial femoral head is located onto the femoral neck, the neck angle away from the transverse plane (α) would not affect the measurement of combined version. Consequently, this inner part is not affected by the measurement of combined version and can be used to measure combined inclination.

The trial femoral head has markings on the surface which measure the amount of combined version on the outer head and combined inclination on the inner head. The blue line on the outer surface is used to align the femoral head with the transverse plane. Once the femoral head is located into the pelvic acetabular cup the measurement of combined version and combined inclination can be determined by where the markings intersect with the rim of the acetabular cup. This should be read when the leg is positioned in the anatomical neutral standing posture so that both the pelvis and femur are aligned.

The process of using the femoral head begins after the surgeon has dislocated the hip joint, prepared the trial acetabular cup, performed the femoral osteotomy and fitted the femoral stem in the medullary canal of the femur. The surgeon then locates the trial femoral head on the tapered interface of the femoral neck and rotates it until the blue line on the trial head is aligned with the transverse plane. Next, the surgeon re-locates the hip joint and holds the treated leg in the standing posture. At this point, both the combined version measurement and combined inclination measurement can be read, using the design presented in Figure 7.9. Combined version is read where the blue line of the outer part of the femoral head and the rim of the acetabular cup intersect. Combined inclination is read where the inner part of the femoral head and the rim of the acetabular cup intersect.

Measurement of both combined version and inclination can be used to define an acceptable range required to be achieved for a particular implant. This can be defined by simple colour coded zones to indicate the acceptable range (green) and the range which is not acceptable (red). Based on the measurements made in the randomised controlled trial a combined version angle of between 30° and 50° and a combined inclination angle of above 45° was defined as acceptable and placed in the green zone. As Figure 7.10 shows, using the coloured zones, combined version is read where the blue line of the outer part of the femoral head and the rim of the acetabular cup intersect. Combined inclination is read where the inner part of the femoral head and the rim of the acetabular cup intersect. Once combined anteversion and combined inclination has been read the surgeon can assess whether the relative orientation of the prosthetic components is correct or whether a different modular neck option needs to be selected to achieve the correct orientation.

This section has presented one possible design solution to aid the surgeon in making the correct modular femoral neck choice. However, adoption of this medical device is dependent upon whether femoral neck modularity is perceived as providing a beneficial post-operative outcome. At present, this is still being evaluated and further long term studies are required before its success can be evaluated.

7.7 Further Work

The research presented in this study has the potential to be exploited further and developed into new areas for research. One such area is the application of the range of motion benchmark in physiotherapy and post-operative recovery. The range of motion benchmark can potentially highlight manouevres which might pose risk to the patient with regard to impingement and dislocation. Therefore, given the findings related to inter-joint adaptation, a patient's post-operative recovery could be tailored to ensure that risk manouevres are avoided by performing activities using an alternative method exploiting other joint movements.

The techniques used to develop the range of motion benchmark can be used to develop similar benchmarks for the other joints within the human body. The shoulder would be the next logical step in which to use the modelling philosophy presented in this study, as it has a similar anatomy to the hip joint and has similar problems with impingement. Also, the range of motion benchmark could be applied to the native hip to understand the clinical problem of femoroacetabular impingement which has been recognised as the pathomechanism for the onset of primary arthritis. However, further research would be required to be able to model hip joint translation to account for a non-spherical head. In addition, there would be a requirement to better model the effect of soft tissue rather than just bony impingement as acknowledged in section 4.4.2 when modelling range of motion using patient CT scans.

The application of this study has focussed upon assessing the effectiveness of femoral neck modularity. However, the vast majority of the operative techniques in THA require the acetabular cup to be fitted first. This sets the impingement limits for the prosthetic hip joint, which femoral neck modularity can influence to a certain extent. Therefore, to improve hip replacement outcome more focus has to be given to being able to consistently fit the acetabular component in the correct orientation. There have been many studies which have attempted to define a safe zone for acetabular component orientation. However, these have suffered from having inconsistent definitions and references. This has meant

there is still a wide distribution of recommended values of what is considered to be the correct prosthetic orientation. Further work needs to be done on establishing this safe zone considering all the modelling variables discussed in this report. Once done this will allow techniques to be developed that fit the acetabular component in the correct orientation. Patient imaging can be employed to achieve this by allowing customised surgical fixtures to be designed and manufactured to aid surgeon fitment intra-operatively.

Finally, the research on hip joint range of motion can be expanded beyond the clinical field. Examples include ergonomic designs to improve the comfort of car seating or modelling to achieve better realism within computer games or manufacturing simulations. These represent a few of the possible options for where the research can be exploited.

7.8 Summary

This chapter has brought together all the key themes of the research and discussed them together in relation to the research question. The key areas of research that have been undertaken to meet the requirements of the research objectives have allowed this research question to be answered, within the identified limitations of the study. Fulfilling the research question and objectives has meant that this study has developed and applied innovation and made a contribution to knowledge to the fields of biomechanics and orthopaedics. The work undertaken has developed further innovation which can be used to improve operative outcome in THA and address a limitation with regard to femoral neck modularity identified in the study allowing it to be used to its full potential. The key findings and recommendations arising from this work can now be made in the next chapter.

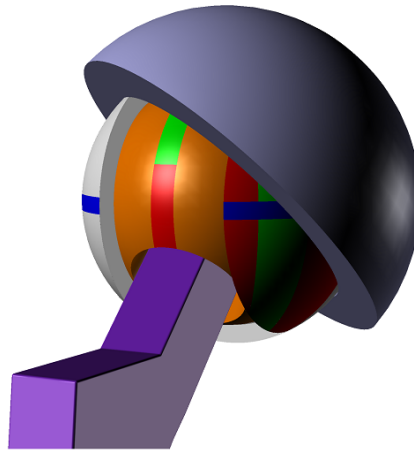


Figure 7.10: The trialling process for the prototype femoral head.

Chapter 8

Conclusion

8.1 Introduction

The research presented in this study set out to answer the following research question.

“How can range of motion be graphically represented and modelled physiologically to assess resistance to dislocation in total hip arthroplasty?”

Chapter 7 detailed how this question was answered through meeting the requirements of five research objectives. These objectives were met using a two stage research design which constructed a graphical representation of hip joint range of motion and applied it in a clinical setting to assess the effectiveness of femoral neck modularity. This chapter will consider the wider consequences of the study’s findings and its possible longer term implications.

8.2 Key findings

This section summarises the key findings of the research. These findings have come from all stages of the research, from establishing the theoretical foundation through to meeting the requirements of all the research objectives.

- **Minimum range of motion requirement** - The findings of this study has provided support for previous studies. These studies found that ability to perform activities of daily living were positively correlated with achieving a certain amount of pure joint motion. This meant a minimum range of motion requirement was able to be graphically represented to assess operative outcome.
- **Congruence of anatomical coordinate frames** - The review of the literature found that different pelvic and femoral coordinate frames were applied in gait analysis studies compared to those used in a clinical setting. This study has found agreement with regard to these coordinate frames so that range of motion data was able to be taken from studies of human movement and applied in a clinical setting.
- **Cartesian representation of hip joint range of motion** - Research contained within this study has found that the clinical pelvic and femoral coordinate frames are aligned. This has meant that both data from gait analysis studies and measurements of prosthetic component orientation were able to be presented on a single Cartesian plot for direct and simplistic comparison of post-operative range of motion.
- **Effectiveness of femoral neck modularity** - This study has found that femoral neck modularity has significant potential to alter prosthetic component orientation to improve range of motion over its equivalent non-modular control. However, this potential is not being maximised because of the limited improvement in range of motion that modular necks with small amounts of ante-retroversion combined with varus-valgus can provide. Further, it is only possible to recognise extreme cases of component mal-orientation. The extent of this mal-orientation goes beyond the current practicable limit which a modular neck can correct.

- **Use of a trial femoral head** - Further work has found that markings on the surface of the prosthetic femoral head can be used to aid the surgeon in their assessment of prosthetic orientation. This makes use of simplifying four orientation parameters into two - combined version and combined inclination. The surgeon can assess relative prosthetic orientation based on whether the rim of the acetabular cup intersects in either the acceptable or unacceptable zone marked on the femoral head.

These five points summarise the key outcomes of the research. These findings have expanded the body of knowledge with regard to both hip joint biomechanics and orthopaedics. How this knowledge can be used will be considered in the following section.

8.3 Implications of the research

The application of the research contained within this study has been focussed upon the post-operative assessment of a total hip arthroplasty technology. There are implications that the research will have for this immediate area but also in the wider orthopaedic field.

- **Femoral neck modularity** - As highlighted in the previous section the effectiveness of femoral neck modularity is being limited by the use of necks with a small amount of combined ante-retroversion with varus-valgus. Further, there are cases where the current maximum amount of neck ante-retroversion or neck varus-valgus is not enough to correct the extent of the prosthetic mal-orientation to bring range of motion into acceptable limits. Therefore, manufacturers supplying modular femoral neck implants should consider the prosthetic options that they offer.
- **Modularity in total hip arthroplasty** - In the review of the literature it was acknowledged that successful THA outcome was dependent upon two factors, joint stability and range of motion until impingement. The experimental analysis contained within this study has determined modular variables which can be considered for aiding joint stability. Those which aid range of motion and those which could influence both. Further, the effect of previous undocumented characteristics has been found to have a significant effect upon range of motion. The knowledge gained by these insights can be used both to design new implants but also to develop detailed guides for surgeons with regard to intra-operative modular selection.
- **Surgical planning** - The research contained within this study has mainly concerned post-operative evaluation of THA outcome. Further work has shown how the research can be applied to aid the surgeon's intra-operative evaluation. The next logical step for the research is for it to be incorporated into the pre-operative planning stage. Computer models of both the range of motion benchmark and trial femoral head could be used by the surgeon to plan prosthetic component orientation, select ideal modular component and visualise post-operative prosthetic range of motion.

These new tools would allow the surgeon to plan the operative procedure taking into account individual patient anatomy and their prosthetic component requirement to achieve the maximised range of motion.

- **Physical Therapy** - The post-operative range of motion results have direct relevance to a patient's recovery. The graphical representation of their prosthetic range of motion can be used to identify any areas or movements which might pose a risk for the patient in terms of dislocation. Compensatory manoeuvres could then be developed to allow the patient to perform their daily activities in the safest possible manner dependent upon the characteristics of their total hip replacement.
- **Femoroacetabular impingement** - The success of THA in restoring lost mobility to patients is well documented. However, there are younger more active patients suffering from this disease not eligible for treatment due to issues regarding its longevity. There is growing consensus that the onset of osteoarthritis is caused by a lack of clearance between the acetabular rim and femoral neck. This results in early contact between these bones during the activities that a person is likely to undertake during the course of their daily routine. Therefore, the research contained within this study can be directly applied into this field to aid both post-operative evaluation and potentially pre-operative planning.

8.4 Final summary

The research that has been undertaken in this study has developed a methodology which can be used to assess the effectiveness of operative outcome in total hip arthroplasty. This has been the first study to provide a clinically meaningful Cartesian representation of hip joint range of motion which permit operative outcome to be directly compared against an established benchmark. This has been used to provide detailed information with regard to the effectiveness of a key hip implant technology. The findings are directly relevant to not only surgeons but also implant manufacturers to improve implant design and together with surgeons and engineers improve the operative process to be more effective. This will deliver benefit to patients and healthcare providers both nationally and internationally.

References

- Ahlberg A, Moussa M, and Al-Nahdi M. On geographical variations in the normal range of joint motion. *Clin Orthop Relat R*, **1988**, 234:229–231.
- Ahn H, Bhandari M, and Schemitsch EH. An evidence-based approach to the adoption of new technology. *J Bone Joint Surg Br*, **2009**, 91(S3):95–98.
- Alton F, Baldey L, Caplan S, and Morrissey MC. A kinematic comparison of overground and treadmill walking. *Clin Biomech*, **1998**, 13(6):434–440.
- Amadi HO, Hansen UN, Wallace AL, and Bull AMJ. A scapular coordinate frame for clinical and kinematic analyses. *J Biomech*, **2008**, 41(10):2144–2149.
- American Academy of Orthopaedic Surgeons. *Joint motion: method of measuring and recording*. Chicago: American Academy of Orthopaedic Surgeons, **1965**.
- Amstutz HC, Ludwig RM, Schurman DJ, and Hodgson AG. Range of motion studies for total hip replacements: a comparative study with a new experimental apparatus. *Clin Orthop Relat R*, **1975**, 111:124–130.
- Anderson J, Neary F, Pickstone JV, and Raftery J. *Surgeons, manufacturers, and patients: a transatlantic history of total hip replacement*. Palgrave Macmillan, **2007**.
- Andrews JG. On the specification of joint configurations and motions. *J Biomech*, **1984**, 17(2):155–158.
- Andriacchi TP, Alexander EJ, Toney MK, Dyrby C, and Sum J. A point cluster method for in vivo motion analysis: applied to a study of knee kinematics. *J Biomech Eng - T ASME*, **1998**, 120(6):743–749.
- Antony J. *Design of experiments for engineers and scientists*. Butterworth-Heinemann, **2003**.
- Baker R. Pelvic angles: a mathematically rigorous definition which is consistent with a conventional clinical understanding of the terms. *Gait Posture*, **2001**, 13(1):1–6.
- Baker R. Comment: ISB recommendation on definition of joint coordinate systems for the

- reporting of human joint motion - part I: ankle, hip and spine. *J Biomech*, **2003**, 36(2): 300–302. Comment on original paper by Wu et al. (2002).
- Barrack RL, Lavernia C, Ries M, Thornberry R, and Tozakoglou E. Virtual reality computer animation of the effect of component position and design on stability after total hip arthroplasty. *Orthop Clin N Am*, **2001**, 32(4):569–578.
- Barsoum WK, Patterson RW, Higuera C, Klika AK, Krebs VE, and Molloy R. A computer model of the position of the combined component in the prevention of impingement in total hip replacement. *J Bone Joint Surg Br*, **2007**, 89(6):839–845.
- Benedetti MG, Berti L, Maselli S, Mariani G, and Giannini S. How do the elderly negotiate a step? A biomechanical assessment. *Clin Biomech*, **2007**, 22(5):567–573.
- Boone DC and Azen SP. Normal range of motion of joints in male subjects. *J Bone Joint Surg Br*, **1979**, 61(5):756–759.
- Boutron I, Ravaud P, and Nizard R. The design and assessment of prospective randomised, controlled trials in orthopaedic surgery. *J Bone Joint Surg Br*, **2007**, 89(7):858–863.
- Boyer KA, Beaupre GS, and Andriacchi TP. Gender differences exist in the hip joint moments of healthy older walkers. *J Biomech*, **2008**, 41(16):3360–3365.
- Brainlab AG. Brainlab Orthopaedic Solutions: Product Portfolio, 2008. url: http://www.brainlab.com/download/pdf/OrthoPortfolioOct07_FINALVERSION.pdf. [Online; accessed 17-May-2011].
- Brinckmann P, Frobin W, and Leivseth G. *Musculoskeletal Biomechanics*. Thieme Publishing, **2002**, 1st edition.
- Burroughs BR, Golladay GJ, Hallstrom B, and Harris WH. A novel constrained acetabular liner design with increased range of motion. *J Arthroplasty*, **2001**, 16(8S1):31–36.
- Burroughs BR, Hallstrom B, Golladay GJ, Hoeffel D, and Harris WH. Range of motion and stability in total hip arthroplasty with 28-, 32-, 38-, and 44-mm femoral head sizes an in vitro study. *J Arthroplasty*, **2005**, 20(1):11–19.
- Cailliet R. *Soft tissue pain and disability*. F.A. Davis Co., Philadelphia, **1978**.
- Camomilla V, Cereatti A, Vannozzi G, and Cappozzo A. An optimized protocol for hip joint centre determination using the functional method. *J Biomech*, **2006**, 39(6):1096–1106.
- Cappozzo A, Della Croce U, Leardini A, and Chiari L. Human movement analysis using stereophotogrammetry - part 1: theoretical background. *Gait Posture*, **2005**, 21(2): 186–196.

- Carman AB and Milburn PD. Determining rigid body transformation parameters from ill-conditioned spatial marker co-ordinates. *J Biomech*, **2006**, 39(10):1778–1786.
- Chandler DR, Glousman R, Hull D, McGuire PJ, Kim IS, Clarke IC, and Sarmiento A. Prosthetic hip range of motion and impingement: the effects of head and neck geometry. *Clin Orthop Relat R*, **1982**, 166:284–291.
- Charnley J. *Low friction arthroplasty of the hip: theory and practice*. Springer-Verlag, **1979**.
- Chen E, Goertz W, and Lill CA. Implant position calculation for acetabular cup placement considering pelvic lateral tilt and inclination. *Comput Aided Surg*, **2006**, 11(6):309–316.
- Cheng PL. Joint rotation between two attitudes in the spherical rotation coordinate system. *J Biomech*, **2004**, 37(10):1475–1482.
- Cheng PL, Nicol AC, and Paul JP. Determination of axial rotation angles of limb segments: a new method. *J Biomech*, **2000**, 33(7):837–843.
- Chezea L, Dumasa R, Comteta JJ, Rumelhart C, and Fayeta M. A joint coordinate system proposal for the study of the trapeziometacarpal joint kinematics. *Comput Method Biomech*, **2009**, 12(3):277–282.
- Cho SH, Park JM, and Kwon OY. Gender differences in three dimensional gait analysis data from 98 healthy Korean adults. *Clin Biomech*, **2004**, 19(2):145–152.
- Chow SC and Liu JP. *Design and analysis of clinical trials: concepts and methodologies*. LibreDigital, **2004**, 2nd edition.
- Chung KC and Burns PB. A guide to planning and executing a surgical randomized controlled trial. *J Hand Surg-Am*, **2008**, 33(3):407–412.
- Cole TM. *Goniometry: The measurement of joint motion*, pp. 40–44. WB Saunders, 2nd edition, 1971.
- Costigan PA, Deluzio KJ, and Wyss UP. Knee and hip kinetics during normal stair climbing. *Gait Posture*, **2002**, 16(1):31–37.
- Cotter SC. A screening design for factorial experiments with interactions. *Biometrika*, **1979**, 66(2):317–320.
- Dandachli W, Richards R, Sauret V, and Cobb JP. The transverse pelvic plane: A new and practical reference frame for hip arthroplasty. *Comput Aided Surg*, **2006**, 11(6): 322–326.
- Daniels L and Worthingham C. *Muscle testing: techniques of manual examination*. W.B. Saunders Company, **1972**, 3rd edition.

- Davis JC. *Statistics and data analysis in geology*. John Wiley & Sons, Inc, **2002**, 3rd edition.
- Davis KE, Ritter MA, Berend ME, and Meding JB. The importance of range of motion after total hip arthroplasty. *Clin Orthop Relat R*, **2007**, 465:180–184.
- Depuy Orthopaedics Inc. Corail Hip System: Surgical Technique, 2010. url: [http://www.depuy.com/sites/default/files/products/files/0612-82-501r5%20SCRN%20\(2\)_0.pdf](http://www.depuy.com/sites/default/files/products/files/0612-82-501r5%20SCRN%20(2)_0.pdf). [Online; accessed 15-May-2011, Revision 5].
- DeVita P and Hortobagyi T. Age causes a redistribution of joint torques and powers during gait. *J Appl Physiol*, **2000**, 88(5):1804–1811.
- DiGioia AM, Jaramaz B, Blackwell M, Simon DA, Morgan F, Moody JE, Nikou C, Colgan BD, Aston CA, Labarca RS, Kischell E, and Kanade T. The Otto Aufranc Award: image guided navigation system to measure intraoperatively acetabular implant alignment. *Clin Orthop Relat R*, **1998**, 355:8–22.
- DiGioia AM, Jaramaz B, Plakseychuk AY, Moody JE, Nikou C, LaBarca RS, Levison TJ, and Picard F. Comparison of a mechanical acetabular alignment guide with computer placement of the socket. *J Arthroplasty*, **2002**, 17(3):359–364.
- D’Lima DD, Urquhart AG, Buehler KO, Walker RH, and Colwell CW. The effect of the orientation of the acetabular and femoral components on the range of motion of the hip at different head-neck ratios. *J Bone Joint Surg Am*, **2000**, 82(3):315–321.
- Dorr LD, Malik A, Dastane M, and Wan Z. Combined anteversion technique for total hip arthroplasty. *Clin Orthop Relat R*, **2009**, 467(1):119–127.
- Duwelius PJ, Hartzband MA, Burkhart R, Carnahan C, Blair S, Wu Y., and Grunke-meier GL. Clinical results of a modular neck hip system: hitting the bulls-eye more accurately. *Am J Orthop*, **2010**, 39(S10):2–6.
- Ehrig RM, Taylor WR, Duda GN, and Heller MO. A survey of formal methods for determining the centre of rotation of ball joints. *J Biomech*, **2006**, 39(15):2798–2809.
- Enocson A, Hedbeck CJ, Tidermark J, Pettersson H, Ponzer S, and Lapidus LJ. Dislocation of total hip replacement in patients with fractures of the femoral neck. *Acta Orthop*, **2009**, 80(2):184–189.
- Ferber R, McClay-Davis I, and Williams DS. Gender differences in lower extremity mechanics during running. *Clin Biomech*, **2003**, 18(4):350–357.
- Fernández O. Obtaining a best fitting plane through 3D georeferenced data. *J Struct Geol*, **2005**, 27(5):855–858.

- Gajdosik RL and Bohannon RW. Clinical measurement of range of motion: review of goniometry emphasizing reliability and validity. *Phys Ther*, **1987**, 67(12):1867–1872.
- Galloway Jr RL. The process and development of image-guided procedures. *Annu Rev Biomed Eng*, **2001**, 3(1):83–108.
- Golub GH and Van Loan CF. An analysis of the total least squares problem. *SIAM J Numer Anal*, **1980**, 17(6):883–893.
- Green WBB and Heckman JD, (eds). *The clinical measurement of joint motion*. Rosemont: American Academy of Orthopaedic Surgeons, **1994**.
- Grood ES and Suntay WJ. A joint coordinate system for the clinical description of three-dimensional motions: application to the knee. *J Biomech Eng - T ASME*, **1983**, 105(2): 136–144.
- Hagio K, Sugano N, Nishii T, Miki H, Otake Y, Hattori A, Suzuki N, Yonenobu K, Yoshikawa H, and Ochi T. A novel system of four-dimensional motion analysis after total hip arthroplasty. *J Orthop Res*, **2004**, 22(3):665–670.
- Halvorsen K. Bias compensated least squares estimate of the center of rotation. *J Biomech*, **2003**, 36(7):999–1008.
- Harris WH. *Advanced concepts in total hip replacement*. Slink Inc., **1985**.
- Heading J. *Matrix theory for physicists*. Longmans, Green, **1958**.
- Heard WB. *Rigid body mechanics: mathematics, physics and applications*. Wiley-VCH, **2005**.
- Hemmerich A, Brown H, Smith S, Marthandam SSK, and Wyss UP. Hip, knee, and ankle kinematics of high range of motion activities of daily living. *J Orthop Res*, **2006**, 24(4): 770–781.
- Hibbeler RC. *Engineering mechanics: dynamics*. Prentice Hall, **2009**, 12th edition.
- Higgins JPT. and Green S. *Cochrane handbook for systematic reviews of interventions*. John Wiley & Sons, Ltd, **2008**.
- Holt CA, Evans SL, Dillon D, and Ahuja S. Three-dimensional measurement of intervertebral kinematics in vitro using optical motion analysis. *P I Mech Eng H - J Med*, **2005**, 219(6):393–399.
- Hoppenfeld S and Hutton R. *Physical examination of the spine and extremities*. New York: Appleton-Century-Crofts, **1976**.

- Huo MH, Parvizi J, Bal BS, and Mont MA. What's new in total hip arthroplasty. *J Bone Joint Surg Am*, **2008**, 90(9):2043–2055.
- Hurd WJ, Chmielewski TL, Axe MJ, Davis I, and Snyder-Mackler L. Differences in normal and perturbed walking kinematics between male and female athletes. *Clin Biomech*, **2004**, 19(5):465–472.
- James B and Parker AW. Active and passive mobility of lower limb joints in elderly men and women. *Am J Phys Med Rehab*, **1989**, 68(4):162–167.
- Japanese Orthopaedic Association. *Range of joint motion and method of measurement*. Tokyo: Japanese Orthopaedic Association, **1995**.
- Jaramaz B, Nikou C, Simon D, and DiGioia A. Range of motion after total hip arthroplasty: experimental verification of the analytical simulator. In Troccaz J, Grimson E, and Mosges R, (eds). *Proceedings of the First Joint Conference on Computer Vision, Virtual Reality and Robotics in Medicine and Medial Robotics and Computer-Assisted Surgery*, **1997**, pp. 573–582.
- Jaramaz B, DiGioia AM, Blackwell M, and Nikou C. Computer assisted measurement of cup placement in total hip replacement: Computer assisted orthopaedic surgery: Medical robotics and image guided surgery. *Clin Orthop Relat R*, **1998**, 354:70–81.
- Johnston RC and Smidt GL. Measurement of hip-joint motion during walking: evaluation of an electrogoniometric method. *J Bone Joint Surg Am*, **1969**, 51(6):1083–1094.
- Johnston RC and Smidt GL. Hip motion measurements for selected activities of daily living. *Clin Orthop Relat R*, **1970**, 72:205–215.
- Jolles BM, Zangger P, and Leyvraz PF. Factors predisposing to dislocation after primary total hip arthroplasty. *J Arthroplasty*, **2002**, 17(3):282–288.
- Judge JO, Davis RB, and Ounpuu S. Step length reductions in advanced age: the role of ankle and hip kinetics. *J Gerontol A-Biol*, **1996**, 51(6):303–312.
- Kadaba MP, Ramakrishnan HK, and Wootten ME. Measurement of lower extremity kinematics during level walking. *J Orthop Res*, **1990**, 8(3):383–392.
- Kelley TC and Swank ML. Role of navigation in total hip arthroplasty. *J Bone Joint Surg Am*, **2009**, 91(S1):153–158.
- Kendall HO, Kendall FP, and Wadsworth GE. *Muscles testing and function*. Baltimore: Williams and Wilkins, **1971**, 2nd edition.
- Kerrigan DC, Todd M, and Della Croce U. Gender differences in joint biomechanics during walking. *Am J Phys Med Rehab*, **1998a**, 77(1):2–7.

- Kerrigan DC, Todd MK, Della Croce U, Lipsitz LA, and Collins JJ. Biomechanical gait alterations independent of speed in the healthy elderly: evidence for specific limiting impairments. *Arch Phys Med Rehab*, **1998b**, 79(3):317–322.
- Kessler O, Patil S, Stefan W, Mayr E, Colwell CW, and D'Lima DD. Bony impingement affects range of motion after total hip arthroplasty: A subject-specific approach. *J Orthop Res*, **2008**, 26(4):443–452.
- Kirkwood RN, Culham EG, and Costigan P. Radiographic and non-invasive determination of the hip joint center location: effect on hip joint moments. *Clin Biomech*, **1999**, 14(4): 227–235.
- Kluess D, Martin H, Mittelmeier W, Schmitz KP, and Bader R. Influence of femoral head size on impingement, dislocation and stress distribution in total hip replacement. *Med Eng Phys*, **2007**, 29(4):465–471.
- Ko BH and Yoon YS. Optimal orientation of implanted components in total hip arthroplasty with polyethylene on metal articulation. *Clin Biomech*, **2008**, 23(8):996–1003.
- Kop AM and Swarts E. Corrosion of a hip stem with a modular neck taper junction: a retrieval study of 16 cases. *J Arthroplasty*, **2009**, 24(7):1019–1023.
- Krushell RJ, Burke DW, and Harris WH. Elevated-rim acetabular components: effect on range of motion and stability in total hip arthroplasty. *J Arthroplasty*, **1991**, 6:S53–S58.
- Kubiak-Langer M, Tannast M, Murphy SB, Siebenrock KA, and Langlotz F. Range of motion in anterior femoroacetabular impingement. *Clin Orthop Relat R*, **2007**, 458: 117–124.
- Kuipers JB. *Quaternions and rotation sequences: A primer with applications to orbits, aerospace, and virtual reality*. Princeton University Press, **1999**, 1st edition.
- Kumar R. *Research methodology: A step-by-step guide for beginners*. Sage Publications Ltd, **2011**, 3rd edition.
- Kummer FJ, Shah S, Iyer S, and DiCesare PE. The effect of acetabular cup orientations on limiting hip rotation. *J Arthroplasty*, **1999**, 14(4):509–513.
- Kurtz S, Ong K, Lau E, Mowat F, and Halpern M. Projections of primary and revision hip and knee arthroplasty in the United States from 2005 to 2030. *J Bone Joint Surg Am*, **2007**, 89(4):780–785.
- Kurtz WB, Ecker TM, Reichmann WM, and Murphy SB. Factors affecting bony impingement in hip arthroplasty. *J Arthroplasty*, **2010**, 25(4):624–634.

- Lembeck B, Mueller O, Reize P, and Wuelker N. Pelvic tilt makes acetabular cup navigation inaccurate. *Acta Orthop*, **2005**, 76(4):517–523.
- Lewinnek GE, Lewis JL, Tarr R, Compere CL, and Zimmerman JR. Dislocations after total hip-replacement arthroplasties. *J Bone Joint Surg Am*, **1978**, 60(2):217–220.
- Luttgens K and Wells KF. *Kinesiology: Scientific basis of human movement*. Dubuque: Brown & Benchmark, **1982**, 7th edition.
- Malchau H, Callanan M, Bragdon C, Zurakowski D, Jarrett B, and Rubash H. An analysis of cup positioning in total hip arthroplasty: quality improvement by use of a local joint registry. *Orthopaedic Proceedings*, **2011**, vol. 93, p. 88.
- Malik A, Maheshwari A, and Dorr LD. Impingement with total hip replacement. *J Bone Joint Surg Am*, **2007**, 89(8):1832–1842.
- Maruyama M, Feinberg JR, Capello WN, and D’Antonio JA. Morphologic features of the acetabulum and femur: anteversion angle and implant positioning. *Clin Orthop Relat R*, **2001**, 393:52–65.
- Mayr E, Thaler M, Williams A, Moctezuma De La Barrera J, Krismer M, and Nogler M. The figure-of-four axis as a reference to determine stem rotation in hip arthroplasty. what does it really measure? a cadaver study. *Acta Orthop*, **2007**, 78(4):458–462.
- McCollum DE and Gray WJ. Dislocation after total hip arthroplasty: causes and prevention. *Clin Orthop Relat R*, **1990**, 261:159–170.
- McCulloch P, Taylor I, Sasako M, Lovett B, and Griffin D. Randomised trials in surgery: problems and possible solutions. *Brit Med J*, **2002**, 324(7351):1448–1451.
- Miki H, Yamanashi W, Nishii T, Sato Y, Yoshikawa H, and Sugano N. Anatomic hip range of motion after implantation during total hip arthroplasty as measured by a navigation system. *J Arthroplasty*, **2007**, 22(7):946–952.
- Miki H, Nishihara S, Otake Y, Suzuki N, Yonenobu K, and Sugano N. The effect of modular neck system on prevention for prosthetic impingement. Presented at the 55th Annual Meeting of the Orthopaedic Research Society - Las Vegas, Nevada, February 22-24, **2009**.
- Mohr T. *Physical Therapy*, chapter Musculoskeletal analysis: the hip, pp. 369–380. Philadelphia: J.B. Lippincott Co., 1989.
- Monnet T, Desailly E, Begon M, Vallée C, and Lacouture P. Comparison of the SCoRE and HA methods for locating in vivo the glenohumeral joint centre. *J Biomech*, **2007**, 40(15):3487–3492.

- Montgomery DC. *Design and analysis of experiments*. John Wiley & Sons Inc, **2008**, 6th edition.
- Morrison JB. The mechanics of the knee joint in relation to normal walking. *J Biomech*, **1970**, 3(1):51–61.
- Mulholland SJ and Wyss UP. Activities of daily living in non-western cultures: range of motion requirements for hip and knee joint implants. *Int J Rehabil Res*, **2001**, 24(3): 191–198.
- Murphy KR, Myers B, and Wolach AH. *Statistical power analysis: a simple and general model for traditional and modern hypothesis tests*. Psychology Press, **2004**, 2nd edition.
- Murphy SB, Simon SR, Kijewski PK, Wilkinson RH, and Griscom NT. Femoral anteversion. *J Bone Joint Surg Am*, **1987**, 69(8):1169–1176.
- Murray DW. The definition and measurement of acetabular orientation. *J Bone Joint Surg Br*, **1993**, 75(2):228–232.
- Murray RM, Li Z, Sastry S, and Sastry SS. *A mathematical introduction to robotic manipulation*. CRC Press, **1994**.
- Nadzadi ME, Pedersen DR, Callaghan JJ, and Brown TD. Effects of acetabular component orientation on dislocation propensity for small-head-size total hip arthroplasty. *Clin Biomech*, **2002**, 17(1):32–40.
- Nadzadi ME, Pedersen DR, Yack HJ, Callaghan JJ, and Brown TD. Kinematics, kinetics, and finite element analysis of commonplace maneuvers at risk for total hip dislocation. *J Biomech*, **2003**, 36(4):577–591.
- Najarian BC, Kilgore JE, and Markel DC. Evaluation of component positioning in primary total hip arthroplasty using an imageless navigation device compared with traditional methods. *J Arthroplasty*, **2009**, 24(1):15–21.
- National Joint Registry. National Joint Registry for England and Wales. 8th annual report, 2011. url: <http://www.njrcentre.org.uk/NjrCentre/Portals/0/Documents/NJR%208th%20Annual%20Report%202011.pdf>. [Online; accessed 10-07-2011].
- National Joint Replacement Registry. Hip and knee arthroplasty: annual report 2011. url: http://www.dmac.adelaide.edu.au/aoanjrr/documents/AnnualReports2011/AnnualReport_2011_WebVersion.pdf. [Online; accessed 10-07-2011].
- Nikou C, Jaramaz B, and DiGioia AM. Range of motion after total hip arthroplasty: simulation of non-axisymmetric implants. In Wells W, Colchester A, and Delp S, (eds).

- Proceedings of the Second International Conference on Medical Image Computing and Computer-Assisted Intervention, **1998**, pp. 700–709.
- Nikou C, Jaramaz B, DiGioia A, and Levison T. Description of anatomic coordinate systems and rationale for use in an image-guided total hip replacement system. Proceedings of the Third International Conference on Medical Image Computing and Computer-Assisted Intervention, **2000**, pp. 1118–1194.
- Nishihara S, Sugano N, Nishii T, Ohzono K, and Yoshikawa H. Measurements of pelvic flexion angle using three-dimensional computed tomography. Clin Orthop Relat R, **2003**, 411:140–151.
- Noble PC, Sugano N, Johnston JD, Thompson MT, Conditt MA, Engh CA, and Mathis KB. Computer simulation: how can it help the surgeon optimize implant position? Clin Orthop Relat R, **2003**, 417:242–252.
- Nonaka H, Mita K, Watakabe M, Akataki K, Suzuki N, Okuwa T, and Yabe K. Age-related changes in the interactive mobility of the hip and knee joints: a geometrical analysis. Gait Posture, **2002**, 15(3):236–243.
- Nordin M and Frankel VH. *Basic biomechanics of the musculoskeletal system*. Lippincott Williams & Wilkins, **2001**, 3rd edition.
- Pedersen DR, Callaghan JJ, and Brown TD. Activity-dependence of the “safe zone” for impingement versus dislocation avoidance. Med Eng Phys, **2005**, 27(4):323–328.
- Perron M, Malouin F, Moffet H, and McFadyen BJ. Three-dimensional gait analysis in women with a total hip arthroplasty. Clin Biomech, **2000**, 15(7):504–515.
- Piantadosi S. *Clinical trials: a methodologic perspective*. Wiley-Interscience, **2005**, 2nd edition.
- Piazza SJ, Erdemir A, Okita N, and Cavanagh PR. Assessment of the functional method of hip joint center location subject to reduced range of hip motion. J Biomech, **2004**, 37(3):349–356.
- Pollard CD, Davis IMC, and Hamill J. Influence of gender on hip and knee mechanics during a randomly cued cutting maneuver. Clin Biomech, **2004**, 19(10):1022–1031.
- Ranawat CS and Maynard MJ. Modern technique of cemented total hip arthroplasty. Tech Orthop, **1991**, 6(3):17–25.
- Rees D.G. *Essential statistics*. CRC Press, **2001**, 4th edition.
- Ritter MA. A treatment plan for the dislocated total hip arthroplasty. Clin Orthop Relat R, **1980**, 153:153–155.

- Roaas A and Andersson GBJ. Normal range of motion of the hip, knee and ankle joints in male subjects, 30–40 years of age. *Acta Orthop*, **1982**, 53(2):205–208.
- Roach KE and Miles TP. Normal hip and knee active range of motion: the relationship to age. *Phys Ther*, **1991**, 71(9):656–665.
- Rowe PJ, Myles CM, Walker C., and Nutton R. Knee joint kinematics in gait and other functional activities measured using flexible electrogoniometry: how much knee motion is sufficient for normal daily life? *Gait Posture*, **2000**, 12(2):143–155.
- Rowley DI and Dent JA. *The musculoskeletal system: Core topics in the new curriculum*. Arnold, **1997**.
- Sakai T, Sugano N, Nishii T, Haraguchi K, Ochi T, and Ohzono K. Optimizing femoral anteversion and offset after total hip arthroplasty, using a modular femoral neck system: an experimental study. *J Orthop Sci*, **2000**, 5(5):489–494.
- Sakai T, Sugano N, Ohzono K, Nishii T, Haraguchi K, and Yoshikawa H. Femoral anteversion, femoral offset, and abductor lever arm after total hip arthroplasty using a modular femoral neck system. *J Orthop Sci*, **2002**, 7(1):62–67.
- Saltelli A, Chan K, and Scott EM, (eds). *Sensitivity analysis*, vol. 134. Wiley: New York, **2000**.
- Schulz K, Altman D, and Moher D. Consort 2010 statement: updated guidelines for reporting parallel group randomised trials. *BMC Med*, **2010**, 8(1):1–18.
- Schwenke H, Neuschaefer-Rube U, Pfeifer T, and Kunzmann H. Optical methods for dimensional metrology in production engineering. *CIRP Ann-Manuf Techn*, **2002**, 51(2):685–699.
- Scifert CF, Noble PC, Brown TD, Bartz RL, Kadakia N, Sugano N, Johnston RC, Pedersen DR, and Callaghan JJ. Experimental and computational simulation of total hip arthroplasty dislocation. *Orthop Clin N Am*, **2001**, 32(4):553–567.
- Seki M, Yuasa N, and Ohkuni K. Analysis of optimal range of socket orientations in total hip arthroplasty with use of computer-aided design simulation. *J Orthop Res*, **1998**, 16(4):513–517.
- Sommer 3rd HJ, Miller NR, and Pijanowski GJ. Three-dimensional osteometric scaling and normative modelling of skeletal segments. *J Biomech*, **1982**, 15(3):171–180.
- Soong M, Rubash HE, and Macaulay W. Dislocation after total hip arthroplasty. *J Am Acad Orthop Sur*, **2004**, 12(5):314–321.

- Spring KW. Euler parameters and the use of quaternion algebra in the manipulation of finite rotations: a review. *Mech Mach Theory*, **1986**, 21(5):365–373.
- Stökdijk M, Nagels J, and Rozing PM. The glenohumeral joint rotation centre in vivo. *J Biomech*, **2000**, 33(12):1629–1636.
- Stuchin SA. Anatomic diameter femoral heads in total hip arthroplasty: a preliminary report. *J Bone Joint Surg Am*, **2008**, 90(S3):52–56.
- Sun H, Inaoka H, Fukuoka Y, Masuda T, Ishida A, and Morita S. Range of motion measurement of an artificial hip joint using CT images. *Med Biol Eng Comput*, **2007**, 45(12):1229–1235.
- Svenningsen S, Terjesen T, Auflem M, and Berg V. Hip motion related to age and sex. *Acta Orthop*, **1989**, 60(1):97–100.
- Tannast M, Langlotz U, Siebenrock KA, Wiese M, Bernsmann K, and Langlotz F. Anatomic referencing of cup orientation in total hip arthroplasty. *Clin Orthop Relat R*, **2005**, 436:144–150.
- Tannast M, Kubiak-Langer M, Langlotz F, Puls M, Murphy SB, and Siebenrock KA. Noninvasive three-dimensional assessment of femoroacetabular impingement. *J Orthop Res*, **2007**, 25(1):122–131.
- Tannast M, Goricki D, Beck M, Murphy SB, and Siebenrock KA. Hip damage occurs at the zone of femoroacetabular impingement. *Clin Orthop Relat R*, **2008**, 466(2):273–280.
- Thornberry RL and Hogan AJ. The combined use of simulation and navigation to demonstrate hip kinematics. *J Bone Joint Surg Am*, **2009**, 91(S1):144–152.
- Toni A, Sudanese A, Paderni S, Guerra E, Bianchi G, Antonietti B, and Giunti A. Cementless hip arthroplasty with a modular neck. *La Chirurgia degli organi di movimento*, **2001**, 86(2):73–85.
- Torgerson C. *Systematic reviews*. Continuum International Publishing Group, **2003**.
- Traina F, Baleani M, Viceconti M, and Toni A. Modular neck primary prosthesis: experimental and clinical outcomes. Presented as a scientific exhibit at the Annual Meeting of the American Academy of Orthopaedic Surgeons, San Francisco, March 10-14, **2004**.
- Traina F, De Clerico M, Biondi F, Pilla F, Tassinari E, and Toni A. Sex differences in hip morphology: is stem modularity effective for total hip replacement? *J Bone Joint Surg Am*, **2009a**, 91(S6):121–128.
- Traina F, De Fine M, Biondi F, Tassinari E, Galvani A, and Toni A. The influence of the

- centre of rotation on implant survival using a modular stem hip prosthesis. *Int Orthop*, **2009b**, 33(6):1513–1518.
- Traina F, De Fine M, Tassinari E, Sudanese A, Calderoni PP, and Toni A. Modular neck prostheses in DDH patients: 11-year results. *J Orthop Sci*, **2011**, 16(1):14–20.
- Turley GA and Griffin DR. A device to prevent prosthetic dislocation and wear, GB1202126.7 - filed: 8 Feb 2012.
- Turley GA, Ahmed SMY, Williams MA, and Griffin DR. Establishing a range of motion boundary for total hip arthroplasty. *P I Mech Eng H - J Med*, **2011**, 225(8):769–782.
- Turley GA, Ahmed SMY, Williams MA, and Griffin DR. Validation of the femoral anteversion measurement method used in imageless navigation. *Comput Aided Surg*, **2012**, 17(4):187–197.
- Veeger HEJ. The position of the rotation center of the glenohumeral joint. *J Biomech*, **2000**, 33(12):1711–1715.
- Viceconti M, Ruggeri O, Toni A, and Giunti A. Design-related fretting wear in modular neck hip prosthesis. *J Biomed Mater Res A*, **1996**, 30(2):181–186.
- Viceconti M, Baleani M, Squarzone S, and Toni A. Fretting wear in a modular neck hip prosthesis. *J Biomed Mater Res A*, **1997**, 35(2):207–216.
- Vidalain J. Outcome of an extensively ha-coated stem at 18-year follow-up: a prospective study of 615 cases. *Orthopaedic Proceedings*, **2010**, vol. 92, p. 532.
- Weiss JM, Noble PC, Conditt MA, Kohl HW, Roberts S, Cook KF, Gordon MJ, and Mathis KB. What functional activities are important to patients with knee replacements? *Clin Orthop Rel R*, **2002**, 404:172–188.
- Welman C, Kruger F, and Mitchell B. *Research methodology*. Oxford University Press, **2005**, 3rd edition.
- Widmer KH. Containment versus impingement: finding a compromise for cup placement in total hip arthroplasty. *Int Orthop*, **2007**, 31(S1):29–33.
- Widmer KH and Majewski M. The impact of the CCD-angle on range of motion and cup positioning in total hip arthroplasty. *Clin Biomech*, **2005**, 20(7):723–728.
- Widmer KH and Zurfluh B. Compliant positioning of total hip components for optimal range of motion. *J Orthop Res*, **2004**, 22(4):815–821.
- Wilson DAJ, Dunbar MJ, Amirault JD, and Farhat Z. Early failure of a modular femoral neck total hip arthroplasty component: A case report. *J Bone Joint Surg Am*, **2010**, 92(6):1514–1517.

- Wolf A, Digioia AM, Mor AB, and Jaramaz B. A kinematic model for calculating cup alignment error during total hip arthroplasty. *J Biomech*, **2005**, 38(11):2257–2265.
- Woltring HJ. Representation and calculation of 3-D joint movement. *Hum Movement Sci*, **1991**, 10(5):603–616.
- Woltring HJ. 3-D attitude representation of human joints: a standardization proposal. *J Biomech*, **1994**, 27(12):1399–1414.
- Wright G, Sporer S, Urban R, and Jacobs J. Fracture of a modular femoral neck after total hip arthroplasty: a case report. *J Bone Joint Surg Am*, **2010**, 92(6):1518–1521.
- Wright Medical Technology, Inc. Procotyl L Acetabular Cup System: Surgical Technique, 2009. url: <http://www.wmt.com/physicians/litProductLit.asp?litType=ed0679c2-25ba-4c84-9fb5-e0b93550e28c&specialty=82f54a41-d110-4750-895a-afaaef9a89a>. [Online; accessed 16-May-2011].
- Wright Medical Technology, Inc. Profemur TL Total Hip System: Surgical Technique, 2010. url: <http://www.wmt.com/physicians/litProductLit.asp?litType=ed0679c2-25ba-4c84-9fb5-e0b93550e28c&specialty=82f54a41-d110-4750-895a-afaaef9a89a>. [Online; accessed 16-May-2011, Revision 5.10].
- Wu G and Cavanagh PR. ISB recommendations for standardization in the reporting of kinematic data. *J Biomech*, **1995**, 28(10):1257–1261.
- Wu G, Siegler S, Allard P, Kirtley C, Leardini A, Rosenbaum D, Whittle M, D’Lima DD, Cristofolini L, Witte H, Schmid O, and Stokes I. ISB recommendation on definitions of joint coordinate system of various joints for the reporting of human joint motion - part I: ankle, hip, and spine. *J Biomech*, **2002**, 35(4):543–548.
- Wu G, van der Helm FCT, Veeger HEJ, Makhsous M, van Roy P, Anglin C, Nagels J, Karduna AR, McQuade K, Wang X, Werner FW, and Buchholz B. ISB recommendation on definitions of joint coordinate systems of various joints for the reporting of human joint motion - part II: shoulder, elbow, wrist and hand. *J Biomech*, **2005**, 38(5):981–992.
- Yoon YS, Hodgson AJ, Tonetti J, Masri BA, and Duncan CP. Resolving inconsistencies in defining the target orientation for the acetabular cup angles in total hip arthroplasty. *Clin Biomech*, **2008**, 23(3):253–259.
- Yoshimine F. The influence of the oscillation angle and the neck anteversion of the prosthesis on the cup safe-zone that fulfills the criteria for range of motion in total hip replacements. The required oscillation angle for an acceptable cup safe-zone. *J Biomech*, **2005**, 38(1):125–132.
- Yoshimine F. The safe-zones for combined cup and neck anteversions that fulfill the

- essential range of motion and their optimum combination in total hip replacements. J Biomech, **2006**, 39(7):1315–1323.
- Yoshimine F and Ginbayashi K. A mathematical formula to calculate the theoretical range of motion for total hip replacement. J Biomech, **2002**, 35(7):989–993.
- Yoshioka Y and Cooke TDV. Femoral anteversion: assessment based on function axes. J Orthop Res, **1987**, 5(1):86–91.

Appendix A

Calculation of hip-joint centre

Landmark definitions:

ASIS - Anterior Superior Iliac Spine.

PSIS - Posterior Superior Iliac Spine.

LEPI - Lateral Femoral Epicondyle.

MEPI - Medial Femoral Epicondyle.

LMAL - Lateral Ankle Malleolus.

MMAL - Medial Ankle Malleolus.

x -axis - medial-lateral axis.

y -axis - anterior-posterior axis.

z -axis - superior-inferior axis.

**All calculations are for a left hip joint*

Step 1: Translate all marker trajectories m_i with the PSIS_{mid} as the origin.

$$m_i - \frac{\text{PSIS}_{\text{left}} + \text{PSIS}_{\text{right}}}{2} \quad (\text{A.1})$$

Step 2a: Pelvic x -axis.

$$v_x = \frac{\text{ASIS}_{\text{right}} - \text{ASIS}_{\text{left}}}{\|\text{ASIS}_{\text{right}} - \text{ASIS}_{\text{left}}\|} \quad (\text{A.2})$$

Step 2b: Pelvic z -axis.

$$v_z = \frac{\text{ASIS}_{\text{right}} \times \text{ASIS}_{\text{left}}}{\|\text{ASIS}_{\text{right}} \times \text{ASIS}_{\text{left}}\|} \quad (\text{A.3})$$

Step 2c: Pelvic y -axis.

$$v_y = v_z \times v_x \quad (\text{A.4})$$

Step 3: Form pelvic body segment rotation matrix.

$$\mathbf{P} = \begin{bmatrix} v_x.u & v_y.u & v_z.u \\ v_x.v & v_y.v & v_z.v \\ v_x.w & v_y.w & v_z.w \end{bmatrix} \quad (\text{A.5})$$

Step 4a: Translate all marker trajectories m_i with the ASIS_{mid} as the origin.

$$m_i - \frac{\text{ASIS}_{\text{left}} + \text{ASIS}_{\text{right}}}{2} \quad (\text{A.6})$$

Step 4b: Transform LEPI and MEPI marker trajectories into the pelvic body segment coordinate frame.

$$\mathbf{P}^T.m_i \quad (\text{A.7})$$

Step 5: Calculate initial estimate of hip joint centre using LEPI and MEPI marker trajectories Halvorsen (2003).

$$A = 2 \sum_{p=1}^m \left[\left(\frac{1}{N} \sum_{k=1}^N v_k^p (v_k^p)^T \right) - \overline{v^p} (\overline{v^p})^T \right] \quad (\text{A.8})$$

$$b = \sum_{p=1}^m ((\overline{v^p})^3 - \overline{v^p} (\overline{v^p})^2) \quad (\text{A.9})$$

$$\text{hip}_{\text{init}} = A^{-1}.b \quad (\text{A.10})$$

Step 6: Compute correction term $\hat{\Delta}b$ and calculate hip_{new} , repeat until convergence Halvorsen (2003).

$$\hat{\Delta}b = 2\hat{\sigma}^2 \sum_{p=1}^m \overline{(v^p - \hat{m})} \quad (\text{A.11})$$

$$\text{hip}_{\text{new}} = A^{-1}.(b - \hat{\Delta}b) \quad (\text{A.12})$$

Appendix B

Validation experiment

Step 1: Translate all marker trajectories m_i with the $\text{hip}_{\text{centre}}$ as the origin.

$$m_i - \text{hip}_{\text{centre}} \quad (\text{B.1})$$

Step 2: Calculate knee centre.

$$\text{Knee} = \frac{\text{LEPI} + \text{MEPI}}{2} \quad (\text{B.2})$$

Step 3: Calculate ankle centre.

$$\text{Ankle} = \frac{\text{LMAL} + \text{MMAL}}{2} \quad (\text{B.3})$$

Step 4a: Femoral z-axis.

$$v_{fz} = \frac{\text{hip}_{\text{centre}} - \text{Knee}}{\|\text{hip}_{\text{centre}} - \text{Knee}\|} \quad (\text{B.4})$$

Step 4b: AEP vector.

$$v_{aep} = \frac{\text{Ankle} \times \text{Knee}}{\|\text{Ankle} \times \text{Knee}\|} \quad (\text{B.5})$$

Step 4c: Femoral y-axis.

$$v_{fy} = v_{aep} \times v_{fz} \quad (\text{B.6})$$

Step 4d: Femoral x-axis.

$$v_{fx} = v_{fy} \times v_{fz} \quad (\text{B.7})$$

Step 5: Calculate angle in transverse plane between pelvic (v_x) and femoral (v_{fx}) medial-lateral axes.

$$v_{fx} = \begin{bmatrix} u & v & w \end{bmatrix}^T \quad (\text{B.8})$$

$$u_{2d} = \frac{u}{\| \begin{bmatrix} u & v \end{bmatrix}^T \|} \quad (\text{B.9})$$

$$angle = \arccos(u_{2d}) \quad (\text{B.10})$$

Appendix C

Inter-observer experiment

Landmark definitions:

ASIS_{treated} - Treated side anterior superior iliac spine.

ASIS_{untreated} - Untreated side anterior superior iliac spine.

Pubis - Midpoint of the pubic tubercles.

I / i - Operative inclination.

A / a - Operative anteversion.

**All calculations are for a left hip joint*

Step 1: Origin coordinate system to the 1st assessor pubis measurement.

$$\begin{aligned} &1^{\text{st}} \text{ assessor landmarks (ASIS}_{\text{treated}}, \text{ASIS}_{\text{untreated}}, \text{Pubis}) - 1^{\text{st}} \text{ assessor Pubis} \\ &2^{\text{nd}} \text{ assessor landmarks (ASIS}_{\text{treated}}, \text{ASIS}_{\text{untreated}}, \text{Pubis}) - 1^{\text{st}} \text{ assessor Pubis} \end{aligned} \quad (\text{C.1})$$

Step 2: Construct the pelvic 1st assessor pelvic coordinate frame.

$$\begin{aligned} v_x &= \frac{\text{ASIS}_{\text{untreated}} - \text{ASIS}_{\text{treated}}}{\|\text{ASIS}_{\text{untreated}} - \text{ASIS}_{\text{treated}}\|} \\ v_y &= \frac{\text{ASIS}_{\text{untreated}} \times \text{ASIS}_{\text{treated}}}{\|\text{ASIS}_{\text{untreated}} \times \text{ASIS}_{\text{treated}}\|} \\ v_z &= v_x \times v_y \end{aligned} \quad (\text{C.2})$$

If:

$$v_x = \begin{bmatrix} u \\ v \\ w \end{bmatrix}$$

Step 3: 1st assessor pelvic coordinate frame orientation relative to 2nd assessor frame.

$$\mathbf{A} = \begin{bmatrix} v_{x.u} & v_{y.u} & v_{z.u} \\ v_{x.v} & v_{y.v} & v_{z.v} \\ v_{x.w} & v_{y.w} & v_{z.w} \end{bmatrix} \quad (\text{C.3})$$

Step 4: 2nd assessor acetabular system rotation matrix - Operative definition $A_x.I_y$.

$$\mathbf{R} = \begin{bmatrix} \cos i & 0 & \sin i \\ \sin i \cdot \sin a & \cos a & -\sin a \cdot \cos i \\ -\sin i \cdot \cos a & \sin a & \cos i \cdot \cos a \end{bmatrix} \quad (\text{C.4})$$

Step 5: 1st assessor acetabular system rotation matrix.

$$A^T \cdot \mathbf{R} \quad (\text{C.5})$$

If:

$$A^T \cdot \mathbf{R} = \begin{bmatrix} a_{11} & a_{12} & a_{13} \\ a_{21} & a_{22} & a_{23} \\ a_{31} & a_{32} & a_{33} \end{bmatrix}$$

Step 6: 1st assessor acetabular system orientation.

$$\begin{aligned} \mathbf{Inclination} &= \text{atan2}(a_{11}, a_{13}) \\ \mathbf{Anteversion} &= \text{atan2}(a_{22}, a_{32}) \end{aligned} \quad (\text{C.6})$$